SYNTHETIC, STRUCTURAL, AND MECHANISTIC STUDIES IN EARLY TRANSITION METAL AND ACTINIDE CHEMISTRY

Thesis by

Janet E. Nelson

In Partial Fulfillment of the Requirements

for the degree of

Doctor of Philosophy

California Institute of Technology

Pasadena, California

1991

(submitted April 22, 1991)

Acknowledgements

First, I would like to thank my advisor, John Bercaw, for the personal and scientific support he has shown through the years. His example has taught me much about how to think about chemistry. I must also thank Jay Labinger for many stimulating discussions and for extensive advice, especially for the work presented in Chapter 2. I also thank the members of the Bercaw group, past and present, for the science I have learned from them and for their help in this work. Pat Anderson has been a great friend as well as a wonderful source of advice over the past five years. Additionally, several people merit special thanks: Ged Parkin, who laid the groundwork for the chemistry in Chapter 1; Larry Henling and Dick Marsh, for solving the crystal structure in Chapter 1; Andy Meyers and Pete Dragavich, for help in the organic synthesis of the labeled thiols; and Jim Brainard, Scott Ross, Dan Jones, and David Live, for assistance obtaining deuterium decoupled NMR spectra.

I am grateful for the opportunity I had to go to Los Alamos National Laboratory and work with Al Sattelberger. The result of this "sabbatical" is Chapter 3. Many thanks also go to Dave Clark who taught me much of the uranium chemistry, to Carol Burns for solving the crystal structure in this chapter, and to all the people in INC-4 for the wonderful and supportive work environment. It was truly a fun experience.

Finally, I need to thank some special people whose support, love, and encouragement made this all possible: My family, Kathy, Russ, Tommy, and Mike. I dedicate this thesis to my daughter, Hannah, whose timely birth made the last weeks of my graduate work exciting and wonderful.

ABSTRACT

A series of permethyltantalocene thioaldehyde hydride complexes is prepared by treatment of $Cp*_2Ta(\eta^2\text{-}C_6H_4)H$ with thiols. The X-ray structure of $Cp*_2Ta(\eta^2\text{-}S=CHCH_2Ph)H$ is reported. These permethyltantalocene thioaldehyde hydride complexes are shown to be in rapid equilibrium with a 16 electron thiolate species through a β-H elimination/migration process. Upon heating, the permethyltantalocene thioaldehyde hydride complexes undergo an α-alkyl migration to the thermodynamically favored tautomer, the permethyltantalocene sulfido alkyl, $Cp*_2Ta(=S)CH_2R$. Derivatives of the permethyltantalocene phenethylthioaldehyde hydride have been prepared from the *erythro-* and *threo*-phenethyl-d_2 mercaptan to elucidate the mechanism of this migration. The migration has been found to proceed primarily with retention of stereochemistry at carbon for the migrating alkyl.

In contrast to the extremely specific regioselectivity and stereoselectivity normally demonstrated by Schwartz's reagent (Cp_2ZrHCl), hydrozirconation of styrene shows two unusual behaviors. First, treatment of Cp_2ZrHCl with styrene leads to a mixture of terminal (85%) and internal (15%) insertion products. The benzylic insertion product is stable, and does not undergo migration to a terminal organozirconium product, even when heated. Second, attempts to prepare stereospecifically labeled deutero organozirconium derivatives result in scrambling of the β positions of both isomers, yielding a statistical distribution of isotopomers. The features of this scrambling process are described and a mechanism involving an organozirconium alkyl hydride species is proposed.

$[K(THF)_2]_2[U(NHAr)_5]\bullet THF$, (Ar = 2,6-diisopropylphenyl) is prepared by treatment of $UI_3(THF)_4$ with five equivalents of potassium 2,6-diisopropylanilide (KNHAr) in THF. Electronic absorption spectra reveal internal f-f transitions characteristic of trivalent uranium. A single crystal X-ray study revealed that the dianion is a monomer containing a trigonal bipyramidal five-coordinate uranium center. The potassium cations each interact in an η^6 and η^4 fashion

with two arene rings of the arylamido ligands, and two THF molecules. Crystal data (at -70° C):

Monoclinic space group P2$_1$/C, with a = 21.726(7) Å, b = 15.378(6) Å, c = 25.007(4) Å, β = 106.07(4)°, and Z = 4.

TABLE OF CONTENTS

LIST OF FIGURES

LIST OF TABLES

ABBREVIATIONS

Anal.	elemental analysis
br	broad
Calcd.	calculated
Cp	η^5-C_5H_5
Cp*	η^5-C_5Me_5
d	doublet
dd	doublet of doublets
IR	Infrared spectroscopy
m	multiplet (NMR), medium (UV-VIS)
Me	methyl
NMR	Nuclear Magnetic Resonance spectroscopy
Ph	phenyl
ppm	parts per million
q	quartet
s	singlet (NMR), strong (UV-VIS)
t	triplet
UV-VIS-NIR	Ultra Violet/ Visible/ Near Infrared spectroscopy
vw	very weak
w	weak

Chapter 1

Synthesis and Characterization of Thioaldehyde-Hydride Derivatives of Permethyltantalocene. Investigations of Their Equilibration with Thiolates and the Stereochemistry of Alkyl Migrations from Sulfur to Tantalum

Abstract:

A series of permethyltantalocene thioaldehyde hydride complexes is prepared by treatment of $Cp*_2Ta(\eta^2-C_6H_4)H$ with thiols. The X-ray structure of $Cp*_2Ta(\eta^2-S=CHCH_2Ph)H$ is reported. These permethyltantalocene thioaldehyde hydride complexes are shown to be in rapid equilibrium with a 16 electron thiolate species through a β-H elimination/migration process. Upon heating, the permethyltantalocene thioaldehyde hydride complexes undergo an α-alkyl migration to the thermodynamically favored tautomer, the permethyltantalocene sulfido alkyl, $Cp*_2Ta(=S)CH_2R$. Derivatives of the permethyltantalocene phenethylthioaldehyde hydride have been prepared from the *erythro-* and *threo*-phenethyl-d_2 mercaptan to elucidate the mechanism of this migration. The migration has been found to proceed primarily with retention of stereochemistry at carbon for the migrating alkyl.

Introduction

The removal of sulfur from crude fossil fuels is an important commercial process, known as HDS or hydrodesulfurization, and has been studied extensively.[1] The basic HDS reaction converts sulfur compounds to hydrocarbons and hydrogen sulfide in a thermodynamically favored reaction. The heterogeneous commercial HDS processes occur at temperatures of 600-750 K and at pressures of 10-100 atm. The usual industrial catalyst is about 3% CoO and 12% MoO_3 on γ-alumina. The metal oxides are converted to sulfides by H_2S to produce the active catalyst. It is generally thought that the $[MoS_2]$ species are actually the active components and that the [Co] species increase the number of active sites. Despite a large amount of research on the mechanism of hydrodesulfurization, the process is still not completely understood, and the results from studies are often conflicting. As thiophene derivatives are more difficult to hydrodesulfurize than thiols, much work has focused on metal reactions of thiophenes. The mode of bonding to the catalyst and the nature of the C-S bond cleavage are two aspects that are not well understood.

Two general modes for binding thiophene to the catalyst surface have been proposed: π-coordination (either η^2-coordination through the carbon-carbon double bond, or η^4- or η^5-coordination through the entire π system) and direct η^1-bonding through the sulfur. While many studies report stable transition metal complexes of thiophene exhibiting these types of bonding,[2] studies demonstrating S-C bond cleavage are more rare. For example, Angelici and coworkers have reported evidence for insertion into a thiophene S-C bond in a π-bonded iridium complex,[3] and Jones and Dong have recently reported insertion of a metal into the C-S bond of a S-bound rhodium complex.[4] At present, however, there is very little hard evidence regarding the mechanisms of the hydrogenation steps leading to alkane and H_2S, or of the C-S bond cleavage. There is a need to develop a system that may model these processes.

A system that has proved to be particularly amenable to study a variety of fundamental organometallic transformations is that of permethyltantalocene. This system has exhibited a variety of α- and β-migratory insertion and elimination reactions of oxygen, nitrogen, and sulfur derivatives. For example, it has been shown that reactions of $Cp^*_2Ta^{III}$-R sources (e.g. $Cp^*_2Ta(=CH_2)H$) with methanol, dimethylamine, or methanethiol produce η^2-complexes with loss of RH.[5] For X = O, S, or NR, the η^2-complex is not the thermodynamically favored tautomer, as shown in Scheme 1. The complex rearranges, presumably via an insertion reaction, giving a $[Cp^*_2Ta\text{-}XCH_3]$ intermediate, followed by an α-alkyl migration to produce $Cp^*_2Ta(=X)CH_3$.

X = O, NMe, S
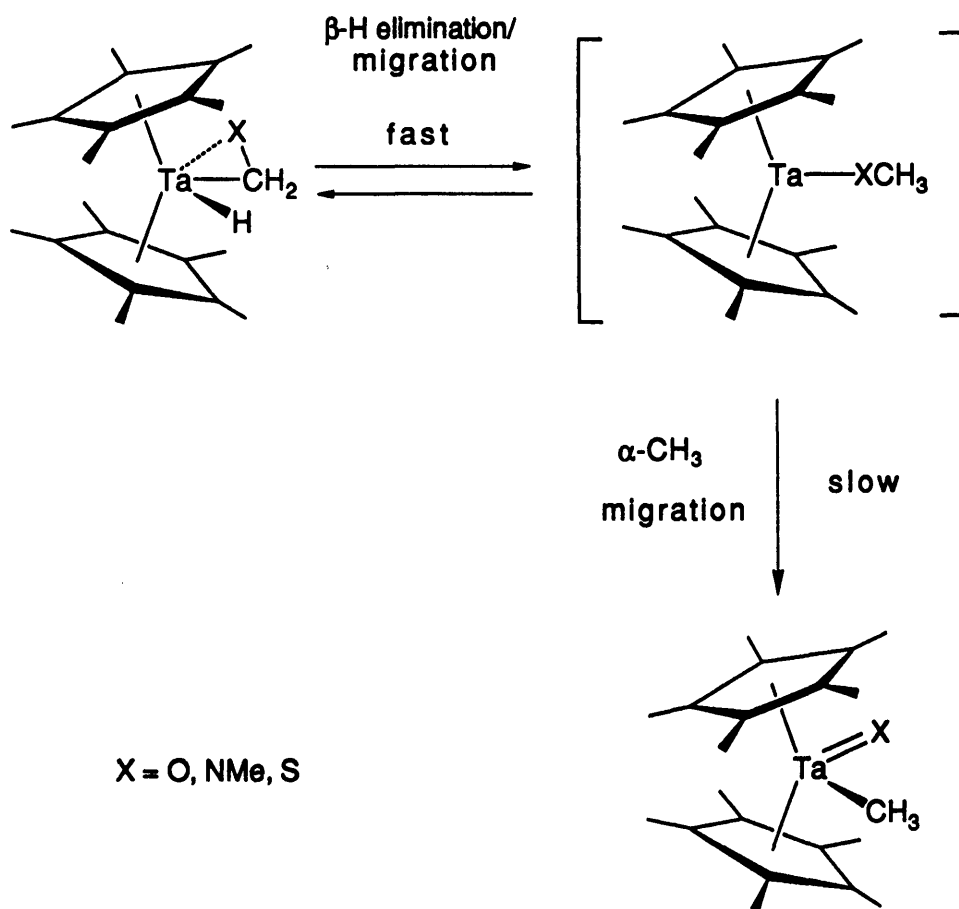
Scheme 1

These results suggest that a study of sulfur derivatives of permethyltantalocene may provide key information regarding the possible mechanisms of the HDS reaction. This chapter discusses studies of the synthesis, characterization, and reactivity of some new permethyltantalocene thioaldehyde, thiolate, and sulfido derivatives.

Results and Discussion

Synthesis of Thioaldehyde Hydride Derivatives of Permethyltantalocene.

Useful starting materials for the synthesis of a number of permethyltantalocene derivatives are [Cp*$_2$Ta-R] (R = alkyl, aryl) sources. Treatment of these complexes (Cp*$_2$Ta(η^2-C$_6$H$_4$)H was used for most of the studies) with thiols has resulted in a series of new permethyltantalocenethioaldehyde hydride complexes.

$$Cp*_2Ta(\eta^2\text{-}C_6H_4)H \ + \ RCH_2SH \ \longrightarrow \ Cp*_2Ta(\eta^2\text{-}S{=}CHR)H \ + \ C_6H_6 \tag{1}$$

$$(R = H, Ph, CH_2CH_2CH_3, CH_2Ph, CH_2C(CH_3)_3)$$
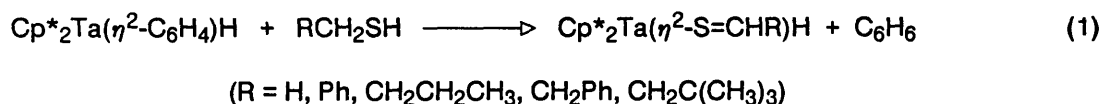
Although this type of addition was found to be unsuccessful with alcohols or amines other than methanol[6] and dimethyl amine,[7] interestingly, the reactions appear to be quite general and to proceed very cleanly with thiols. No reaction was found to occur, however, with thiophene. The reactions are carried out in toluene under an Ar atmosphere. After stirring 2-12 hours, the reaction mixtures are filtered and the products precipitated from pentane. Although NMR tube reactions proceed quantitatively, isolated yields are often lower due to high solubilities of the complexes. These complexes have been characterized by NMR (Table 1).

Structure and Bonding of Cp*$_2$Ta(η^2-S=CHCH$_2$Ph)H.

A typical permethyltantalocene thioaldehyde hydride complex, Cp*$_2$Ta(η^2-S=CHCH$_2$Ph)H, has been structurally characterized. An ORTEP drawing of the complex is shown in Figure 1. While several thioaldehyde transition metal complexes have been reported,[8] examples involving early transition metals are uncommon. To our knowledge, no other tantalum complexes thioaldehyde have been reported; the only other early transition metal examples are the zirconium complexes, Cp$_2$Zr(η^2-S=CHR) (R = Me, Ph), reported by Buchwald and coworkers,[9] and the titanium complex, Cp$_2$Ti(η^2-S=CH$_2$)(PMe$_3$), reported by Grubbs and coworkers.[10]

Figure 2 shows a drawing of the molecules packing in the unit cell of the structure. Selected bond distances and angles are given in Table 2. The [Cp*$_2$Ta] geometry is unexceptional, with a ring centroid-Ta-ring centroid angle of 139.2°. A hydrogen atom and the thioaldehyde ligand are coordinated in the wedge between the rings. The sulfur atom is in the exo position, with the carbon next to the hydride ligand in the wedge. Disorder results from the superposition of two enantiomers, with the thioaldehyde carbon C1 being the asymmetric atom. Figure 3 shows a view of the two components of the disordered structure. The two conformations are related by the approximate interchange of the sulfur and the hydrogen positions in the wedge. The major component at each site has a population of 0.68(1). Because the space group is centrosymmetric, there are equal proportions of both enantiomers in the crystal.

The bonding of the ligand to the metal center is of interest in thioaldehyde complexes. Two resonance structures, a Ta(III) π-thioaldehyde (1) and a Ta(V) thia-metalacyclopropane (2), contribute to the bonding of the complex.
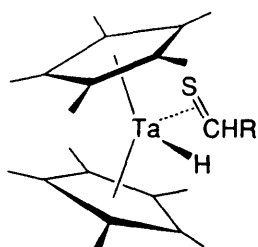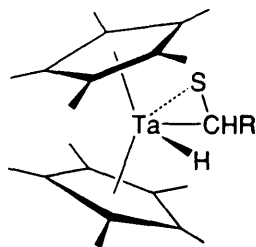
1   2

In this structure, the disorder affects the accuracy of the bond lengths and angles, those involving the S' (the minor site) being particularly unreliable. Nonetheless, the S-C1 bond lengths of 1.86(2) and 1.96(3) Å for the major and minor components strongly suggest a single bond. This compares to 1.819(3) Å for a $C(sp^3)$-S single bond, and 1.671 (24) Å for a $(X)_2$-C=S double bond, X = C, N, O, S.[11] The Ta-C1 distance of 2.28(2) Å is consistent with a single bond (2.22(4) Å for terminal Ta-CH_3)[12] as are the Ta-S and Ta-S' distances of 2.418(9) and 2.517(17) Å (compared to 2.529(3) and 2.520(3) Å for Zr-S in Buchwald's zirconium thioaldehyde complexes and to 2.452(1) Å for Ti-S in Grubbs' titanium thioformaldehyde complex). Although the disorder in the solid state structure precludes a definitive conclusion, these results suggest that the complex is primarily thia-tantalacyclopropane, **2**, in nature.

Figure 1: ORTEP Drawing of Cp*₂Ta(η^2-S=CHCH₂Ph)H
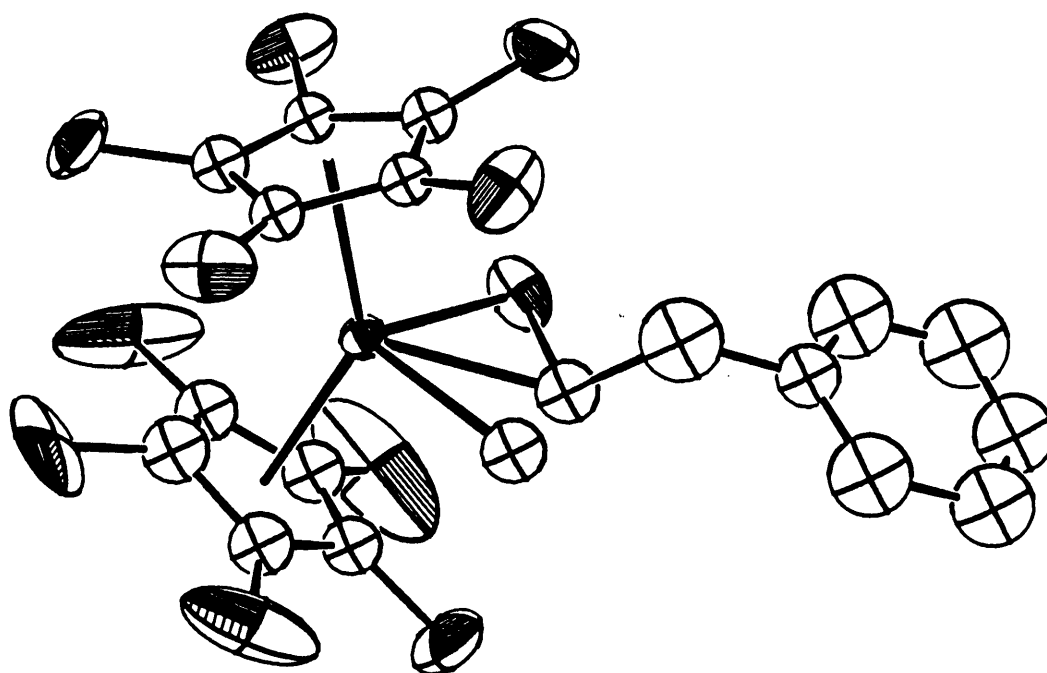
Figure 2: Crystal Packing of Cp*$_2$Ta(η^2-S=CHCH$_2$Ph)H
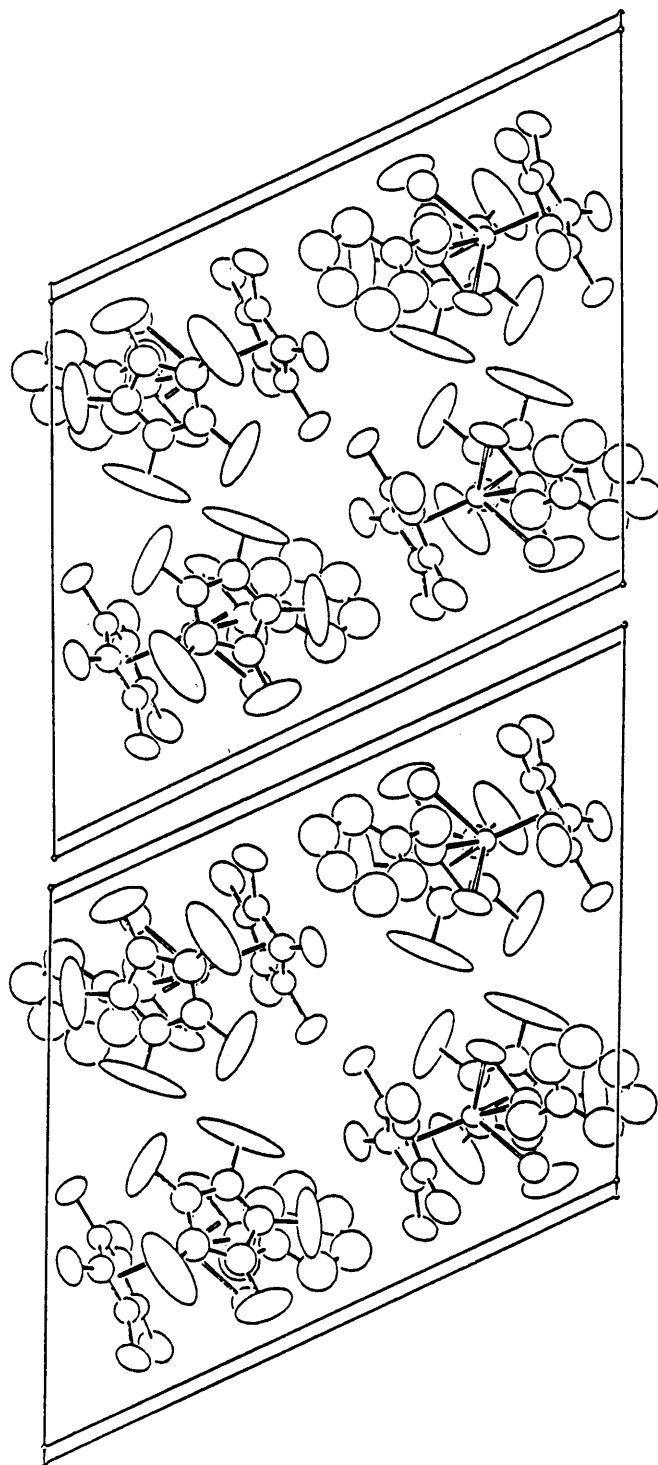
Table 2: Selected Bond Distances (Å) and Angles (°) for Cp*$_2$Ta(η^2-S=CHCH$_2$Ph)H

	Distance(Å)				Angle(°)
Ta –C1	2.28(2)	C1	–Ta –S		46.6(5)
Ta –S	2.418(9)	Ta	–S –C1		62.8(7)
S –C1	1.86(2)	S	–C1 –Ta		70.6(7)
Ta –S'	2.517(17)	C1	–Ta –S'		47.9(6)
S' –C1	1.96(3)	Ta	–S' –C1		59.7(7)
Ta –CpA‡	2.156	S'	–C1 –Ta		72.4(8)
Ta –CpB‡	2.132	Ta	–C1 –C2		128.5(16)
		S	–C1 –C2		111.2(16)
		S'	–C1 –C2		86.3(15)
		CpA‡ –Ta –S			104.5
		CpB‡ –Ta –S			104.0
		CpA‡ –Ta –S'			104.4
		CpB‡ –Ta –S'			101.9
		CpA‡ –Ta –C1			115.7
		CpB‡ –Ta –C1			105.1
		CpB‡ –Ta –CpA‡			139.2

‡ Ring centroids

Figure 3: View of the Major (68%) and Minor (32%)

Components of Cp*$_2$Ta(η^2-S=CHCH$_2$Ph)H
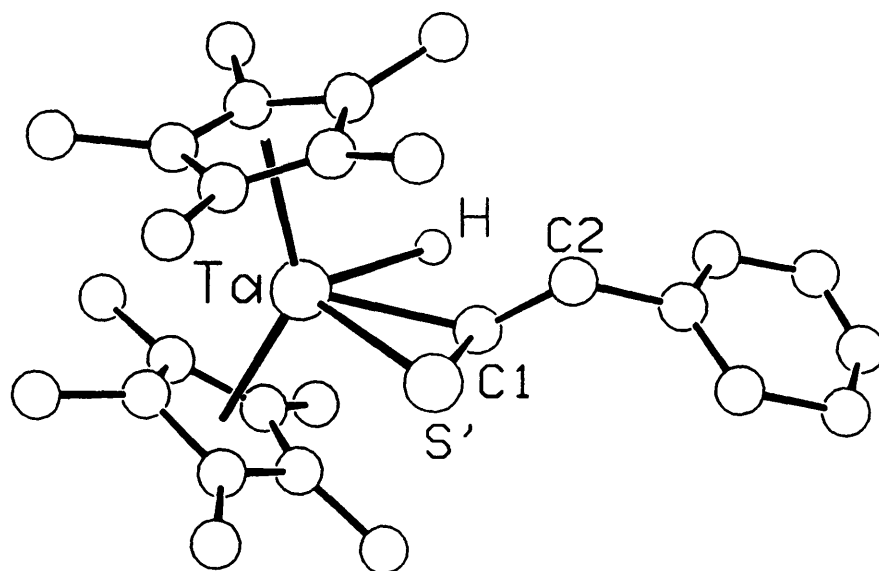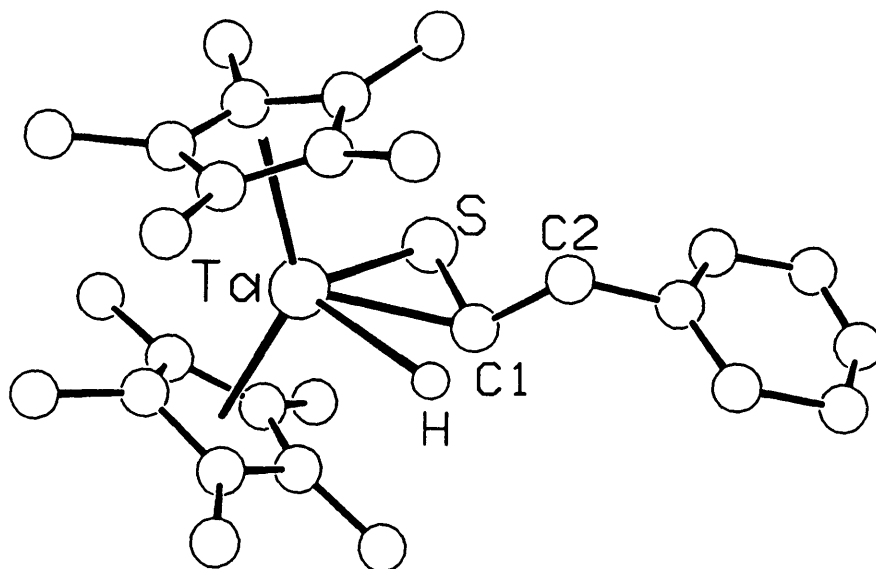
Reactivity of Permethyltantalocenethioaldehyde Hydride Complexes.

The Ta (V) thioaldehyde hydride complexes, $Cp^*_2Ta(\eta^2\text{-}S\text{=}CHR)H$, appear to be in equilibrium with Ta (III), 16 electron thiolate complexes, $[Cp^*_2Ta\text{-}SCH_2R]$.

$$Cp^*_2Ta(\eta^2\text{-}S\text{=}CHR)H \rightleftharpoons [Cp^*_2Ta\text{-}SCH_2R] \qquad (2)$$
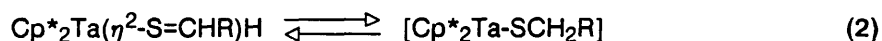
Although these 16 electron complexes are in such low concentration as to preclude direct detection or isolation, evidence supporting their presence comes from (1) reactivity studies in which they can be trapped by the addition of suitable donor ligand (L) to give isolated $Cp^*_2Ta(L)(SCH_2R)$, (2) the observation of an inverse kinetic isotope effect for the conversion of $Cp^*_2Ta(\eta^2\text{-}S\text{=}CH_2)H$ to $Cp^*_2Ta(S)CH_3$ observed by Parkin, and (3) dynamic NMR experiments. Thus, the exchange of H_A with H_B as shown in Equation 3 is observed by ^1H NMR and is interpreted as proceeding via the 16 electron thiolate intermediate in which rotation about the S-C bond renders H_A and H_B equivalent.
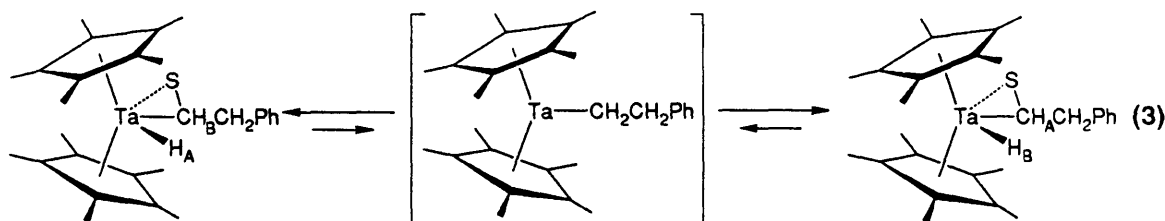
This equilibrium for $Cp^*_2Ta(\eta^2\text{-}S\text{=}CHCH_2Ph)H$ has not been studied quantitatively; however, magnetization transfer is observed at approximately 65° C, establishing an approximate activation barrier for β-hydrogen migration of 19 kcal/mol.[13]

As mentioned, these reactions of thiol with $[Cp^*_2Ta\text{-}R]$ sources are quite general. An interesting reactivity for the reaction of permethyltantalocene vinylidene hydride complex with benzyl mercaptan has been observed. The expected thioaldehyde hydride complex is not the first observed reaction product, as monitored by ^1H NMR. The reaction proceeds cleanly to give

an initial product which may be isolated by running the reaction in cold petroleum ether. ^{1}H

NMR studies show this complex to be Cp*$_2$Ta(CHCH$_2$)(SCH$_2$C$_6$H$_5$)H. Upon heating, this

thiolate intermediate eliminates ethylene and rearranges to produce the expected

permethyltantalocene thioaldehyde hydride complex.

$$(4)$$
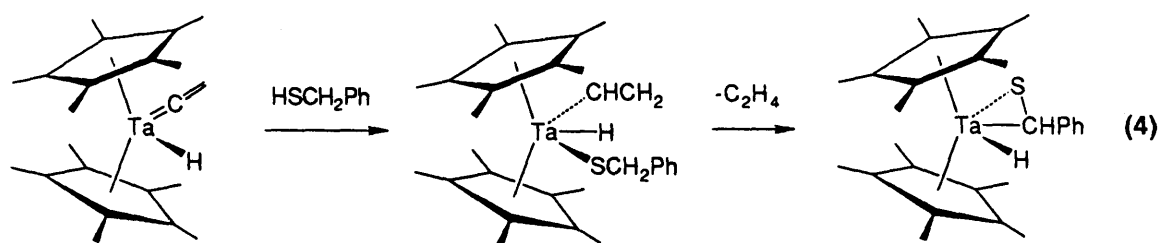
The kinetics of the ethylene loss for this reaction have been followed. The reaction is first order

with k = 3.7(4) x 10^{-5}/sec and ΔG‡ = 24(3) kcal/mol at 35° C (Figure 4).

$$y = -0.29071 - 3.6765e\text{-}5x \quad R^2 = 0.981$$
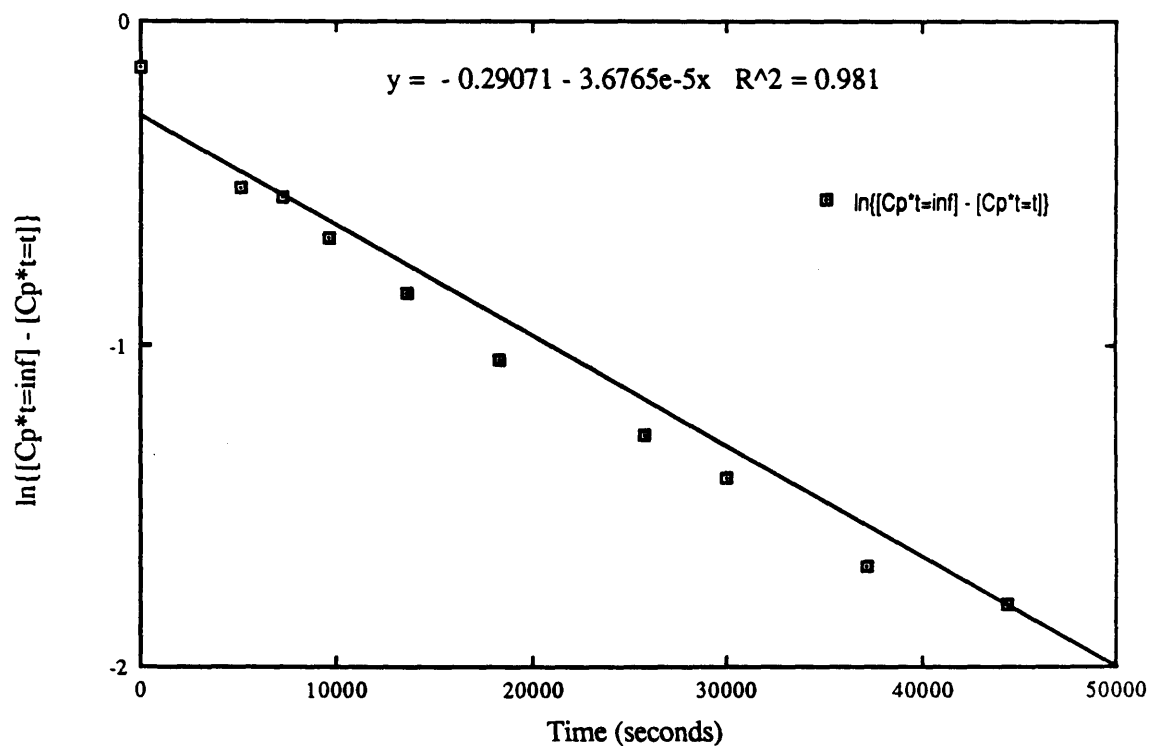
Figure 4: Kinetic Plot for Conversion of Cp*$_2$Ta(CHCH$_2$)(SCH$_2$C$_6$H$_5$)H

to Cp*$_2$Ta(η^2-S=CHC$_6$H$_5$)H

The isolation of this $Cp^*_2Ta(CHCH_2)(SCH_2C_6H_5)H$ intermediate supports a mechanism where the incoming thiol oxidatively adds to the $[Cp^*_2Ta\text{-}R]$ center. Reductive elimination of alkene generates a Ta (III) thiolate intermediate, which β-H eliminates to the thioaldehyde hydride complex (Scheme 2).
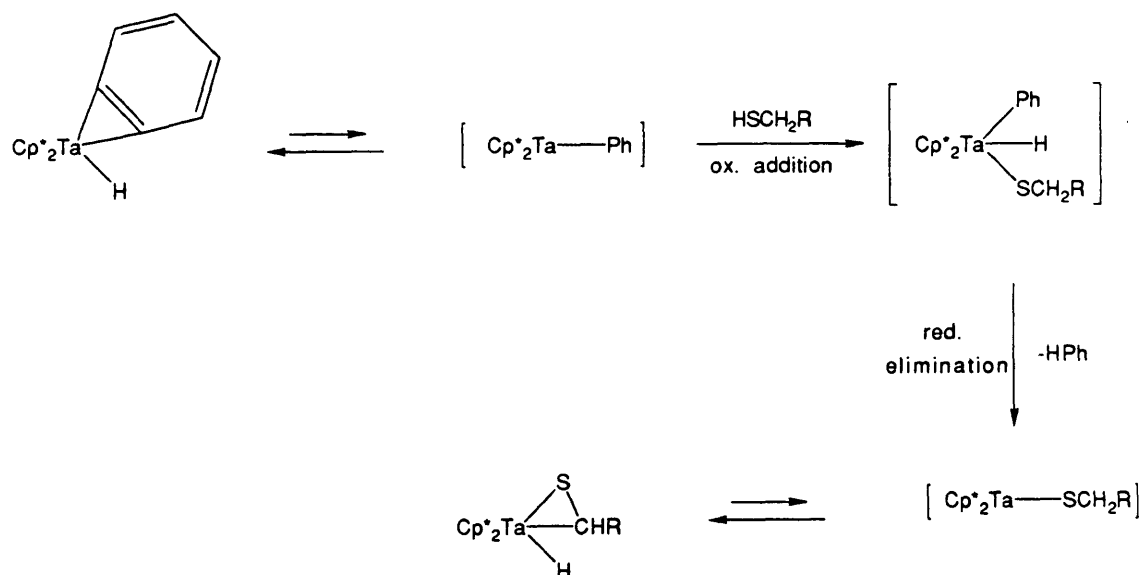
Scheme 2

These observations appear to rule out another likely mechanism for the formation of the η^2-thioaldehyde complex: coordination of the thiol through the sulfur, followed by PhH loss *via* a α-abstraction to give the Ta(III) thiolate, which β-H eliminates to give the product (Scheme 3).
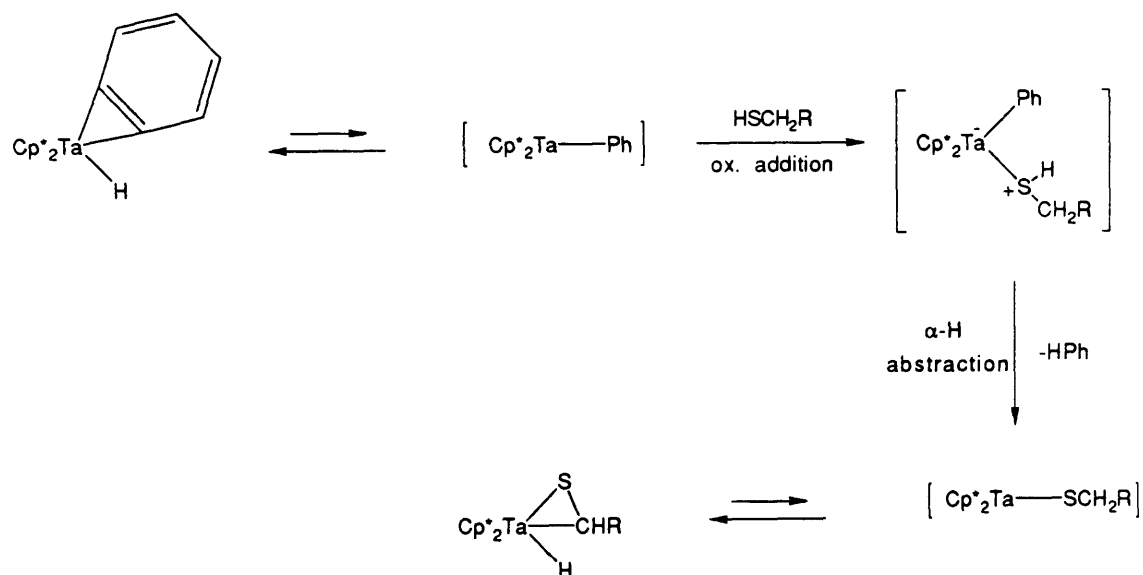
Scheme 3

Some of the reactivity of these permethyltantalocene thioaldehyde hydride complexes with other substrates has been investigated. As mentioned, they may be trapped with CO or MeNC to yield the trapped thiolate species. The permethyltantalocene thioaldehyde hydride complexes react cleanly with H_2O to produce $Cp^*{}_2Ta(=O)H$. Similar reactivity for $Cp^*{}_2Ta(=S)H$ and $Cp^*{}_2Ta(=NR)H$ (R = H. Ph) complexes has been explored by St. Clair.[7]

Many of the permethyltantalocene thioaldehyde hydride complexes react with excess thiol to produce the permethyltantalocene dithiolate hydride complexes, 3. These dithiolate complexes are not formed in the reaction with excess benzyl mercaptan, presumably for steric reasons. Although these dithiolate complexes have not been isolated, ^1H NMR data are given in Table 1.
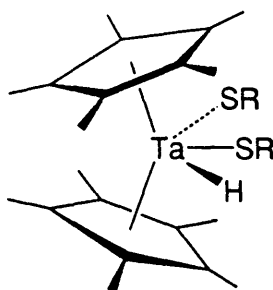
3

Thermal Chemistry of Thioaldehyde Hydrides.

Upon heating, the permethyltantalocene thioaldehyde hydride complexes undergo an α-alkyl migration to the thermodynamic product.

$$Cp^*{}_2Ta(\eta^2\text{-}S=CHR)H \longrightarrow Cp^*{}_2Ta(=S)CH_2R \qquad (5)$$

The permethyltantalocene sulfido alkyls may also be prepared by direct transfer of sulfur to a Ta(III) source. Based on similar chemistry with ethylene oxide,[14] [Cp*$_2$Ta-R] sources have been treated with ethylene sulfide to produce the tantalum sulfido alkyl products as monitored by ^{1}H NMR.[15]

$$Cp*_2Ta(\eta^2\text{-}C_6H_4)H \ + \ \overline{SCH_2CH_2} \ \longrightarrow \ Cp*_2Ta(=S)C_6H_5 \ + \ C_2H_4 \qquad (6)$$

$$Cp*_2Ta(\eta^2\text{-}CH_2=CHC_6H_5)H \ + \ \overline{SCH_2CH_2} \ \longrightarrow \ Cp*_2Ta(=S)CH_2CH_2C_6H_5 \ + \ C_2H_4 \qquad (7)$$
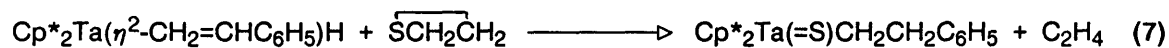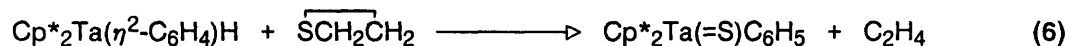
Stereochemistry of the α-Migration.

An investigation of the mechanism of the rearrangement from the permethyltantalocene thioaldehyde hydride to the permethyltantalocene sulfido alkyl is important to better understand this rare example of S-C bond cleavage. In order to determine the mechanism of the α-alkyl elimination of the permethyltantalocene thioaldehyde hydride complexes, it is important to ascertain the stereochemistry at carbon for the migration. Examination of diastereomeric organometallic compounds by using NMR to probe the relative stereochemistry has been thoroughly developed.[16] The $^3J_{H\text{-}H}$ coupling constants for *erythro-* and *threo-d$_2$* derivatives are particularly distinctive. Thus, diastereotopically labeled thiols have been prepared for use as NMR probes in this migration.

Although the derivatives derived from neohexyl mercaptan can be prepared, the reaction of neohexyl mercaptan with the permethyltantalocene starting materials is not as clean as with other thiols. Even under varied reaction conditions (diluting the reactants, using different [Cp*$_2$Ta-R] sources, lowering reaction temperatures), contamination with a small amount of permethyltantalocene dithiolate hydride complex, which made the NMR spectrum

complicated, is always observed. Therefore, analogous derivatives derived from phenethyl

mercaptan were chosen as the diastereomeric probes since $PhCH_2CH_2SH$ reacts very cleanly

with the [Cp^*_2Ta-R] sources. Initial attempts to prepare pure *erythro-* and *threo-d_2* labeled

derivatives for phenethyl mercaptan using established routes[17] failed. (The results of this have

been published,[18] and will be discussed in detail in Chapter 2.) Therefore, another route to the

diastereomeric thiols has been developed. The synthetic strategy is shown in Scheme 4.
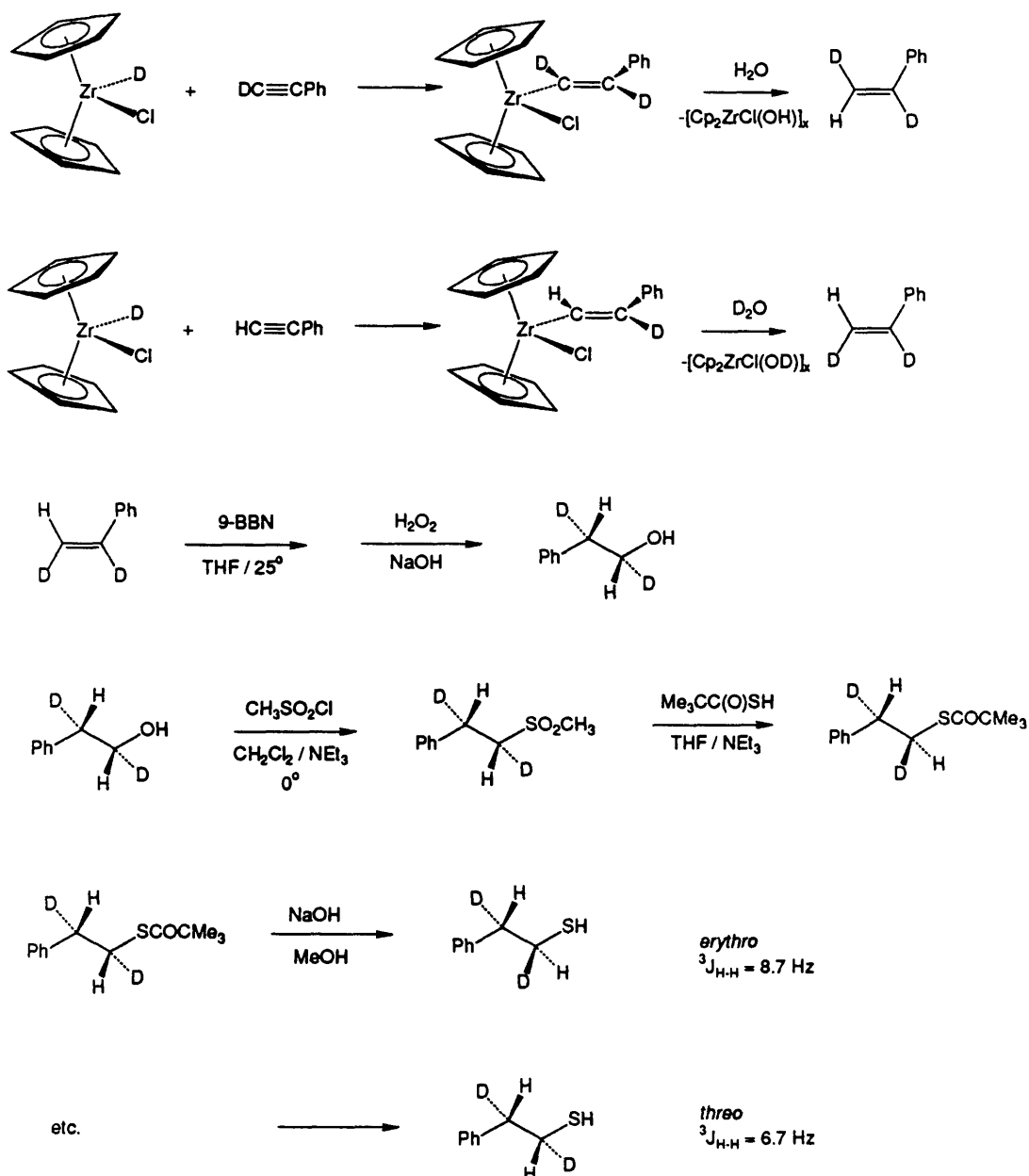
Scheme 4

Cis- and *trans*-styrene-d_2 are cleanly prepared by hydrozirconation of phenylacetylene or deuterophenylacetylene. Hydroboration is used to convert the olefin to the *erythro-* or *threo-* phenethyl alcohol. 9-BBN was chosen as the hydroborating reagent as it adds to hindered alkenes with much greater selectivity than is observed with other hydroborating reagents.[19] The alcohol is treated with methylsulfonylchloride to produce the mesolate derivative, which is then treated with thiopivalic acid to yield the pivalate. Although this step goes with inversion of stereochemistry, the resulting complex is still diastereotopically pure. All other steps in this sequence proceed with retention of stereochemistry. Finally, the pivalate is cleaved in the presence of base to yield the labeled phenethyl mercaptan. In isolating the thiol, it is important to neutralize the reaction mixture at this point before exposure to air as thiols tend to form disulfides in the presence of base. Table 3 shows the $^3J_{H-H}$ coupling constants for the *erythro* and *threo* derivatives.

Table 3: $^3J_{H-H}$ **Coupling Constants (in Hz) for** *Erythro-* **and** *Threo-* **Phenethyl-**d_2 **Derivatives**

Compound (R = CHDCHDPh)	*Erythro*	*Threo*
ROH	7.2	5.7
RSC(O)C(CH₃)₃	9.0	5.9
RSH	8.7	6.7
Cp*₂Ta(=S)R	12.7	3.4

Cp*₂Ta(η^2-C₆H₄)H was treated with the diastereotopic thiols to produce the corresponding permethyltantalocene thioaldehyde hydride complexes. The rearrangement to the sulfido alkyl was followed by ^{1}H NMR. The migration proceeds predominantly (c. a. 85%) with retention of stereochemical identity. However for each case, a moderate amount of the opposite diastereomer is produced. This is clear from the ^{1}H NMR spectra shown in Figure 5.

Thus, although the migration goes primarily with retention of stereochemistry at carbon, the source of the moderate epimerization has been investigated. To try to establish whether the label loss occurs before migration, the *erythro* and *threo* derivatives of d_2-Cp*₂Ta(η^2-S=CHCH₂Ph)H have been trapped with methylisonitrile to produce the *erythro* and *threo* Cp*₂Ta(SCHDCHDPh)(CNMe). Unfortunately, these diastereomeric complexes, unlike the permethyltantalocene sulfido alkyls, do not have sufficiently different chemical shifts to cleanly resolve the mixtures, and the *erythro* and *threo* coupling constants are too similar to determine if a small amount of the other diastereomer is present.

Figure 5: ^{1}H NMR of Alkyl Region of *Erythro-* and *Threo*-Cp*$_2$Ta(=S)CHDCHDPh

threo

$^3J_{HH}$ = 3.4 Hz

erythro

$^3J_{HH}$ = 12.7 Hz

.7
PPM
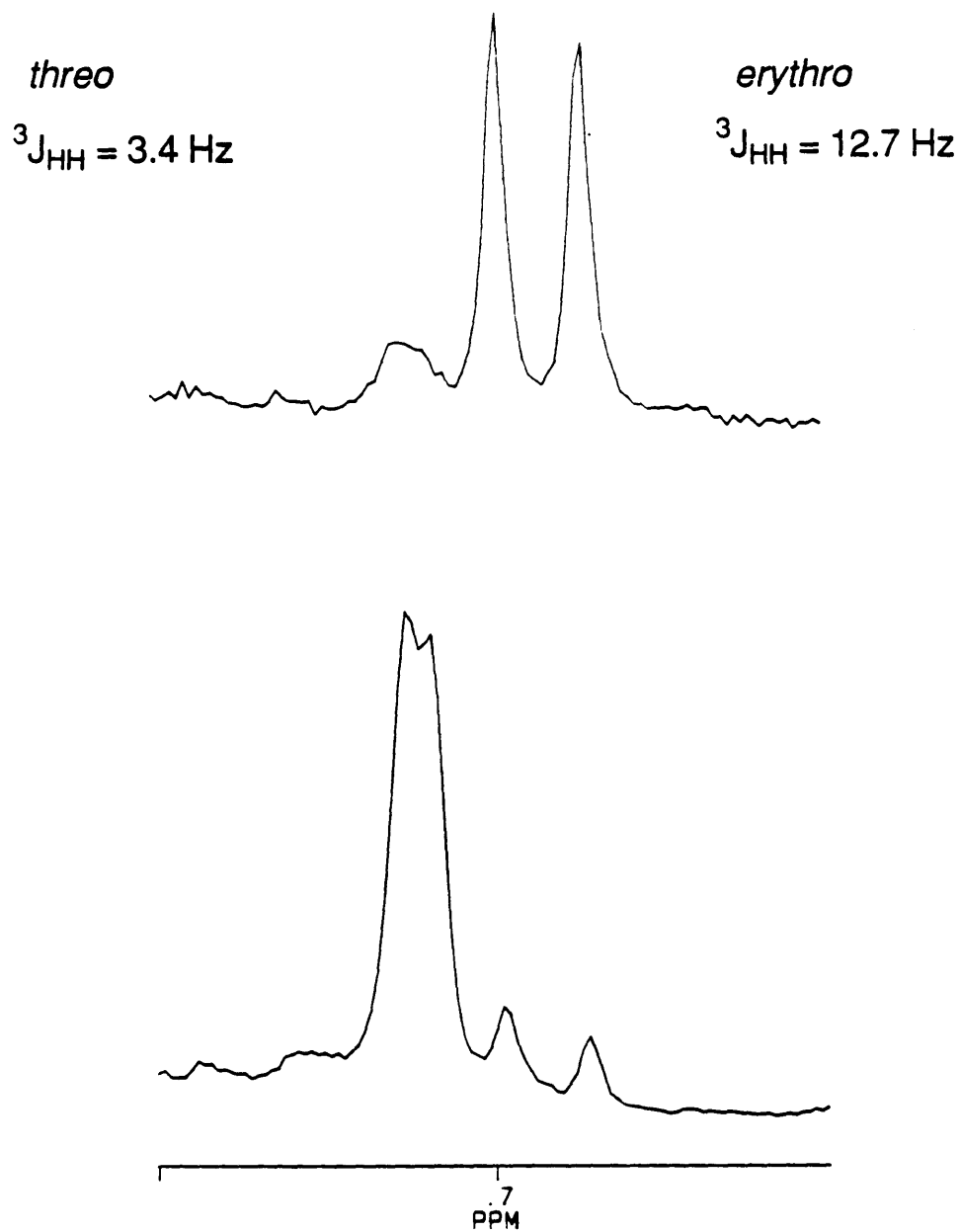
This result led us to investigate the purity of the starting *erythro* and *threo* phenethyl mercaptans. Although the ^{1}H NMR spectra looked pure for each diastereomer, the ratio of components could not be determined for a sample made with 70:30 *erythro:threo* phenethyl mercaptan. Even using ^{2}H decoupled ^{1}H NMR techniques, the mixed sample appeared to have an averaged $^3J_{H-H}$ coupling rather than showing two distinct sets of doublets for the two diastereomers. The ^{1}H decoupled ^{13}C NMR spectra were examined for the thiols to see if perhaps a difference in chemical shifts could be seen for the diastereomers. Unfortunately, again the patterns showed the identical chemical shift within the resolution of the instrument, and no further information could be obtained. Therefore, we cannot say that the approximately 15% label loss is not present in the starting thiols.

It is also possible a side reaction occurring around the migration temperature is responsible for the label loss. An important resonance structure for these thioaldehyde complexes is the π-thioaldehyde coordination of the ligand. Rotation of the thioaldehyde ligand to coordinate the opposite face, possibly utilizing the lone pairs of electrons on sulfur, would explain scrambling as shown in Scheme 5.

Therefore, the migration reaction was run at two different temperatures to see if this possible side reaction could be "shut down." At 122° C, the ratios of diastereomers in the products were 84:16 and 83:17 for two runs. At 96° C, the ratios of diastereomers in the products were 86:14 and 88:12 for two runs. Although the amount of label loss is slightly lower for the migration at the lower temperature, it is not significant enough to draw any solid conclusions about this mechanism for label loss.
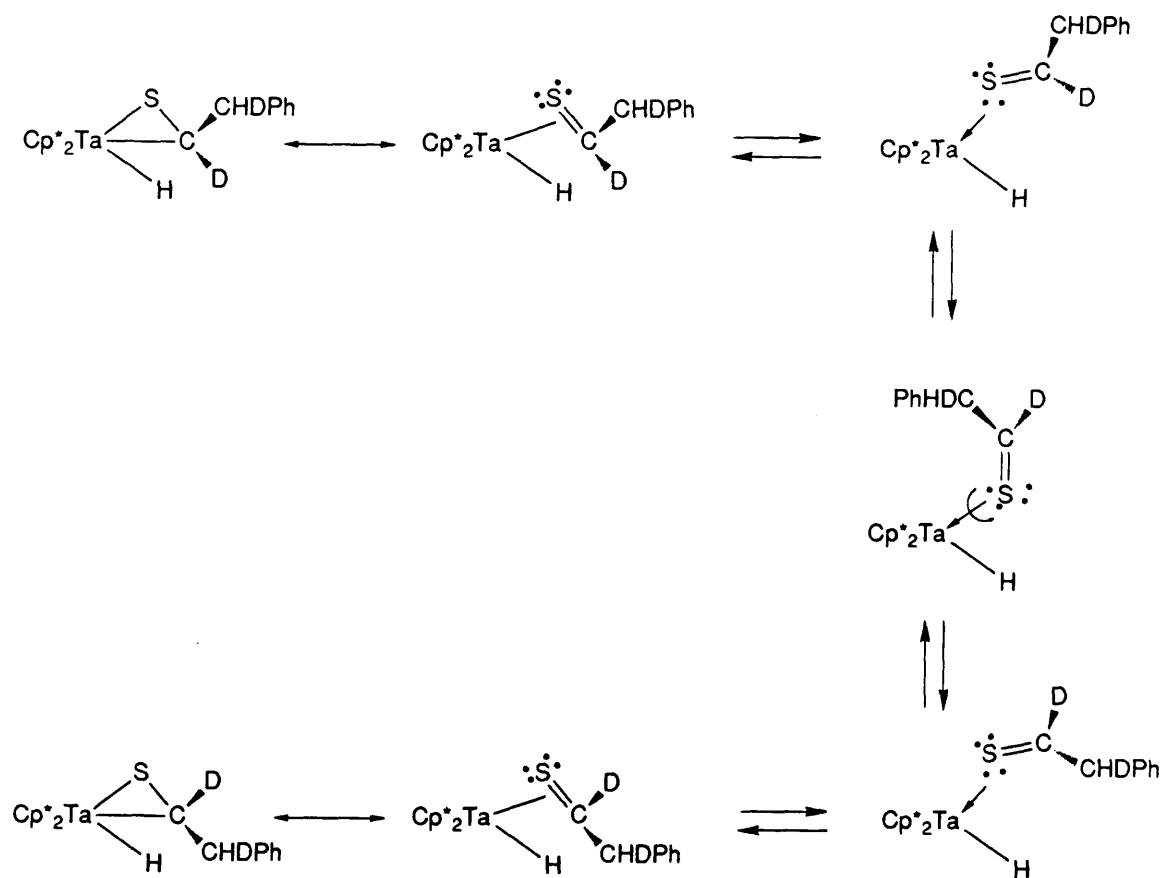
Scheme 5

In regard to the mechanism of the S-C bond cleavage from the permethyltantalocene thioaldehyde hydride to the permethyltantalocene sulfido alkyl, it is strongly implied from deuterium isotope effects that the migration involves the pre-equilibrium of a 16 electron thiolate intermediate. The α-migration from this thiolate intermediate occurs with retention of stereochemical identity at carbon, possibly with some unexplained loss of label. If a free radical process is involved in this migration, any free radical intermediate must be extremely short lived.

Reactivity of the Permethyltantalocene Sulfido Hydride and Alkyl Derivatives.

Photolysis of the $Cp*_2Ta(=S)Me$ complex has been shown by Parkin to yield the permethyltantalocene thioaldehyde hydride complex, along with decomposition products.[20] This result, however, is not observed for other permethyltantalocene sulfido alkyl derivatives. Photolysis leads only to unidentified decomposition, presumably to "tuck-in" products. Interestingly, photolysis of $Cp*_2Ta(=O)Me$ as well leads to only decomposition products.[21] It is not clear what makes the permethyltantalocene sulfido methyl complex unique in this regard.

Permethyltantalocene sulfido hydride showed no reactivity towards H_2, even at elevated temperature and pressure. This result is not surprising in light of the oxophilic, hence sulfophilic, character of these early transition metal complexes. In fact, $Cp*_2TaH_3$ reacts with H_2S at room temperature to give the permethyltantalocene sulfido hydride complex.

$$Cp*_2Ta(=S)H \ + \ H_2 \ \longrightarrow \ \text{no reaction} \qquad (8)$$

$$Cp*_2TaH_3 \ + \ H_2S \ \longrightarrow \ Cp*_2Ta(=S)H \ + \ H_2 \qquad (9)$$

In light of these results, the use of these permethyltantalocene complexes to effect hydrodesulfurization in a catalytic manner is doubtful. One observation is particularly encouraging: $Cp*_2Ta(=S)Me$ reacts with H_2, albeit slowly, at elevated temperatures and pressures to produce the permethyltantalocene sulfido hydride and liberate methane.

$$Cp*_2Ta(=S)Me \; + \; H_2 \; \longrightarrow \; Cp*_2Ta(=S)H \; + \; CH_4 \qquad\qquad (10)$$

This result led to the proposal of a catalytic cycle containing the features of hydrodesulfurization

(i.e., RSH + H_2 ————————▷ H_2S + RH) involving a tantalum sulfido species (Scheme 6).
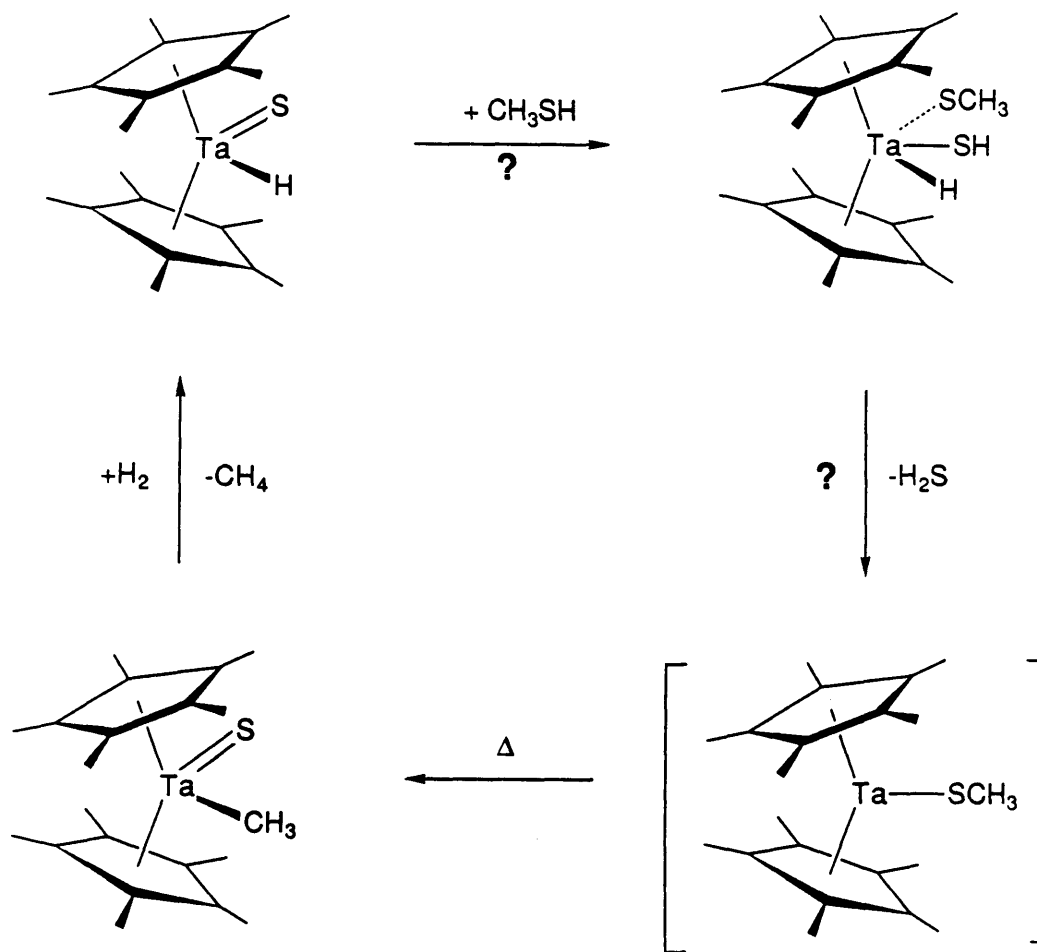
Scheme 6

The cycle involves four fundamental steps. First, a 1,2 addition of thiol to the $Cp*_2Ta(=S)H$ complex must occur. These 1,2 addition reactions have been shown to be facile for similar $Cp*_2W=O$ systems.[22] Second, a reductive elimination of H_2S must occur to yield the thiolate complex. Third, the thiolate complex, in equilibrium with the permethyltantalocene thioaldhyde hydride, must undergo S-C bond cleavage. This has been shown to occur in this system. Finally, hydrogenation of the sulfido alkyl to liberate alkane and regenerate the sulfido hydride completes the catalytic cycle. Unfortunately, no reactivity for the $Cp*_2Ta(=S)H$ is observed with thiols, so this cycle has not been realized.

Conclusions

Attempts to extend the synthetic methodology for the preparation of permethyltantalocene thioaldehyde hydride complexes has been successful. Permethyltantalocene benzyne hydride has served as an excellent starting material to cleanly generate a number of these complexes. One of these, $Cp^*_2Ta(\eta^2\text{-}S{=}CHCH_2Ph)H$, has been crystallographically characterized. The solid state structure indicates the complex is primarily thia-metalacyclopropane in nature.
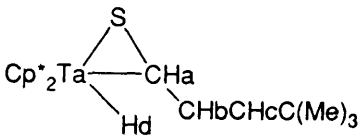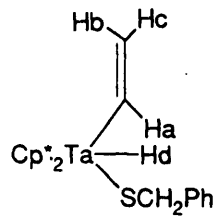
The permethyltantalocene thioaldyhyde hydride complexes are shown to be in equilibrium with a tantalum (III) thiolate complex through a β-H elimination/migration process. These thiolate complexes are reactive towards a number of substrates, including CO, isonitriles, water, and additional thiol.

The permethyltantalocene thioaldyhyde hydride complexes undergo a rare sulfur carbon bond cleavage step to form the thermodynamically favored structure, the permethyltantalocene sulfido alkyl. Stereochemical studies have shown this α-alkyl migration to proceed primarily with retention of stereochemistry. While it is disappointing that no catalytic behavior with respect to hydrodesulfurization is observed for the system, information about a very key step in that catalytic cycle, namely S-C bond cleavage, has been obtained.

Table 1: Summary of ^{1}H and ^{13}C NMR Data[a]

Compound	Assignment	δ (ppm)	J (Hz)
Cp*$_2$Ta(η^2-S=CH$_2$)H	(η^5-C$_5$(CH$_3$)$_5$)	1.72 s	
	S=CH$_2$	1.70 d	$^4J_{H\text{-}H}$ = 3
	Ta-H	0.39 br t	
	(η^5-C$_5$(CH$_3$)$_5$)	11.9 q	$^1J_{C\text{-}H}$ =126
	(η^5-C$_5$(CH$_3$)$_5$)	106.6 s	
	S=CH$_2$	40.2 dt	$^1J_{C\text{-}H}$ = 155, $^2J_{C\text{-}H}$ = 10
Cp*$_2$Ta(η^2-S=CHC$_6$H$_5$)H	(η^5-C$_5$(CH$_3$)$_5$)	1.71 s	
		1.55 s	
	CHC$_6$H$_5$	7.76 d	7.8
		7.27 t	7.6
		7.01	
	SCH	b	
	Ta-H	c	
	(η^5-C$_5$(CH$_3$)$_5$)	11.4	
	(η^5-C$_5$(CH$_3$)$_5$)	11.7	
	(η^5-C$_5$(CH$_3$)$_5$)	108.1	
	(η^5-C$_5$(CH$_3$)$_5$)	108.3	
	CHC$_6$H$_5$	58.2	
	CHC$_6$H$_5$	123.1	
		127.1	
		129.2	
		151.4	
Cp*$_2$Ta(η^2-S=CHCH$_2$C$_6$H$_5$)H	(η^5-C$_5$(CH$_3$)$_5$)	1.64 s	
		1.80 s	
	H$_a$	2.2 m	J$_{ab}$= 10.8
	H$_b$	3.0 dd	J$_{bc}$= 14.2
	H$_c$	3.8 dd	J$_{ac}$= 3.1
	Ta-H$_d$	1 br s	J$_{ad}$= 1.17
	CHCH$_2$C$_6$H$_5$	6.9-7.8 m	
	(η^5-C$_5$(CH$_3$)$_5$)	11.4	
		12.2	
	(η^5-C$_5$(CH$_3$)$_5$)	107.3	
		108.5	
	S=CH	48.4	
	CH$_2$C$_6$H$_5$	60.7	
	CHC$_6$H$_5$	125.5	
		128.9	
		d	
Cp*$_2$Ta(η^2-S=CHCH$_2$CH$_2$CH$_3$)H	(η^5-C$_5$(CH$_3$)$_5$)	1.78 s	
	(η^5-C$_5$(CH$_3$)$_5$)	1.70 s	
	Ta-H$_d$	b	
	CH$_2$CH$_2$CH$_3$	f	

Structure (for Cp*$_2$Ta(η^2-S=CHCH$_2$C$_6$H$_5$)H):

Cp*$_2$Ta bonded to S and CHa in a three-membered ring, with Hd bridging, and CHa bearing CHbCHcPh.

Cp*$_2$Ta(η^2-S=CHCH$_2$C(CH$_3$)$_3$)H	(η^5-C$_5$(CH$_3$)$_5$)	1.78 s	
	(η^5-C$_5$(CH$_3$)$_5$)	1.70 s	
	C(CH$_3$)	1.33 s	
	H$_a$	1.93 m	J$_{ab}$ = 11.6
	H$_b$	1.55 dd	J$_{bc}$ = 13.7
	H$_c$	2.45 dd	J$_{ac}$ = 1.8
	Ta-H$_d$	0.64 br	
	(η^5-C$_5$(CH$_3$)$_5$)	11.3	
	(η^5-C$_5$(CH$_3$)$_5$)	12.1	
	(η^5-C$_5$(CH$_3$)$_5$)	106.8	
	(η^5-C$_5$(CH$_3$)$_5$)	107.9	
	S=CH	51.8	
	CH$_2$C(CH$_3$)$_3$	56.6	
	CH$_2$C(CH$_3$)$_3$	30.3	

Cp*$_2$Ta(CHCH$_2$)(SCH$_2$C$_6$H$_5$)H[e]	(η^5-C$_5$(CH$_3$)$_5$)	1.76 s	
	H$_a$	6.80 m	J$_{ab}$= 12.4
	H$_b$	6.38 m	J$_{ac}$= 18.0
	H$_c$	6.14 dd	J$_{bc}$= 3.2
	CH$_2$C$_6$H$_5$	3.99 s	
	CH$_2$C$_6$H$_5$	7.69 d	6.9
		7.28 dd	7.5
		7.12 dd	7.4
	Ta-H$_d$	7.95 d	J$_{ad}$= 9.1
	(η^5-C$_5$(CH$_3$)$_5$)	11.58 q	127
	(η^5-C$_5$(CH$_3$)$_5$)	108.97 s	
	CH$_2$C$_6$H$_5$	49.1 t	138
	CHC$_6$H$_5$	108.0 d	41.1
		149.8 s d	
	CHCH$_2$	179.1 d	123
	CHCH$_2$	117.9 t	152

Cp*$_2$Ta(=S)H	(η^5-C$_5$(CH$_3$)$_5$)	1.97 s	
	Ta-H	8.05 s	
	(η^5-C$_5$(CH$_3$)$_5$)	13.1 q	^{1}J$_{C-H}$ =127
	(η^5-C$_5$(CH$_3$)$_5$)	114.6 s	

Cp*$_2$Ta(=S)CH$_3$	(η^5-C$_5$(CH$_3$)$_5$)	1.81 s	
	CH$_3$	-0.02 s	
	(η^5-C$_5$(CH$_3$)$_5$)	12.7 q	^{1}J$_{C-H}$ = 126
	(η^5-C$_5$(CH$_3$)$_5$)	116 s	
	CH$_3$	24.6 q	^{1}J$_{C-H}$ = 124

Cp*$_2$Ta(S)C$_6$H$_5$	(η^5-C$_5$(CH$_3$)$_5$)	1.77 s	
	C$_6$H$_5$	6.52-7.71 m	

Cp*$_2$Ta(S)CH$_2$C$_6$H$_5$	(η^5-C$_5$(CH$_3$)$_5$)	1.77 s	
	C$_6$H$_5$	7.43 d	7.6
		7.21 t	7.5
		6.94 t	7.2
	CH$_2$	b	

$Cp*_2Ta(S)CH_2CH_2C_6H_5$	$(\eta^5\text{-}C_5(CH_3)_5)$	1.83 s
	$CH_2CH_2C_6H_5$	0.79 m
AA'XX' pattern	$CH_2CH_2C_6H_5$	2.92 m
	$CH_2CH_2C_6H_5$	6.8-7.8m
$Cp*_2Ta(S)CH_2CH_2C(CH_3)_3$	$(\eta^5\text{-}C_5(CH_3)_5)$	1.85 s
	$CH_2CH_2C(CH_3)_3$	0.45
AA'XX' pattern	$CH_2CH_2C(CH_3)_3$	b
	$CH_2CH_2C(CH_3)_3$	1.02
$Cp*_2Ta(SCH_2CH_2C(CH_3)_3)_2H$	$(\eta^5\text{-}C_5(CH_3)_5)$	1.92 s
	$CH_2CH_2C(CH_3)_3$	f
	$CH_2CH_2C(CH_3)_3$	1.01
		1.05
	H	b
$Cp*_2Ta(SCH_2CH_2Ph)_2H$	$(\eta^5\text{-}C_5(CH_3)_5)$	1.83 s
	CH_2CH_2Ph	3.05-3.30 f
	CH_2CH_2Ph	7.0-7.2 f
	H	b
$Cp*_2Ta(SCH_3)_2H$	$(\eta^5\text{-}C_5(CH_3)_5)$	1.85 s
	CH_3	
	H	
$Cp*_2Ta(SCH_2CH_2Ph)(CNMe)$	$(\eta^5\text{-}C_5(CH_3)_5)$	1.79 s
	CH_2CH_2Ph	2.93 dd
	CH_2CH_2Ph	3.19 dd
	Ph	f
	Me	3.10 s

(a) NMR spectra in benzene-d_6 at ambient temperature unless noted. Chemical shifts are reported in ppm (δ) from tetramethylsilane added as an internal reference or to residual proton in solvent. Coupling constants reported in Hz. (b) Resonance not found. (c) Peak assumed to be under Cp* resonance. (d) Remainder of phenyl resonances hidden under solvent or not assigned. (e) Spectrum in toluene-d_8. (f) Resonances not well enough resolved to make definite assignments.

Experimental Section

General Considerations. All air sensitive manipulations were performed by using high vacuum line or glovebox techniques.[23] Argon, hydrogen, and nitrogen gases were purified by passage over MnO on vermiculite and activated 4 Å molecular sieves. Solvents were dried over CaH_2, $LiAlH_4$ or Na/benzophenone and stored under vacuum over "titanocene"[24] or sodium benzophenone ketyl. Solvents for organic work up and purification were reagent grade and used as received unless otherwise noted. Benzene-d_6 was dried over activated 4 Å sieves and stored over titanocene.

Starting Materials. Hydrogen sulfide, methanethiol, $DSCD_3$, butanethiol, thiophenol, benzylmercaptan, phenethyl mercaptan, ethylene sulfide, styrene, neohexyl alcohol, triphenyl phosphene, Br_2, potassium thioacetate, phenylacetylene, n-butyl lithium (1.6 M in hexanes), thiopivalic acid, methylsulfonylchloride, and Cp_2ZrCl_2 were commercially available and used without further purification. (**Caution: H_2S is extremely toxic.**) Triethylamine was dried over CaH_2 and distilled prior to use. Methylisonitrile was vacuum transferred and stored over molecular sieves prior to use. $LiAlH_4$ and $LiAlD_4$ (Aldrich, received as a grey powder) were dissolved in ether, the solutions filtered, and the solvent removed *in vacuo* to yield a white ether-soluble powder. $Cp*_2TaCl_2$ and $Cp*_2TaH_3$ were prepared as previously reported.[25] $Cp*_2Ta(=CCH_2)H$ was prepared according to published procedure.[26] $Cp*_2Ta(\eta^2-C_6H_4)H$ was prepared as described elsewhere.[27] Cp_2ZrHCl and Cp_2ZrDCl were prepared according to Buchwald's published procedure[28] with the following modifications: (1) $LiAlH_4$ and $LiAlD_4$ were *always* isolated from ether and redissolved before use and (2) the entire procedure was done in a glovebox, thus eliminating cannula filtration and slow line filtration.

Spectra. ^{1}H NMR spectra were recorded with Varian EM-390 (90 MHz), JEOL FX90Q (89.56 MHz), JEOL GX400 (400 MHz), and Bruker WM500 (500.13 MHz) spectrometers. [13]C spectra were recorded on a Bruker WM500 (125.767 MHz) spectrometer. [2]H spectra were recorded on a Bruker WM500 (76.775 MHz) spectrometer. IR spectra were obtained on a Beckman 4240 spectrometer as Nujol mulls. Elemental analyses were performed by the analytical services at C.I.T.

Procedures. Many of the reactions reported were carried out in septum-capped NMR tubes. Approximately 15 mg of $Cp^*_2Ta(\eta^2\text{-}C_6H_4)H$, or other [$Cp^*Ta$-R] starting material, was dissolved in 0.4 ml of C_6D_6 and capped with a rubber septum. Known amounts of the appropriate reagent were syringed in through the septum, and the reaction was followed by NMR. For reactions that needed to be monitored longer than two days, starting material and solvent were added to a sealable tube in the glovebox. The reagents were syringed in against an Ar counterflow or condensed in from a calibrated gas bulb. The tube was sealed and the reaction monitored by NMR.

$(CH_3)_3CCH_2CH_2Br$. Neohexanol (8.44 g, 0.083 mol) and PPh_3 (22 g, 1.1 eq) was added to 100 mL DMF under N_2. After stirring until dissolved, Br_2 (4 mL) was added dropwise over 20 minutes until the orange color persisted. This solution was stirred for 2 hr and the alkyl bromide was vacuum distilled. The distillate was extracted into ether and washed with three 50 mL portions of water. The ether was removed *in vacuo*, yielding 5.80 g (43%) neohexyl bromide.

^{1}H NMR Data (C_6H_6, 25° C): δ 0.61 (s, 3 H, CH_3), δ 1.61 (t, 2 H, CH_2), δ 3.02 (t, 2 H CH_2).

(CH₃)₃CCH₂CH₂SH. Neohexyl bromide (8.3 g, 0.050 mol) and potassium thioacetate (5.7 g, 0.050 mol) were dissolved in 25 mL absolute ethanol and refluxed for 2 hr under N_2. KOH (10 g) in 25 mL H_2O was added and the mixture stirred for 1 hour under N_2. After neutralization with glacial acetic acid, the product was extracted into ether and washed with three 50 mL portions of water. The ether was removed *in vacuo*, and the product was distilled and dried over calcium sulfate to yield 5.2 g (0.044 mol, 88%) thiol.

Anal. Calcd. for $C_6H_{14}S$: C, 60.95; H, 11.93. Found: C, 61.33; H, 11.22.

^{1}H NMR Data (C_6H_6, 25° C): δ 0.68 (s, 3 H, CH_3), δ 1.32 (m, 2 H, CH_2), δ 2.15 (m, 2 H CH_2), δ 1.07 (t, 1 H, SH).

PhCH₂CH₂OH. Styrene (2.0 mL, 17 mmol) was added *via* syringe against an Ar counterflow to a 3 neck round bottom flask. 9-BBN (2.1 g, 17 mmol, suspended in 40 mL THF) was added over a 30 min period. The solution was stirred for 2 hr. H_2O (2 mL) and NaOH (5.8 mL, 3 M) were added *via* syringe, followed by the slow addition of H_2O_2 (5.8 mL, 30 %). The solution was stirred 3 hr and quenched with sat. NaCl solution. The water phase was extracted with 50:50 EtOAc/hexanes and the combined organic phases were dried over $MgSO_4$. The solution was reduced in volume to 50 mL. (CAUTION: To avoid a potential explosion due to peroxides in the solution, 10 mL DMF and 50 mL methanol were added and the solution was stirred 12 hr until a peroxide test was negative.) The solution was concentrated and the alcohol was purified by column chromatography on silica gel, eluting with 50:50 EtOAc/toluene to yield 2 mL $PhCH_2CH_2OH$.

PhCH₂CH₂OSO₂CH₃. PhCH₂CH₂OH (2.0 mL, 17 mmol) was dissolved in 30 mL dry CH_2Cl_2.

Et_3N (4.0 mL, 1.3 eq) was added *via* syringe against an Ar counterflow. The solution was cooled

to 0° C. CH_3SO_2Cl (2.0 mL, 1.5 eq) was added dropwise *via* syringe against an Ar counterflow

to the rapidly stirring solution over a 5 min period. The solution was quenched with 50 mL H_2O

and extracted with two 75 mL portions of 50:50 EtOAc/hexanes. The combined organic layers

were dried over Na_2SO_4, and the solvent was removed under reduced pressure to yield 2.0 mL

PhCH₂CH₂OSO₂CH₃. The product was not further purified.

PhCH₂CH₂SC(O)C(CH₃)₃. PhCH₂CH₂OSO₂CH₃ (2.0 mL) was dissolved in 15 mL THF and the

solution was cooled to 0° C. Et_3N (14.0 mL, 6 eq) was added *via* syringe against an Ar

counterflow. Thiopivalic acid (6.6 mL, 3 eq) was added *via* syringe against an Ar counterflow.

The solution was allowed to stir 10 min at 0° C, warmed to 50° C, and stirred for 1 hour. The

solution was quenched with 100 mL H_2O and extracted with three 75 mL portions of 50:50

EtOAc/hexanes. The combined organic layers were dried over Na_2SO_4 and the solvent was

removed under reduced pressure. The residue was purified by column chromatography on

silica gel, eluting with 5:95 EtOAc/hexanes to yield 3.4 g PhCH₂CH₂SC(O)C(CH₃)₃.

^{1}H NMR data (C_6D_6, 25° C): δ 1.06 (s, 9 H, CMe₃), δ 2.66 (t, 2 H, CH₂), delta 2.97 (t, 2 H, CH₂), δ

7.00 (t, 2H, phenyl), δ 7.07 (d, 2H, phenyl).

PHCH₂CH₂SH. PhCH₂CH₂SC(O)C(CH₃)₃ (2.0 mL) was dissolved in 15 mL degassed MeOH

and the solution was cooled to 0° C. NaOH (10 mL, 50%) was added *via* syringe against an Ar

counterflow . The solution was stirred for 5 hr at 0° C, warmed to room temperature, and

stirred for 1 hr until tlc showed the reaction complete. The solution was quenched with 100 mL

sat. NH_4Cl solution, and the product was extracted into 150 mL 50:50 EtOAc/hexanes. The

organic phase was washed with three 50 mL portions of H_2O, dried over Na_2SO_4, and the solvent was removed under reduced pressure. The thiol was purified by column chromatography on silica gel, eluting with 15:85 toluene/hexane to yield 2.0 mL $PhCH_2CH_2SH$.

Erythro- and *threo-***PhCHDCHDSH-d_2**. These derivatives were made as described for $PhCH_2CH_2SH$ above, starting from *cis-* and *trans-*styrene-d_2, respectively.

D-C≡C-Ph. Phenylacetylene (10.0 mL, 91 mmol) was dissolved in 70 mL THF and the solution was cooled to -78° C. n-BuLi (60 mL, 1.6 M in hexanes) was added *via* syringe against an Ar counterflow. The solution was stirred at -78° C for one hour and at room temperature for 2 hours. D_2O (2 mL) was added *via* syringe against an Ar counterflow to produce a yellow solution with much white ppt. The solution was washed with three 50 mL portions of saturated NH_4Cl, and the water phases were extracted into diethyl ether. The combined organic phases were combined, dried over Na_2SO_4, and stripped to dryness to yield 9 mL D-C≡C-Ph. ^{1}H NMR showed > 95% deuterium incorporation.

*Cis-***Styrene-d_2**. Cp_2ZrDCl (10.5 g, 40.5 mmol) was suspended in 50 mL toluene. Phenylacetylene (5.0 mL, 1.1 eq) was added *via* syringe against an Ar counterflow. The solution was stirred 2 hr until all Cp_2ZrDCl dissolved, yielding a dark orange solution. The toluene was removed *in vacuo*, and the remaining orange goo was dissolved in 50 mL diethyl ether. The solution was cooled to 0° C, and 1.0 mL degassed D_2O was slowly added *via* syringe against an Ar counterflow over 30 min. The $[Cp_2ZrO]_x$ was filtered and the styrene was vacuum distilled to yield 5.1 mL *cis*-styrene-d_2. ^{1}H NMR showed greater than 95% deuterium incorporation.

Trans-**Styrene-*d*₂.** Cp$_2$ZrDCl (11 g, 41 mmol) was suspended in 60 mL toluene. Deutero-phenylacetylene (5.0 mL, 1.1 eq) was added *via* syringe against an Ar counterflow. The solution was stirred 3 hr until all Cp$_2$ZrDCl dissolved, yielding a dark orange solution. The toluene was removed *in vacuo,* and the remaining orange goo was dissolved in 50 mL diethyl ether. The solution was cooled to 0° C, and 1.0 mL degassed D$_2$O was slowly added *via* syringe against an Ar counterflow over 30 min. The [Cp$_2$ZrO]$_x$ was filtered, and the styrene was vacuum distilled to yield 2.75 mL *trans*-styrene-*d*$_2$. ^{1}H NMR showed greater than 95% deuterium incorporation.

Cp*$_2$Ta(CH$_2$=CHPh)H.[29] Cp*$_2$TaH$_3$ (0.75 g, 1.7 mmol) was dissolved in 3 mL benzene in a glass bomb. Styrene (0.57 mL, 5 eq) was added *via* syringe against an Ar counterflow. The bomb was placed in a 110° C oil bath for three days. The solvent was removed *in vacuo* and the residue was washed with pentane to yield 0.62 g (1.1 mmol, 65%) tan product.

Anal. Calcd. for C$_{28}$H$_{39}$Ta: C, 60.43; H, 7.06. Found: C, 60.26; H, 6.81.

^{1}H NMR Data (C$_6$H$_6$, 25° C): δ -1.25 (s, 1 H, Ta-H), δ 0.15 (d , 2 H, CH$_2$), δ 1.53 (s, 15 H, Cp*), δ 1.67 (s, 15 H, Cp*), δ 1.90 (t , 1 H, CH), δ 6.97 (t, 2 H, phenyl), δ 7.27 (t, 2 H, phenyl), δ 7.70 (d, 1 H, phenyl).

Cp*$_2$Ta(=S)H. A solution of Cp*$_2$Ta(=C=CH$_2$)H (0.200 g, 0.42 mmol) was stirred in 10 mL of toluene under an atmosphere of H$_2$S for 2 hours at room temperature, giving a rose-pink solution. The solvent was removed *in vacuo* and the residue was extracted into 25 mL pentane and filtered. The filtrate was concentrated to *ca.* 10 mL and placed at -80° C, giving pink needles that were isolated by filtration and washed with cold pentane. Yield of Cp*$_2$Ta(=S)H 0.120 g (0.25 mmol, 59%).

Anal. Calcd. for C$_{20}$H$_{31}$STa: C, 49.6; H, 6.4. Found: C, 49.6; H, 6.4.

Cp*₂Ta(η^2-S=CH₂)H. CH₃SH (ca. 0.6 mmol) was added to a solution of Cp*₂Ta(=C=CH₂)H (0.190 g, 0.40 mmol) in 10 mL pentane, and the mixture was stirred at room temperature for 24 hours. The solvent was removed *in vacuo* and the residue was extracted into 20 mL pentane, filtered, and concentrated to *ca.* 5 mL and placed at -80° C. The white needles that formed were separated by filtration, washed with cold pentane, and dried *in vacuo* to yield 0.100 g (0.20 mmol, 50%) Cp*₂Ta(η^2-S=CH₂)H. The d_3-complex was prepared in a similar manner using CD₃SD.

Anal. Calcd. for $C_{21}H_{33}STa$: C, 50.7; H, 6.7. Found: C, 50.6; H, 6.6.

IR data (Nujol mull, cm⁻¹): 1780 (Ta-H).

Cp*₂Ta(η^2-S=CHC₆H₅)H. Cp*₂Ta(η^2-C₆H₄)H (0.880 g, 1.67 mmol) was dissolved in 15 mL of toluene. While cold (-78°C), HSCH₂C₆H₅ (200 μL, 1 eq) was added *via* syringe. The solution was warmed to room temperature, stirred for 18 hours, and filtered. The toluene was removed *in vacuo*. Petroleum ether was added and removed *in vacuo* for four cycles to remove excess thiol. Isolation from pentane at -78° C afforded 0.61 g (1.07 mmol, 64% yield) pale tan solid.

Anal. Calcd. for $C_{27}H_{37}STa$: C, 56.44; H, 6.50. Found: C, 56.14; H, 6.24.

Cp*₂Ta(CHCH₂)(SCH₂C₆H₅)H. Cp*₂Ta(=CCH₂)H (0.560 g, 1.17 mmol) was dissolved in 15 mL of petroleum ether. While cold (0° C), HSCH₂C₆H₅ (135 μL, 1 eq) was added *via* syringe. The solution was stirred for 30 minutes at 0° C during which time product precipitated. The reaction was cooled to -78° C and filtered to yield 0.26 g (0.43 mmol, 37% yield) tan solid.

Anal. Calcd. for $C_{29}H_{41}STa$: C, 57.80; H, 6.86. Found: C, 56.60; H, 6.25.[30]

IR data (Nujol mull, cm⁻¹): 1950 (Ta-H).

Cp*$_2$Ta(η^2-S=CHCH$_2$C(CH$_3$)$_3$)H. Cp*$_2$Ta(η^2-C$_6$H$_4$)H (0.525 g, 0.947 mmol) was dissolved in 15 mL toluene. Neohexyl mercaptan (100 μL, 1 eq) was added *via* syringe against an Ar counterflow. The solution was stirred for 12 hours and filtered. The toluene was removed *in vacuo*. Petroleum ether was added and removed *in vacuo* for three cycles to remove excess thiol. Isolation from pentane at -78° C afforded 0.075 g (0.132 mmol, 15% yield) light green solid.

Anal. Calcd. for C$_{26}$H$_{43}$STa: C, 54.92; H, 7.62. Found: C, 54.45; H, 6.33.

Cp*$_2$Ta(η^2-S=CHCH$_2$C$_6$H$_5$)H. Cp*$_2$Ta(η^2-C$_6$H$_4$)H (0.220 g, 0.417 mmol) was dissolved in 10 mL toluene. Phenethyl mercaptan (48 μl, 0.85 eq) was syringed in against an Ar counterflow. The solution was stirred for two hours and filtered. The toluene was removed *in vacuo*. Petroleum ether was added and removed *in vacuo* for three cycles to remove excess thiol. Isolation from pentane at -78° C afforded 0.175 g (0.297 mmol, 87% yield) solid.

Anal. Calcd. for C$_{28}$H$_{39}$STa: C, 57.13; H, 6.68. Found: C, 57.41 H, 6.55

Cp*$_2$Ta(=S)CH$_3$. A solution of Cp*$_2$Ta(η^2-S=CH$_2$)H (0.055 g, 0.11 mmol) in 20 mL toluene was heated at 130° C in a glass ampoule for 5 days. The solvent was removed under reduced pressure and the residue was washed with pentane to yield 0.50 g pink flakes (91%).

Anal. Calcd. for C$_{21}$H$_{33}$STa: C, 50.6; H, 6.6. Found: C, 50.6; H, 6.6.

Production of Cp*$_2$Ta(=S)R.

Method 1: A sample of permethyltantalocene thioaldehyde hydride (*ca.* 15 mg) was dissolved in C$_6$D$_6$ in a sealed NMR tube. The sample was heated in an oil bath to 110° C, and the reaction was monitored by ^{1}H NMR until the migration was complete.

Method 2: A sealable NMR tube was charged with *ca.* 15 mg Cp*$_2$Ta(η^2-C$_6$H$_4$)H or Cp*$_2$Ta(η^2-CHCH$_2$C$_6$H$_5$)H dissolved in C$_6$D$_6$. Approximately 1.1 eq ethylene sulfide was condensed into the solution, and the NMR tube was sealed. The reaction was monitored by ^{1}H NMR.

Kinetics of the Conversion of Cp*$_2$Ta(CHCH$_2$)(SCH$_2$C$_6$H$_5$)H to Cp*$_2$Ta(η^2-SCHC$_6$H$_5$)H.

A sample of Cp*$_2$Ta(CHCH$_2$)(SCH$_2$C$_6$H$_5$)H, dissolved in benzene-d$_6$ in a sealed NMR tube, was submerged in an oil bath at 35° C. Approximately ten spectra were taken over three half lives. The rate of the reaction was determined by measuring the increases of Cp* resonances for the product relative to an internal standard (ferrocene) as a function of time. A first order rate constant was obtained from a plot of ln[Cp*$_{t=\infty}$ - Cp*$_{t=t}$] versus time.

Kinetic Isotope Effect for Conversion of Cp*$_2$Ta(η^2-S=CH$_2$)H to Cp*$_2$Ta(=S)CH$_3$.

Two independent samples of Cp*$_2$Ta(η^2-S=CH$_2$)H and Cp*$_2$Ta(η^2-S=CD$_2$)D, dissolved in C$_6$H$_6$ in sealed NMR tubes, were heated side-by-side submerged in an oil bath at 138° C. The rates of the reactions were determined by measuring the decreases in intensity of the Cp* resonances of the starting material, relative to an internal standard (ferrocene), as a function of time. The measured rate constants were k_H = 2.07(3) x 10^{-4} s^{-1} and k_D = 2.87(3) x 10^{-4} s^{-1}, thus giving rise to an *inverse* primary kinetic isotope effect of k_H/k_D = 0.72(3) at 138° C.

Photolysis of Cp*$_2$Ta(=S)CH$_3$.

A sample of Cp*$_2$Ta(=S)CH$_3$ in C$_6$D$_6$ was photolysed with a mercury lamp for 4 hours. After this time, examination of the ^{1}H NMR spectrum demonstrated that conversion to Cp*$_2$Ta(η^2-S=CH$_2$)H had occurred, accompanied by decomposition.

Structural Determination of Cp*$_2$Ta(η^2-S=CHCH$_2$Ph)H. Crystallographic data are summarized in Table 4. Single peach colored crystals of Cp*$_2$Ta(η^2-S=CHCH$_2$Ph)H were grown by cooling a saturated THF solution to -58° C. A tabular crystal fragment measuring 0.09 X 0.32 X 0.52 mm was mounted with grease in a capillary which was then sealed. Oscillation and Weissenberg photographs identified the space group as P2$_1$/c. The crystal was mounted on an Enraf-Nonius CAD4 automated diffractometer. Cell constants and the orientation matrix were determined from the setting angles of 24 reflections with 29° < 2θ < 33°. Data were collected utilizing MoKα radiation. An ω scan was used to collect two quadrants of data for 3° < 2θ < 40° with a $(\sin\theta/\lambda)_{max}$ of 0.48. Indices ranged from -15 to 13 for h, -9 to 9 for k, and -16 to 16 for l. Peak broadening and substantial falloff in three standard reflections, $\bar{3}10$, $\bar{2}20$, and $1\bar{3}\bar{2}$, led to the rejection of the final 763 of the 4962 reflections measured (2345 independent).

The data were corrected for Lorentz and polarization effects; an absorption correction was done by Gaussian integration over an 8 X 8 X 8 grid with μr_{max} of 1.5 and transmission range of 0.26 to 0.69. The goodness of fit for merging was 3.32, due primarily to peak broadening with time, but also to residual absorption effects. The R$_{merge}$ was 0.049 for 1310 reflections with exactly two observations; 12 reflections with background inconsistencies were rejected.

The tantalum coordinates were found by inspection of the data; the locations of the rest of the non-hydrogen atoms were determined by successive structure factor-Fourier calculations. The sulfur atom was found to partially occupy two different sites. Hydrogen atoms were placed at calculated positions 0.95 Å from the bonded carbon atom with B_{iso} = 1.2B_{eq} for the carbon. All methyl groups were modeled by six half-weight H atom positions. The H atom HC1 on the thioaldehyde carbon C1 was disordered in conjunction with the sulfur atom. The H atom on the tantalum was obscured by the disorder involving the sulfur atom and subsequently ignored.

The data were refined by full matrix least squares using F^2 values. The variances of

$\sigma^2(I)$ of the individual data were derived from counting statistics plus an additional term,

$(0.014I)^2$; the variances of the merged data, by propagation of error plus an additional term,

$(0.014\bar{I})^2$. The H atom parameters were recalculated several times during refinement of the 186

parameters, which included a scale factor, the coordinates of non-hydrogen atoms, anisotropic

displacement parameters for Ta, S, and methyl C atoms, isotropic displacement parameters for

the remainder of the non-hydrogen atoms, and a single population factor for the two atoms S

and HC1. The final R-index was 0.068 for the 2179 reflections with $F_o^2 > 0$, and 0.054 for the

1751 reflections with $F_o^2 > 3\sigma(F_o^2)$. The final goodness of fit was 2.55, with a maximum shift to

estimated standard deviation ratio of 0.01 in the final least squares cycle. The final difference

map showed deviations ranging from -1.7 e$\mathring{A}^{-3}$ to 2.6 e$\mathring{A}^{-3}$ near the Ta atom position. The

programs used were those of the CRYM crystallographic computing system and ORTEP,[31] with

atomic scattering factors and dispersion corrections taken from a standard reference.[32]

Crystal and intensity collection data are given in Table 4. Figure 6 shows an ORTEP

drawing of the molecule with the labeling scheme. Final parameters are given in Table 5.

Anisotropic displacement parameters are given in Table 6, hydrogen atom parameters in Table

7. Table 8 gives complete distances and angles for the compound.

Table 4: Crystal and Intensity Collection Data for Cp*$_2$Ta(η^2-S=CHCH$_2$Ph)H

Formula: TaC$_{28}$H$_{39}$S   Formula weight: 588.626

Crystal color: Peach   Habit: Tabular

Crystal size: 0.09 × 0.32 × 0.52 mm

Space group: P2$_1$/c (#14)

$a = 15.729(5)$Å

$b = 10.203(2)$Å $\beta = 116.18(2)°$

$c = 17.599(5)$Å

$V = 2534.6(12)$Å^3 $Z = 4$

$\rho_{calc} = 1.543$ g cm^{-3}

$\mu = 46.63$ cm^{-1} ($\mu r_{max} = 1.5$)   Transmission coeff. = 0.26 − 0.69

CAD-4 diffractometer ω scan

$\lambda = 0.7107$Å   Graphite monochromator

2θ range: 2°–40°   Octants collected: $-h, \pm k, \pm l$

T = 289°K

Number of reflections measured: 4962

Number of independent reflections: 2332

Number with F$_o^2$ > 0: 2178

Number with F$_o^2$ > 3σ(F$_o^2$): 1750

Number of reflections used in refinement: 2332

Goodness of fit for merging data: 3.32

Final R-index: 0.0679 for 2178 reflections with F$_o^2$ > 0

Final R-index: 0.0535 for 1750 reflections with F$_o^2$ > 3σ(F$_o^2$)

Final goodness of fit: 2.54 for 186 parameters and 2332 reflections

Figure 6: Labeling Scheme for Cp*$_2$Ta(η^2-S=CHCH$_2$Ph)H
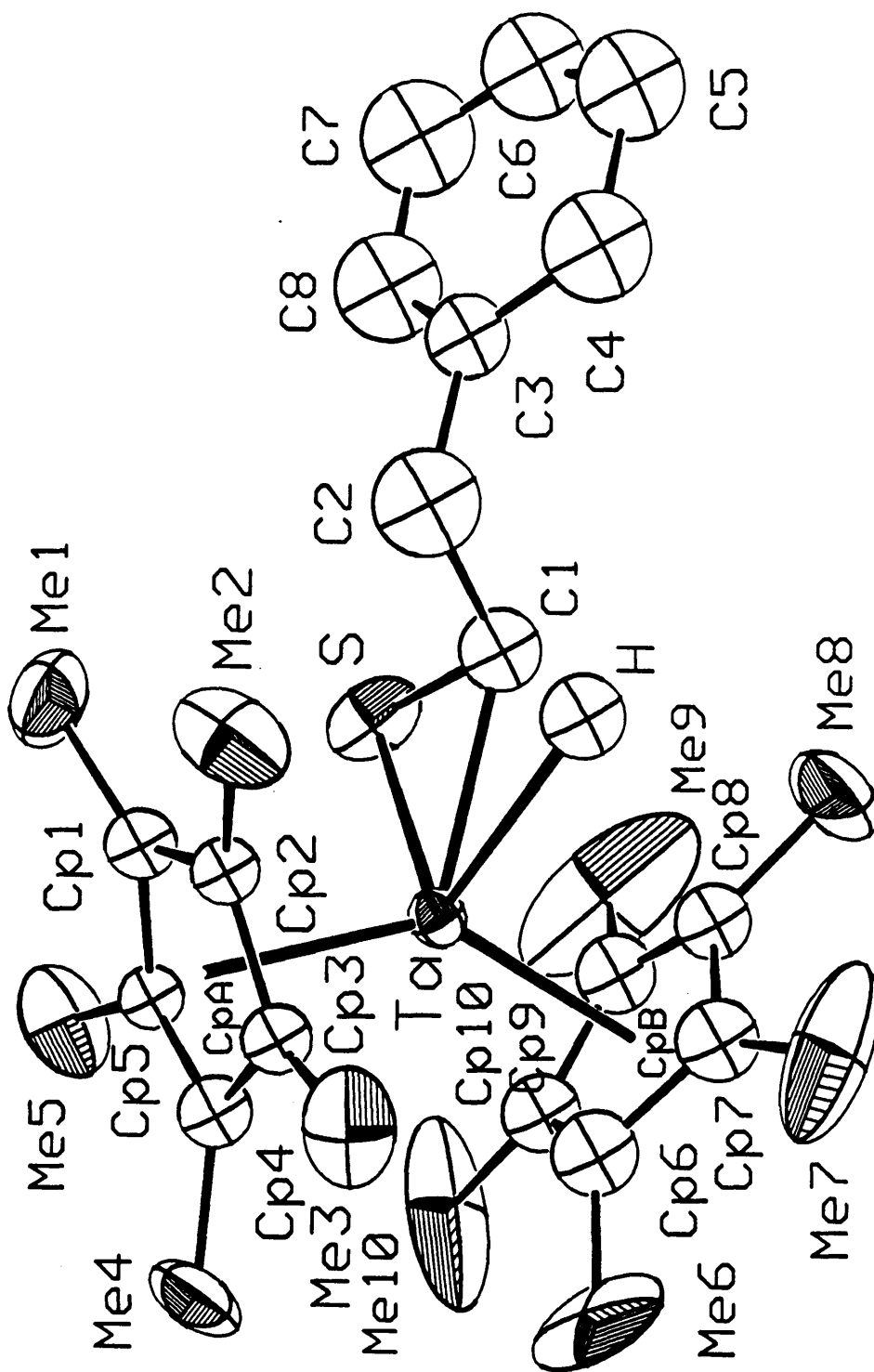
Table 5: Final Atomic Coordinates and Parameters for $Cp*_2Ta(\eta^2\text{-}S=CHCH_2Ph)H$

x, y, z and $U_{eq}{}^a \times 10^4$

Atom	x	y	z	U_{eq} or B
Ta	7377(.4)	−2109(.7)	7423(.4)	405(2)
S †	6338(6)	−3641(7)	7648(6)	826(25)
S′ †	8867(11)	−3137(15)	8521(10)	6.1(5) *
C1	7625(14)	−3754(19)	8374(12)	6.3(5) *
C2	7992(18)	−5108(26)	8377(16)	10.6(8) *
C3	7968(15)	−6115(19)	8987(13)	6.3(5) *
C4	8803(18)	−6268(24)	9750(17)	10.5(7) *
C5	8687(20)	−7260(25)	10333(16)	10.7(7) *
C6	7881(21)	−7773(25)	10008(17)	10.4(7) *
C7	7152(22)	−7713(29)	9324(21)	12.7(9) *
C8	7184(19)	−6751(26)	8789(17)	10.9(7) *
Cp1	7042(12)	−3777(18)	6266(10)	4.5(4) *
Cp2	8017(11)	−3385(16)	6590(10)	3.9(4) *
Cp3	8045(11)	−2066(18)	6420(9)	4.2(3) *
Cp4	7098(12)	−1639(16)	5952(11)	4.7(4) *
Cp5	6500(11)	−2594(14)	5925(9)	3.8(4) *
Me1	6637(16)	−5103(20)	6199(13)	1078(80)
Me2	8860(15)	−4339(20)	6931(13)	1051(71)
Me3	8963(14)	−1385(21)	6541(13)	1011(71)
Me4	6824(15)	−388(19)	5411(11)	954(74)

Atom	x	y	z	U_{eq} or	B
Me5	5422(12)	−2618(21)	5423(12)	1093(88)	
Cp6	7482(16)	190(19)	7565(14)	6.9(5)	*
Cp7	8120(15)	−223(18)	8394(13)	6.3(5)	*
Cp8	7545(13)	−928(17)	8708(12)	5.5(4)	*
Cp9	6651(14)	−789(18)	8151(13)	6.3(5)	*
Cp10	6576(14)	−100(18)	7433(12)	6.1(5)	*
Me6	7745(32)	1279(22)	7153(21)	2345(208)	
Me7	9155(17)	65(27)	8816(19)	1952(152)	
Me8	7997(25)	−1400(24)	9589(14)	1963(170)	
Me9	5875(30)	−1236(30)	8363(32)	3028(186)	
Me10	5651(22)	423(34)	6728(17)	2851(189)	

^{a} $U_{eq} = \frac{1}{3} \sum_i \sum_j [U_{ij}(a_i^* a_j^*)(\vec{a}_i \cdot \vec{a}_j)]$

† Populations: S, 0.68(1); S', 0.32(1).

* Isotropic displacement parameter, B

Table 6: Anisotropic Displacement Parameters for Cp*$_2$Ta(η^2-S=CHCH$_2$Ph)H

Atom	U_{11}	U_{22}	U_{33}	U_{12}	U_{13}	U_{23}
Ta	399(5)	443(5)	384(4)	−9(5)	183(3)	5(5)
S	865(64)	696(61)	1299(75)	−148(43)	826(59)	−101(50)
Me1	1391(213)	869(179)	952(176)	−470(149)	496(161)	−305(133)
Me2	1097(185)	1305(203)	971(167)	678(147)	656(151)	328(141)
Me3	793(157)	1503(218)	974(170)	−405(133)	606(142)	−299(140)
Me4	1347(197)	1037(186)	547(134)	176(137)	480(138)	305(119)
Me5	432(117)	1788(241)	788(146)	130(125)	22(108)	15(139)
Me6	5587(648)	442(175)	2446(345)	−331(265)	3085(444)	−567(194)
Me7	651(182)	2210(328)	2596(373)	−575(180)	353(213)	−1507(275)
Me8	3776(482)	1166(228)	521(163)	441(246)	558(234)	89(141)
Me9	3790(547)	1901(331)	6065(809)	−1021(322)	4613(621)	−1334(399)
Me10	1990(330)	3562(440)	1232(243)	2338(327)	−905(225)	−1043(262)

$U_{i,j}$ values have been multiplied by 10^4

The form of the displacement factor is:

$$\exp -2\pi^2(U_{11}h^2a^{*^2}+U_{22}k^2b^{*^2}+U_{33}\ell^2c^{*^2}+2U_{12}hka^*b^*+2U_{13}h\ell a^*c^*+2U_{23}k\ell b^*c^*)$$

Table 7: Hydrogen Atom Parameters for Cp*$_2$Ta(η^2-S=CHCH$_2$Ph)H

x, y and $z \times 10^4$

Atom	x	y	z	B
HC1	8030	−3667	8956	7.6
HC1′	7158	−3835	8573	7.6
HC2a	8629	−5023	8469	12.9
HC2b	7625	−5461	7820	12.9
HC4	9376	−5792	9888	12.6
HC5	9172	−7470	10873	12.8
HC6	7822	−8372	10398	12.3
HC7	6636	−8279	9209	15.2
HC8	6636	−6570	8279	13.3
HMe1a	7132	−5716	6473	10.3
HMe1b	6222	−5109	6461	10.3
HMe1c	6292	−5330	5618	10.3
HMe1d	5965	−5041	5955	10.3
HMe1e	6816	−5633	5850	10.3
HMe1f	6866	−5481	6746	10.3
HMe2a	9437	−3857	7117	9.9
HMe2b	8866	−4810	7403	9.9
HMe2c	8810	−4935	6504	9.9
HMe2d	8651	−5186	6997	9.9
HMe2e	9140	−4378	6554	9.9
HMe2f	9323	−4038	7473	9.9
HMe3a	8841	−487	6395	9.7
HMe3b	9417	−1456	7121	9.7
HMe3c	9205	−1793	6194	9.7
HMe3d	9490	−1912	6895	9.7
HMe3e	8966	−1267	6010	9.7
HMe3f	9007	−557	6805	9.7
HMe4a	6152	−291	5149	9.0
HMe4b	7104	351	5758	9.0
HMe4c	7037	−447	4983	9.0
HMe4d	7369	135	5544	9.0
HMe4e	6551	−617	4826	9.0
HMe4f	6372	95	5521	9.0
HMe5a	5182	−3421	5521	10.4
HMe5b	5155	−1907	5591	10.4
HMe5c	5252	−2542	4832	10.4
HMe5d	5194	−1753	5248	10.4
HMe5e	5248	−3156	4933	10.4
HMe5f	5148	−2961	5764	10.4

Atom	x	y	z	B
HMe6a	7996	1979	7554	22.0
HMe6b	8221	984	7001	22.0
HMe6c	7210	1567	6676	22.0
HMe6d	7255	1436	6614	22.0
HMe6e	7859	2043	7499	22.0
HMe6f	8313	1051	7118	22.0
HMe7a	9429	−313	9367	19.1
HMe7b	9448	−295	8494	19.1
HMe7c	9251	987	8862	19.1
HMe7d	9325	550	8444	19.1
HMe7e	9302	562	9316	19.1
HMe7f	9501	−735	8963	19.1
HMe8a	7569	−1927	9701	18.5
HMe8b	8547	−1902	9684	18.5
HMe8c	8185	−669	9968	18.5
HMe8d	8671	−1364	9802	18.5
HMe8e	7816	−858	9935	18.5
HMe8f	7813	−2277	9617	18.5
HMe9a	5270	−1060	7881	28.7
HMe9b	5924	−2146	8464	28.7
HMe9c	5901	−773	8832	28.7
HMe9d	6126	−1680	8876	28.7
HMe9e	5515	−493	8383	28.7
HMe9f	5455	−1807	7918	28.7
HMe10a	5780	858	6320	27.1
HMe10b	5231	−286	6482	27.1
HMe10c	5372	1023	6972	27.1
HMe10d	5132	61	6800	27.1
HMe10e	5640	1351	6774	27.1
HMe10f	5611	183	6199	27.1

Table 8: Complete Distances (Å) and Angles (°) for Cp*$_2$Ta(η^2-S=CHCH$_2$Ph)H

		Distance(Å)			Distance(Å)
Ta	–C1	2.28(2)	Cp3	–Me3	1.53(3)
Ta	–S	2.418(9)	Cp4	–Cp5	1.34(2)
S	–C1	1.86(2)	Cp4	–Me4	1.54(3)
Ta	–S′	2.517(17)	Cp5	–Me5	1.53(3)
S′	–C1	1.96(3)	Me1	–HMe1a	0.948
Ta	–CpA	2.156	Me1	–HMe1b	0.950
Ta	–CpB	2.132	Me1	–HMe1c	0.951
Ta	–Cp1	2.524(18)	Me1	–HMe1d	0.951
Ta	–Cp2	2.481(17)	Me1	–HMe1e	0.949
Ta	–Cp3	2.419(17)	Me1	–HMe1f	0.948
Ta	–Cp4	2.474(18)	Me2	–HMe2a	0.955
Ta	–Cp5	2.426(16)	Me2	–HMe2b	0.957
Ta	–Cp6	2.36(2)	Me2	–HMe2c	0.942
Ta	–Cp7	2.49(2)	Me2	–HMe2d	0.949
Ta	–Cp8	2.47(2)	Me2	–HMe2e	0.944
Ta	–Cp9	2.46(2)	Me2	–HMe2f	0.960
Ta	–Cp10	2.41(2)	Me3	–HMe3a	0.948
C1	–C2	1.50(4)	Me3	–HMe3b	0.955
C1	–HC1	0.942	Me3	–HMe3c	0.947
C1	–HC1′	0.947	Me3	–HMe3d	0.953
C2	–C3	1.50(4)	Me3	–HMe3e	0.945
C2	–HC2a	0.945	Me3	–HMe3f	0.952
C2	–HC2b	0.961	Me4	–HMe4a	0.954
C3	–C4	1.41(4)	Me4	–HMe4b	0.948
C3	–C8	1.30(4)	Me4	–HMe4c	0.952
C4	–C5	1.51(4)	Me4	–HMe4d	0.948
C4	–HC4	0.956	Me4	–HMe4e	0.954
C5	–C6	1.25(4)	Me4	–HMe4f	0.952
C5	–HC5	0.944	Me5	–HMe5a	0.949
C6	–C7	1.25(4)	Me5	–HMe5b	0.947
C6	–HC6	0.953	Me5	–HMe5c	0.957
C7	–C8	1.38(4)	Me5	–HMe5d	0.951
C7	–HC7	0.943	Me5	–HMe5e	0.956
C8	–HC8	0.949	Me5	–HMe5f	0.946
Cp1	–Cp2	1.44(3)	Cp6	–Cp7	1.42(3)
Cp1	–Cp5	1.45(2)	Cp6	–Cp10	1.37(3)
Cp1	–Me1	1.48(3)	Cp6	–Me6	1.48(4)
Cp2	–Cp3	1.38(2)	Cp7	–Cp8	1.44(3)
Cp2	–Me2	1.54(3)	Cp7	–Me7	1.49(4)
Cp3	–Cp4	1.42(3)	Cp8	–Cp9	1.32(3)

		Distance(Å)				Angle(°)
Cp8	−Me8	1.47(4)	C1	−Ta	−S	46.6(5)
Cp9	−Cp10	1.40(3)	C1	−Ta	−S'	47.9(6)
Cp9	−Me9	1.50(5)	C1	−S	−Ta	62.8(7)
Cp10	−Me10	1.53(4)	C1	−S'	−Ta	59.7(7)
Me6	−HMe6a	0.957	S	−C1	−Ta	70.6(7)
Me6	−HMe6b	0.949	S'	−C1	−Ta	72.4(8)
Me6	−HMe6c	0.937	Ta	−C1	−C2	128.5(16)
Me6	−HMe6d	0.936	S	−C1	−C2	111.2(16)
Me6	−HMe6e	0.956	S'	−C1	−C2	86.3(15)
Me6	−HMe6f	0.952	CpB	−Ta	−CpA	139.2
Me7	−HMe7a	0.952	CpA	−Ta	−S	104.5
Me7	−HMe7b	0.949	CpB	−Ta	−S	104.0
Me7	−HMe7c	0.950	CpA	−Ta	−S'	104.4
Me7	−HMe7d	0.949	CpB	−Ta	−S'	101.9
Me7	−HMe7e	0.951	CpA	−Ta	−C1	115.7
Me7	−HMe7f	0.951	CpB	−Ta	−C1	105.1
Me8	−HMe8a	0.948	S	−C1	−HC1	138.5
Me8	−HMe8b	0.955	S'	−C1	−HC1'	150.6
Me8	−HMe8c	0.956	HC1	−C1	−C2	90.5
Me8	−HMe8d	0.957	HC1'	−C1	−C2	106.2
Me8	−HMe8e	0.953	C3	−C2	−C1	120.2(22)
Me8	−HMe8f	0.948	HC2a	−C2	−C1	107.2
Me9	−HMe9a	0.972	HC2b	−C2	−C1	106.6
Me9	−HMe9b	0.942	HC2a	−C2	−C3	107.4
Me9	−HMe9c	0.937	HC2b	−C2	−C3	106.3
Me9	−HMe9d	0.929	HC2b	−C2	−HC2a	108.9
Me9	−HMe9e	0.956	C4	−C3	−C2	116.7(21)
Me9	−HMe9f	0.965	C8	−C3	−C2	118.2(23)
Me10	−HMe10a	0.940	C8	−C3	−C4	125.1(24)
Me10	−HMe10b	0.946	C5	−C4	−C3	112.3(23)
Me10	−HMe10c	0.957	HC4	−C4	−C3	124.2
Me10	−HMe10d	0.954	HC4	−C4	−C5	123.5
Me10	−HMe10e	0.951	C6	−C5	−C4	111.8(26)
Me10	−HMe10f	0.938	HC5	−C5	−C4	123.3
			HC5	−C5	−C6	124.8
			C7	−C6	−C5	137.4(32)
			HC6	−C6	−C5	109.9
			HC6	−C6	−C7	112.8
			C8	−C7	−C6	113.7(30)
			HC7	−C7	−C6	121.0

			Angle(°)				Angle(°)
HC7	–C7	–C8	125.3	HMe2e	–Me2	–HMe2d	110.0
C7	–C8	–C3	119.3(27)	HMe2f	–Me2	–HMe2d	108.7
HC8	–C8	–C3	121.0	HMe2f	–Me2	–HMe2e	109.1
HC8	–C8	–C7	119.6	HMe3a	–Me3	–Cp3	109.6
Cp5	–Cp1	–Cp2	105.2(15)	HMe3b	–Me3	–Cp3	109.2
Me1	–Cp1	–Cp2	129.3(17)	HMe3c	–Me3	–Cp3	109.6
Me1	–Cp1	–Cp5	125.2(17)	HMe3d	–Me3	–Cp3	109.3
Cp3	–Cp2	–Cp1	108.3(15)	HMe3e	–Me3	–Cp3	109.7
Me2	–Cp2	–Cp1	124.3(16)	HMe3f	–Me3	–Cp3	109.4
Me2	–Cp2	–Cp3	126.6(16)	HMe3b	–Me3	–HMe3a	109.2
Cp4	–Cp3	–Cp2	107.5(15)	HMe3c	–Me3	–HMe3a	109.9
Me3	–Cp3	–Cp2	121.9(16)	HMe3c	–Me3	–HMe3b	109.3
Me3	–Cp3	–Cp4	128.8(16)	HMe3e	–Me3	–HMe3d	109.7
Cp5	–Cp4	–Cp3	109.8(16)	HMe3f	–Me3	–HMe3d	109.1
Me4	–Cp4	–Cp3	123.6(16)	HMe3f	–Me3	–HMe3e	109.8
Me4	–Cp4	–Cp5	125.5(17)	HMe4a	–Me4	–Cp4	109.5
Cp4	–Cp5	–Cp1	108.4(15)	HMe4b	–Me4	–Cp4	109.8
Me5	–Cp5	–Cp1	121.8(15)	HMe4c	–Me4	–Cp4	109.7
Me5	–Cp5	–Cp4	127.9(16)	HMe4d	–Me4	–Cp4	109.8
HMe1a	–Me1	–Cp1	109.6	HMe4e	–Me4	–Cp4	109.6
HMe1b	–Me1	–Cp1	109.4	HMe4f	–Me4	–Cp4	109.6
HMe1c	–Me1	–Cp1	109.3	HMe4b	–Me4	–HMe4a	109.3
HMe1d	–Me1	–Cp1	109.3	HMe4c	–Me4	–HMe4a	109.0
HMe1e	–Me1	–Cp1	109.4	HMe4c	–Me4	–HMe4b	109.5
HMe1f	–Me1	–Cp1	109.6	HMe4e	–Me4	–HMe4d	109.3
HMe1b	–Me1	–HMe1a	109.6	HMe4f	–Me4	–HMe4d	109.5
HMe1c	–Me1	–HMe1a	109.6	HMe4f	–Me4	–HMe4e	109.0
HMe1c	–Me1	–HMe1b	109.4	HMe5a	–Me5	–Cp5	109.7
HMe1e	–Me1	–HMe1d	109.4	HMe5b	–Me5	–Cp5	109.8
HMe1f	–Me1	–HMe1d	109.5	HMe5c	–Me5	–Cp5	109.4
HMe1f	–Me1	–HMe1e	109.7	HMe5d	–Me5	–Cp5	109.6
HMe2a	–Me2	–Cp2	109.5	HMe5e	–Me5	–Cp5	109.4
HMe2b	–Me2	–Cp2	109.4	HMe5f	–Me5	–Cp5	109.9
HMe2c	–Me2	–Cp2	110.1	HMe5b	–Me5	–HMe5a	109.8
HMe2d	–Me2	–Cp2	109.8	HMe5c	–Me5	–HMe5a	109.0
HMe2e	–Me2	–Cp2	110.0	HMe5c	–Me5	–HMe5b	109.2
HMe2f	–Me2	–Cp2	109.2	HMe5e	–Me5	–HMe5d	108.9
HMe2b	–Me2	–HMe2a	108.5	HMe5f	–Me5	–HMe5d	109.7
HMe2c	–Me2	–HMe2a	109.7	HMe5f	–Me5	–HMe5e	109.3
HMe2c	–Me2	–HMe2b	109.6	Cp10	–Cp6	–Cp7	108.7(20)

			Angle(°)				Angle(°)
Me6	–Cp6	–Cp7	120.1(23)	HMe8c	–Me8	–Cp8	109.7
Me6	–Cp6	–Cp10	124.9(23)	HMe8d	–Me8	–Cp8	109.6
Cp8	–Cp7	–Cp6	105.2(18)	HMe8e	–Me8	–Cp8	109.9
Me7	–Cp7	–Cp6	125.1(21)	HMe8f	–Me8	–Cp8	110.3
Me7	–Cp7	–Cp8	129.7(20)	HMe8b	–Me8	–HMe8a	109.3
Cp9	–Cp8	–Cp7	107.7(18)	HMe8c	–Me8	–HMe8a	109.1
Me8	–Cp8	–Cp7	118.3(19)	HMe8c	–Me8	–HMe8b	108.6
Me8	–Cp8	–Cp9	132.6(21)	HMe8e	–Me8	–HMe8d	108.6
Cp10	–Cp9	–Cp8	111.2(19)	HMe8f	–Me8	–HMe8d	109.0
Me9	–Cp9	–Cp8	120.1(24)	HMe8f	–Me8	–HMe8e	109.4
Me9	–Cp9	–Cp10	128.5(24)	HMe9a	–Me9	–Cp9	108.6
Cp9	–Cp10	–Cp6	106.6(19)	HMe9b	–Me9	–Cp9	109.8
Me10	–Cp10	–Cp6	127.4(21)	HMe9c	–Me9	–Cp9	110.0
Me10	–Cp10	–Cp9	125.2(21)	HMe9d	–Me9	–Cp9	110.3
HMe6a	–Me6	–Cp6	108.2	HMe9e	–Me9	–Cp9	109.2
HMe6b	–Me6	–Cp6	109.0	HMe9f	–Me9	–Cp9	108.9
HMe6c	–Me6	–Cp6	109.9	HMe9b	–Me9	–HMe9a	108.3
HMe6d	–Me6	–Cp6	110.0	HMe9c	–Me9	–HMe9a	108.7
HMe6e	–Me6	–Cp6	108.3	HMe9c	–Me9	–HMe9b	111.3
HMe6f	–Me6	–Cp6	108.8	HMe9e	–Me9	–HMe9d	110.8
HMe6b	–Me6	–HMe6a	108.9	HMe9f	–Me9	–HMe9d	109.9
HMe6c	–Me6	–HMe6a	110.0	HMe9f	–Me9	–HMe9e	107.7
HMe6c	–Me6	–HMe6b	110.7	HMe10a	–Me10	–Cp10	109.6
HMe6e	–Me6	–HMe6d	110.2	HMe10b	–Me10	–Cp10	109.1
HMe6f	–Me6	–HMe6d	110.6	HMe10c	–Me10	–Cp10	108.5
HMe6f	–Me6	–HMe6e	108.9	HMe10d	–Me10	–Cp10	108.6
HMe7a	–Me7	–Cp7	109.3	HMe10e	–Me10	–Cp10	108.9
HMe7b	–Me7	–Cp7	109.7	HMe10f	–Me10	–Cp10	109.6
HMe7c	–Me7	–Cp7	109.6	HMe10b	–Me10	–HMe10a	110.7
HMe7d	–Me7	–Cp7	109.7	HMe10c	–Me10	–HMe10a	109.7
HMe7e	–Me7	–Cp7	109.3	HMe10c	–Me10	–HMe10b	109.2
HMe7f	–Me7	–Cp7	109.5	HMe10e	–Me10	–HMe10d	109.0
HMe7b	–Me7	–HMe7a	109.4	HMe10f	–Me10	–HMe10d	110.2
HMe7c	–Me7	–HMe7a	109.3	HMe10f	–Me10	–HMe10e	110.4
HMe7c	–Me7	–HMe7b	109.6				
HMe7e	–Me7	–HMe7d	109.5				
HMe7f	–Me7	–HMe7d	109.5				
HMe7f	–Me7	–HMe7e	109.3				
HMe8a	–Me8	–Cp8	110.3				
HMe8b	–Me8	–Cp8	109.8				

References

1   For general reviews, see (a) Mitchell, P.C.H. in *Catalysis*, Kemball, C. Ed. The Chemical

Society: London **1977**, *1*, 223. (b) Mitchell, P.C.H. in *Catalysis*, Kemball, C. Ed. The

Chemical Society: London **1977**, *4*, 203. (c) Gates, B.C.; Katzer, J.R.; Schuit, G.C.A.

"Chemistry of Catalytic Processes"; McGraw-Hill Book Company: New York, **1979**. (d)

Weisser, O.; Landa, S. "Sulphide Catalysts, Their Properties and Applications";

Pergamon Press: Oxford, **1973**. (d) Angelici, R. J. *Acc. Chem. Res.* **1988**, *21*, 382.

2   See, for example: (a) Bucknor, S. M.; Draganjac, M.; Rauchfuss, T. B.; Ruffing, C. J.;

Fultz, W. C.; Rheingold, A. L. *J. Am. Chem. Soc.* **1984**, *106*, 5379. (b) Lockemeyer, J.

R.; Rauchfuss, T. B.; Rheingold, A. L.; Wilson, S. R. *J. Am. Chem. Soc.* **1989**, *111*, 8828.

(c) Huckett, S. C.; Miller, L.L.; Jacobson, R. A.; Angelici, R. J. *Organometallics* **1988**, *7*,

686. (d) Wang, C. J.; Angelici, R. J. *Organometallics* **1990**, *9*, 1770.

3   Chen, J.; Daniels, L. M.; Angelici, R. J. *J. Am. Chem. Soc.* **1190**, *112*, 199.

4   Jones, W. D.; Lingzhen, D. *J. Am. Chem. Soc.* **1991**, *113*, 559.

5   Parkin, G.; Bunel, E.; Burger, B. J.; Trimmer, M. S.; van Asselt, A.; Bercaw, J. E. *J. Mol.

Cat.* **1987**, *41*, 21.

6   Burger, B. J., Ph.D. Dissertation, California Institute of Technology, Pasadena, California,

1987.

7   St. Clair, M. A. Ph.D. Dissertation, California Institute of Technology, Pasadena,

California, 1989. Note: $HN(CH_3(CH_2C_6H_5)$ was also shown to react with

$Cp*_2Ta(=CH_2)H$ at 130° C over a period of days to give, among other products,

$Cp*_2Ta(\eta^2-CH_2=NCH_2C_6H_5)H$. Reactions with other amines gave only "tuck-in"

products.

8   See, for example: (a) Mayr, A.; McDermott, G. A.; Dorriew, A. M., Holder, A. K.; Fulz, W. C.; Rheingold, A. L. *J. Am. Chem. Soc.* **1986**, *108*, 310. (b) Hofman, L.; Werner, H. *Chem. Ber,* **1985**, *118*, 4229. (c) Buhro, W. E.; Etter, M. C.; Georgiou, S.; Gladysz, J. A.; McCormick, F. B. *Organometallics,* **1987**, *6*, 1150.

9   Buchwald, S. L.; Nielsen, R. B.; Dewan, J. C. *J. Am. Chem. Soc.* **1987**, *109*, 1590.

10   Park, J. W.; Henling, L. M.; Schaefer, W. P.; Grubbs, R. H. *Organometallics* **1990**, *9*, 1650.

11   Allen, F. H.; Kennard, O.; Watson, D. G.; Brammer, L.; Orpen, A. G.; Taylor, R. *J. Chem. Soc. Perkin Trans. II* **1987**, S14.

12   Orpen, A. G.; Brammer, L.; Allen, F. H.; Kennard, O.; Watson, D. G.; Taylor, R. *J. Chem. Soc Dalton Trans.* **1989**, S1.

13   Note: This is almost identical to the activation barrier seen for Cp*$_2$Ta(η^2-OCH$_2$)H, reference 5.

14   Whinnery, L., unpublished results.

15   Note: Although permethyltantalocene styrene hydride reacts with ethylene sulfide cleanly, it does not exhibit analogous reactivity toward ethylene oxide or nitrous. The Cp*$_2$Ta(=O)(CH$_2$CH$_2$C$_6$H$_5$) complex may be prepared, however from PHIO. Nelson, J., unpublished results.

16   Bock, P. L.; Boschetto, D. J.; Rasmussen, J. R.; Demers, J. P.; Whitesides, G. M. *J. Am. Chem. Soc.* **1974**, *96*, 2814.

17   Schwartz, J.; Labinger, J. A.; *Angew. Chem. Int. Ed. Eng.* **1976**, *15*, 333.

18   Nelson, J. E.; Labinger, J. A.; Bercaw, J.E. *Organometallics* **1989**, *8*, 2484.

19   Roberts, J. D.; Caserio, M. C. *Basic Principles of Organic Chemistry* W. A. Benjamin, Inc.: Menlo Park, California **1977**, p. 423.

20   Parkin, G., unpublished results.

21   Quan, R., unpublished results.

22   Parkin, G.; Bercaw, J. E. *Polyhedron* **1988**, *7*, 2053.

23 Burger, B. J.; Bercaw, J. E. in "New Developments in the Synthesis, Manipulation, and Characterization of Organometallic Compounds"; Wayda, A. and Darensbourg, M. eds.; ACS Symposium Series, **1987**, *357*, 79-98.

24 Marvich, R. H.; Brintzinger, H. H. *J. Am. Chem. Soc.* **1971**, *93*, 2046.

25 Gibson, V. C.; Bercaw, J. E.; Bruton, W. J.; Sanner, R. D. *Organometallics* **1986**, *5*, 986.

26 van Asselt, A.; Burger, B. J.; Gibson, V. C.; Bercaw, J. E. *J. Am. Chem. Soc.* **1986**, *108*, 5347.

27 Trimmer, M. S., Ph.D. Dissertation, California Institute of Technology, Pasadena, California, 1989.

28 Buchwald, S. L.; LaMaire, S. J.; Nielsen, R. B.; Watson, B. T.; King, S. M. *Tetrahedron Lett.* **1987**, *28*, 918.

29 Note: The $Cp*_2Ta(CH_2=CHC(CH_3)_3)H$ complex could not be prepared by this method, Nelson, J. and Quan, R., unpublished results.

30 Note: The elemental analysis for this compound appears low, probably due to a significant amount of $Cp*_2Ta(\eta^2\text{-S=CHPh})H$ present.

31 Johnson, C. K. *ORTEP-II: A FORTRAN Thermal Ellipsoid Program for Crystal Structure Illustrations.* Report ORNL-3794, Third Revision, Oak Ridge National Laboratory, Oak Ridge, Tennessee, **1976**.

32 Cromer, D. T.; Waber, J.T. in *International Tables for X-ray Crystallography, Vol. IV* Ibers, J. A.; Hamilton, W. C. eds. The Kynoch Press: Birmingham, England **1974**, p. 71, p. 148.

Chapter 2

Investigations of the Hydrozirconation of Styrene: Observations of Unusual Regioselectivity and An Unusual Isotope Scrambling Process[1]

Abstract:

In contrast to the extremely specific regioselectivity and stereoselectivity normally demonstrated by Schwartz's reagent (Cp_2ZrHCl), hydrozirconation of styrene shows two unusual behaviors. First, treatment of Cp_2ZrHCl with styrene leads to a mixture of terminal (85%) and internal (15%) insertion products. The benzylic insertion product is stable, and does not undergo migration to a terminal organozirconium product, even when heated.   Second, attempts to prepare stereospecifically labeled deutero organozirconium derivatives result in scrambling of the β positions of both isomers, yielding a statistical distribution of isotopomers. The features of this scrambling process are described and a mechanism involving an organozirconium alkyl hydride species is proposed.

Introduction

Hydrometallation is the addition of a metal-hydrogen bond across an unsaturated group, usually alkenes or alkynes, to produce a σ-alkyl transition metal complex.[2]

$$M\text{-}H \; + \; C=C \; \xrightarrow{\hspace{2cm}} \; M\text{-}C\text{-}C\text{-}H \tag{1}$$

This process is often a key step in the catalytic hydrogenation of olefins. Hydroboration, until twenty years ago, was the most useful and well studied of these hydrometallation processes.[3]

Hydrozirconation was developed in the mid 1970's by Schwartz and coworkers, and has been the most extensively studied hydrometallation reaction. The zirconocene hydrido chloride (Cp_2ZrHCl), known now as Schwartz's reagent, is a 16 electron, d^0, Zr(IV) complex which reacts with alkenes and alkynes to form stable organozirconium products. The synthesis of Cp_2ZrHCl was first reported by Wailes and Weigold in 1970 from treatment of Cp_2ZrCl_2 with $LiAlH_4$ or $LiAl(O^tBu)_3H$ to produce the insoluble polymer, $(Cp_2ZrHCl)_n$.[4] It was subsequently shown that Cp_2ZrHCl reacted with alkynes and alkenes.[5] Schwartz modified the preparation, using Red-Al ($Na[AlH_2(OCH_2CH_2OCH_3)_2]$) as the reductant,[6] and demonstrated the synthetic utility of the system.[7] Recently, Buchwald and coworkers have reported another modification of the Cp_2ZrHCl synthesis which utilizes a purified $LiAlH_4$ solution as a reductant (to eliminate contaminants in the reducing agent) and a final CH_2Cl_2 rinse (to convert over-reduced Cp_2ZrH_2 back to Cp_2ZrHCl).[8] Now, hydrometallation is a powerful synthetic tool, as Cp_2ZrHCl is conveniently prepared as well as possessing many other attributes.

Hydrozirconation affords a stable transition metal hydride complex available to effect a wide number of synthetic transformations. Cp_2ZrHCl has been used extensively as it reduces a wide range of functional groups. Electrophilic cleavage of organozirconium compounds leads to useful organic products. For example, protonation of the organozirconium product leads to the

the corresponding hydrocarbon, bromination to the alkyl bromide, and oxidation to the alcohol. Hydrozirconation also proceeds with high selectivity, especially regio- and stereoselectivity.

The regioselectivity of this system is striking. Hydrozirconation of olefins always results in terminal alkylzirconium products (except for cyclic olefins), regardless of the original position of the double bond in the olefin. Rapid migration by addition-elimination reactions places the zirconium in the least hindered position, presumably due to the steric demands of the two cyclopentadienyl rings.

However, less than complete regiospecificity has been observed by examination of cleavage products of hydrozirconation. Hydrozirconation of aromatic olefins has been shown to give mixtures of benzylic as well as terminal cleavage products, as shown in Equations 2-4.

$$Cp_2ZrHCl \xrightarrow{\text{PhCH=CH}_2} \xrightarrow{\text{isocyanide}} \xrightarrow{I_2} \qquad (2)[9]$$

2.6 : 1

$$Cp_2ZrHCl \xrightarrow{\text{PhCH=CH}_2} \xrightarrow{O_2} \qquad (3)[10]$$

3.4 : 1

$$Cp_2ZrHCl \xrightarrow{\text{PhCH=CH}_2} \xrightarrow{I_2} \qquad (4)[11]$$

9 : 1
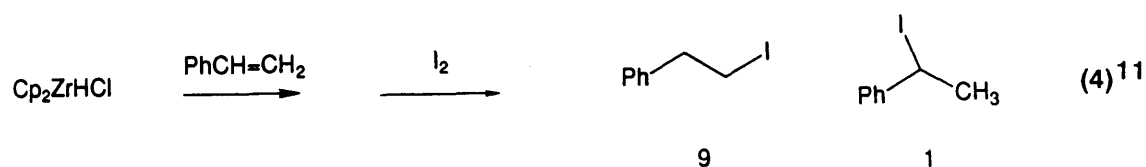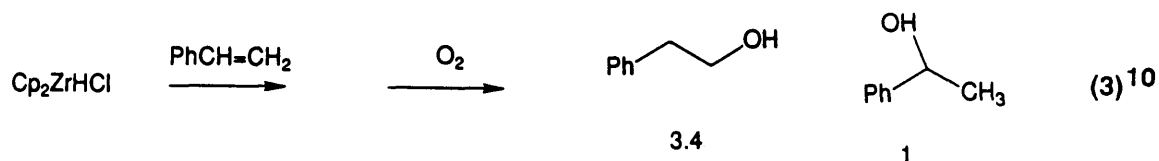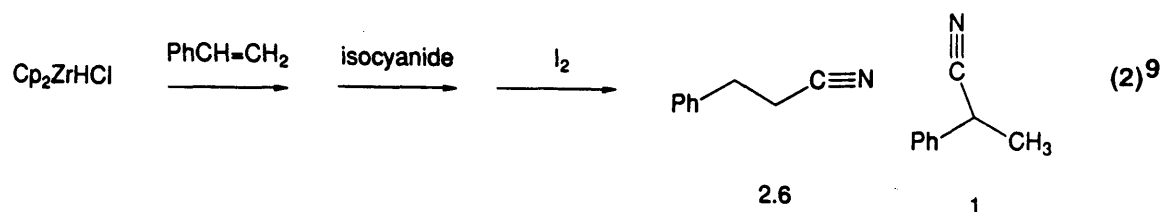
The ratio of the terminal to benzylic cleavage products for the hydrozirconation of styrene seems to depend on the reagent used. For example, Gibson and coworkers report that oxidation with O_2 yields a higher benzylic to terminal alcohol ratio than if ^tBuOOH is used.[11] It is not clear from these studies if two organozirconium isomers, a terminal and a benzylic, are present, or if isomerization is induced by the cleavage reaction.

Another issue in the mechanism of hydrozirconation is the stereoselectivity of the insertion. Although the mechanism of hydrozirconation is not completely defined, alkynes and alkenes always react with Cp_2ZrHCl in a cis manner. Also, cleavage has been shown to occur with retention of configuration about carbon.[12]

The use of NMR stereochemical probes such as $Me_3CCHDCHDX$ as a mechanistic tool was introduced to organometallic chemistry by Whitesides.[13] It was recognized that hydrozirconation itself provides a particularly convenient synthetic route to these desired stereolabeled compounds,[14] as it generally proceeds with high stereo- and regioselectivity. For example, subsequent hydrozirconation of t-butylacetylene and 3,3-dimethyl-1-butene has been shown to give stereospecifically labeled bromides (Equations 5-6).

(5)

Threo

(6)

Erythro
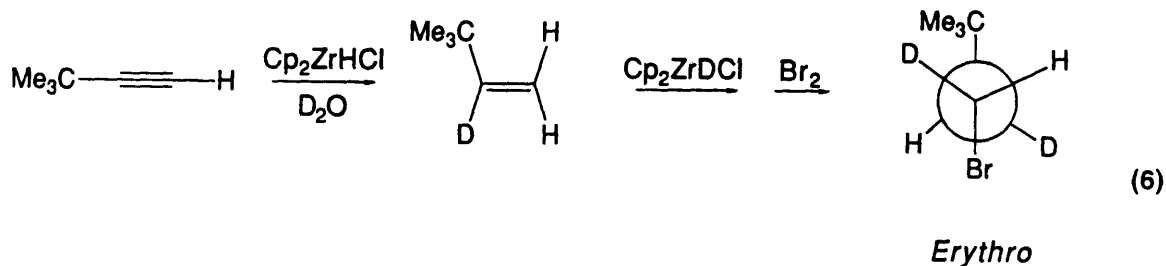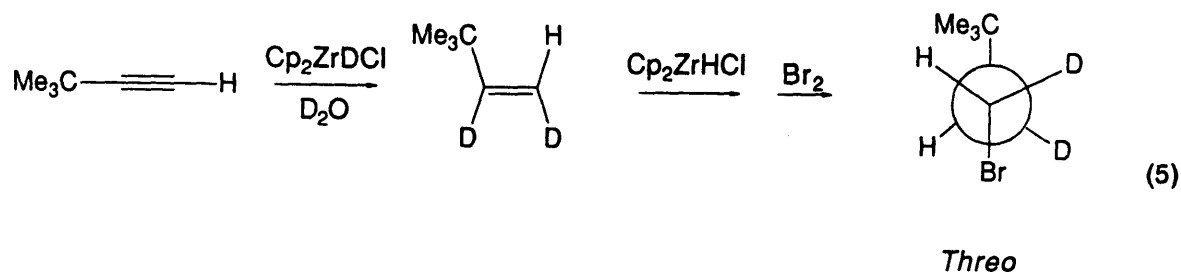
As discussed in Chapter 1, analogous diastereotopic labeled phenethyl derivatives were needed. In utilizing hydrozirconation to produce these derivatives, unusual behaviors for the hydrozirconation of styrene have been observed. This chapter will address the regio- and stereoselective issues of this reaction.

Results and Discussion

Unusual Regioselectivity for the Hydrozirconation of Styrene.

As mentioned, hydrozirconation of styrene, in contrast to most olefins, gives *both* terminal (1) and internal (2) cleavage products. Although analysis of cleavage products from the hydrozirconation of styrene shows products consistent with both the normal and benzylic insertion,[15] the sole report of the direct NMR examination of the organozirconium product(s) produced for the hydrozirconation of styrene reports on only the terminal insertion product.[16] Monitoring the reaction between Cp_2ZrHCl and styrene by high field ^{1}H NMR spectroscopy (Figure 1) reveals that at room temperature 1 and 2 are formed in a ratio of 85:15 (Eqn. 7). This ratio does not change appreciably even upon heating the products in benzene at 100° C.

$$(7)$$

(1)   (2)

85%   15%
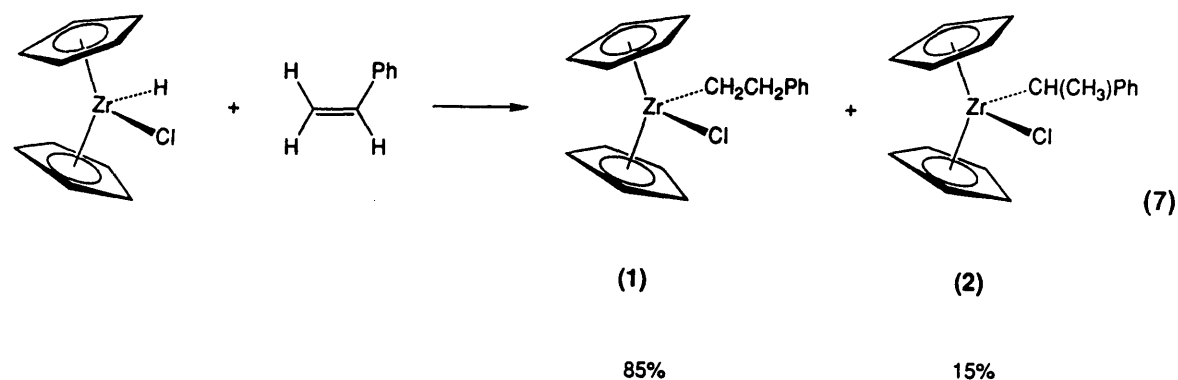
The peaks attributable to 1 are as reported previously, and the AA'XX' pattern may be fully analyzed.[17] The assignment of resonances due to 2 is also straightforward. (See Table 1 for ^{1}H NMR data.)

Figure 1: 500 MHz ^{1}H NMR Spectrum (in Benzene-d_6) of Products of

Reaction of Cp$_2$ZrHCl and CH$_2$=CHPh.
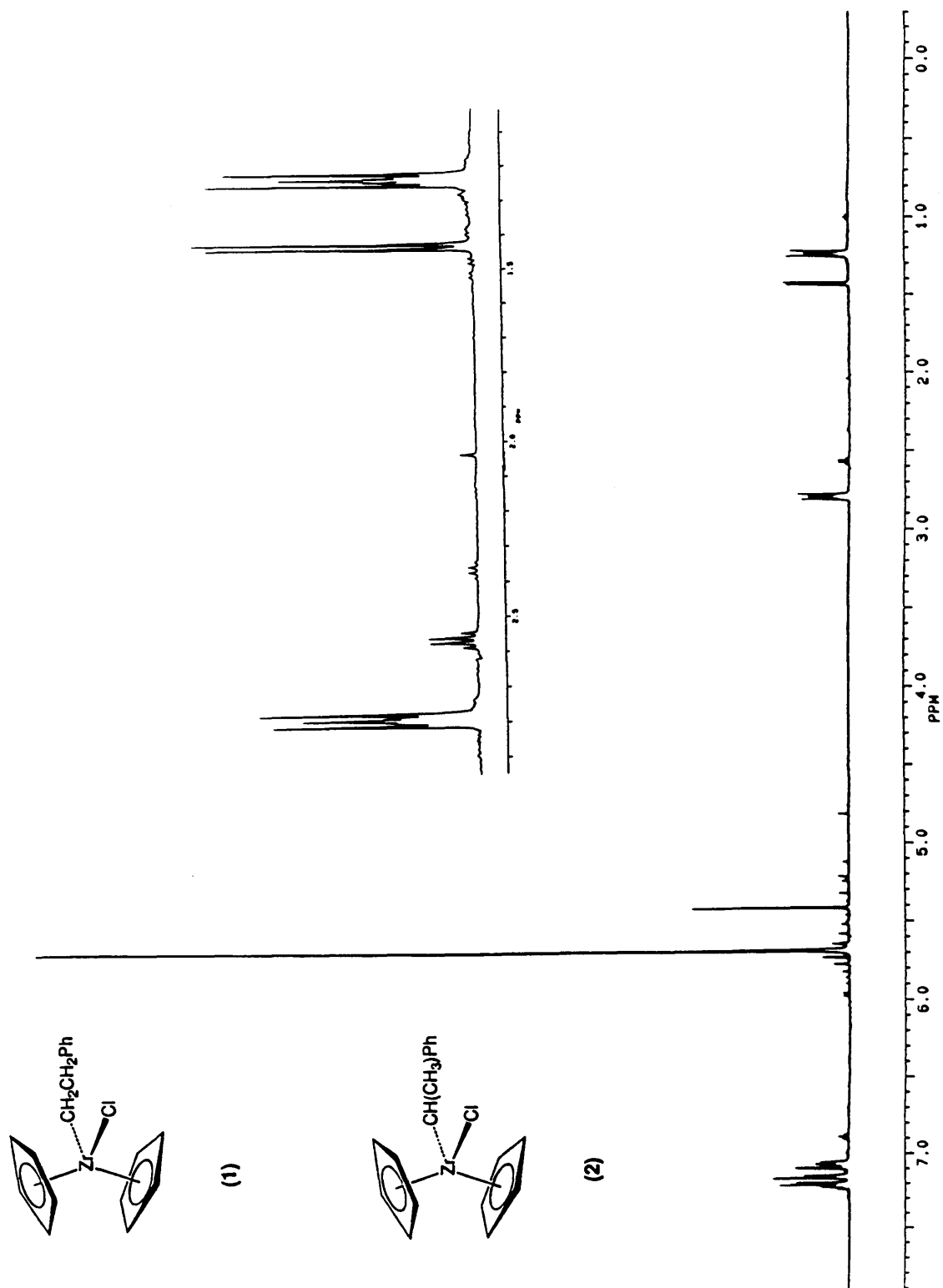
Examination of Regioselectivity for Hydrozirconation of Other Aromatic Olefins.

This striking result of the regioselectivity is the first report of a stable non-terminal hydrozirconation product. We chose to investigate the organozirconium products for the hydrozirconation of other aromatic olefins to see if this is a general observation or simply a special observation for styrene.

^1H NMR spectrum of the hydrozirconation products of Cp_2ZrHCl and allyl benzene ($PhCH_2CH=CH_2$) shows that the terminal insertion product is exclusively obtained. Reaction of Cp_2ZrHCl with *trans*-α-methylstyrene ($PhCH=CHCH_3$) initially yields the benzylic insertion product which slowly rearranges (two days at room temperature) to the terminal product.

Reactions of Cp_2ZrHCl with *para* substituted styrenes ($CH_2=CHC_6H_4X$ with X = Me, OMe, Cl, F) have also been investigated. The ^1H NMR data for these insertions are given in Table 2. They show no significant deviation of the ratio of terminal and benzylic organozirconium insertion products from that shown by hydrozirconation of styrene.

We have also examined the insertion reaction of styrene with another potential hydrozirconation reagent, Cp^*_2ZrHCl. Here, only one organozirconium insertion product, the terminal one, is observed by ^1H NMR spectroscopy. This is almost certainly due to the steric interactions from the pentamethylcyclopentadienyl rings.

Unusual Isotope Scrambling for the Hydrozirconation of Styrene.

In contrast to the neohexyl system,[18] a complicated mixture of products is obtained when employing hydrozirconation to make stereospecific labeled PhCHDCHDX derivatives. In fact, the ^1H NMR spectra of what should be *threo* and *erythro* PhCHDCHDBr are identical. To simplify the investigation of these products, the reaction of Cp_2ZrDCl with $CH_2=CHPh$, to produce the *mono*-deutero derivative, has been followed.

Surprisingly, the ^{1}H NMR spectrum of the products for the reaction of $Cp_2(Cl)ZrD$ with

$CH_2=CHPh$ (Figure 2) *is not* that predicted for simple replacement of D for H in the β positions of

1 and 2. Rather, the signals clearly include as well patterns for $Cp_2(Cl)ZrCH_2CH_2Ph$ (1-d_0) and

$Cp_2(Cl)ZrCH_2CD_2Ph$ (1-βd_2) together with $Cp_2(Cl)ZrCHPhCH_3$ (2-d_0), $Cp_2(Cl)ZrCHPhCHD_2$

(2-βd_2) and $Cp_2(Cl)ZrCHPhCD_3$ (2-βd_3), in roughly statistical amounts (1-d_0: 1-βd_1: 1-βd_2 $\approx$

1:2:1; 2-d_0: 2-βd_1: 2-βd_2: 2-βd_3 $\approx$ 8:12:6:1)

$(n=0,1,2)$ $(n=0,1,2,3)$

$(1$-d_0, 1-βd_1, 1-$\beta d_2)$ $(2$-d_0, 2-βd_1, 2-βd_2, 2-$\beta d_3)$
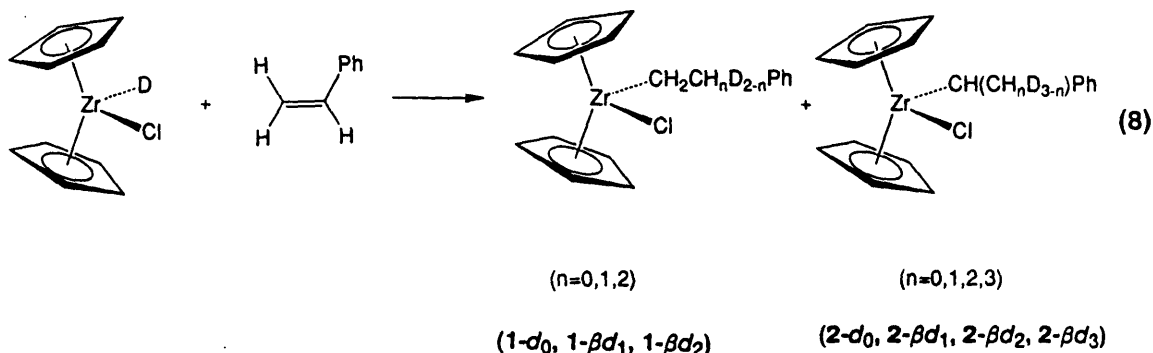
^{1}H NMR decoupling experiments confirm the presence of these isotopomers. Examination of the reaction of *cis-d_2*-styrene with Cp_2ZrHCl shows even more complicated ^{1}H NMR patterns, which were not fully assigned.

The source of the proton in the β position yielding these isotopomers has been examined. Initially, the Cp_2ZrDCl reagent was thought to be contaminated by Cp_2ZrHCl. Treatment of the Cp_2ZrDCl with acetone, however, shows no detectable protio signal for $Cp_2(Cl)Zr(-OCHMe_2)$. Therefore, some exchange process may be responsible for scrambling the organozirconium products. One easily envisioned method of scrambling the deuterium label is the reversible insertion of the olefin. This mechanism would require complete D/H exchange.

Significantly, ^{2}H NMR spectroscopy (Figure 3) reveals that *isotopomers which contain deuterium in the α positions* (1-αd_1, 1-αd_2 or 2-αd_1) *are initially obtained in no more than 10% yield.* Deuterium scrambling into the α positions is very slow, so that even after one week at room temperature the amount of deuterium in the α positions of **1** and **2** is less than 20% of statistical.

Figure 2: 500 MHz ^{1}H NMR Spectra (in Benzene-d_6) of Alkyl Region of

Products of Reaction of (a) Cp$_2$ZrHCl and CH$_2$=CHPh

## and (b) Cp$_2$ZrDCl and CH$_2$=CHPh
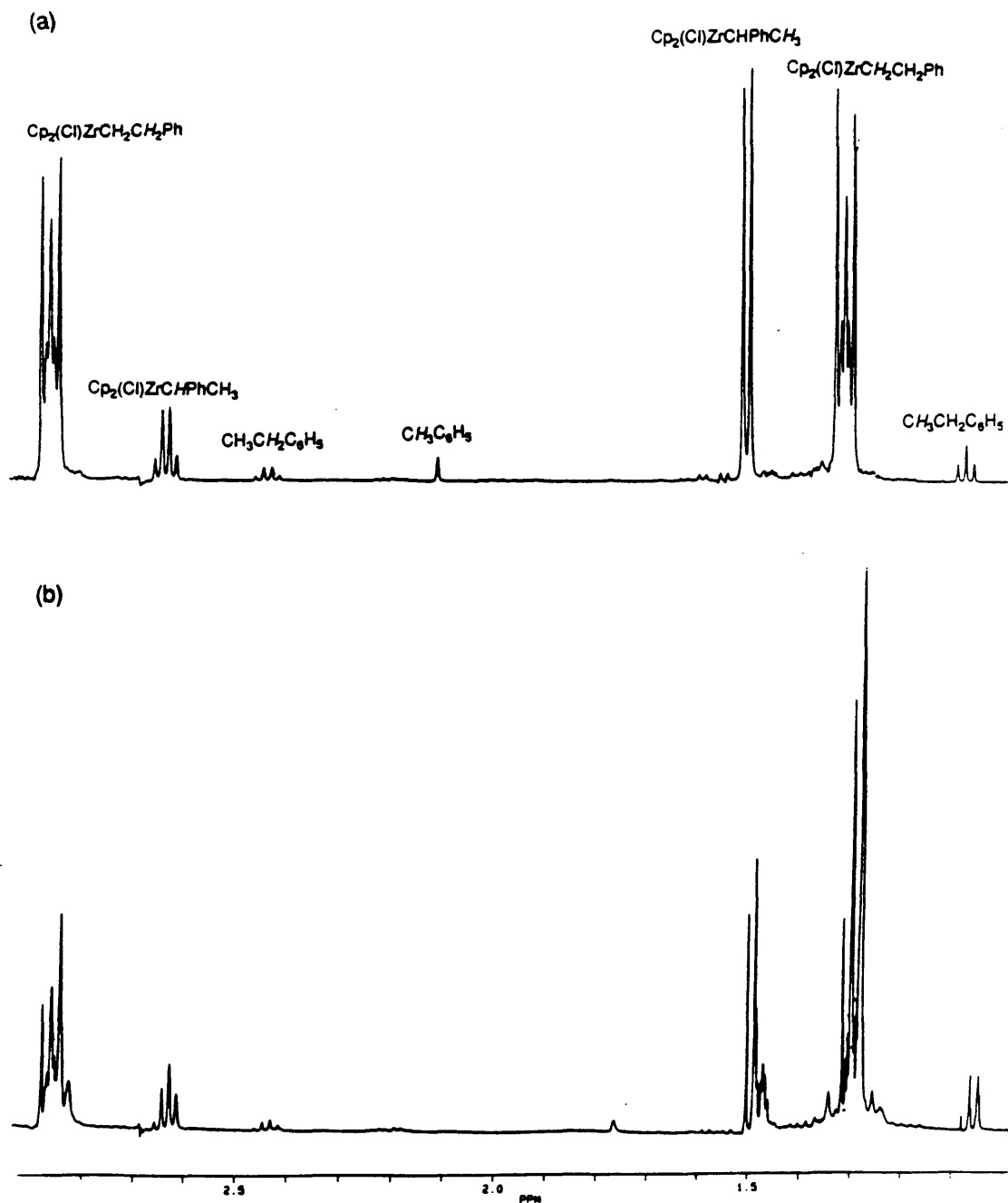
Figure 3: ^{2}H NMR Spectrum (^{1}H Decoupled in C_6H_6) of Products of

Reaction of Cp_2ZrDCl and $CH_2=CHPh$
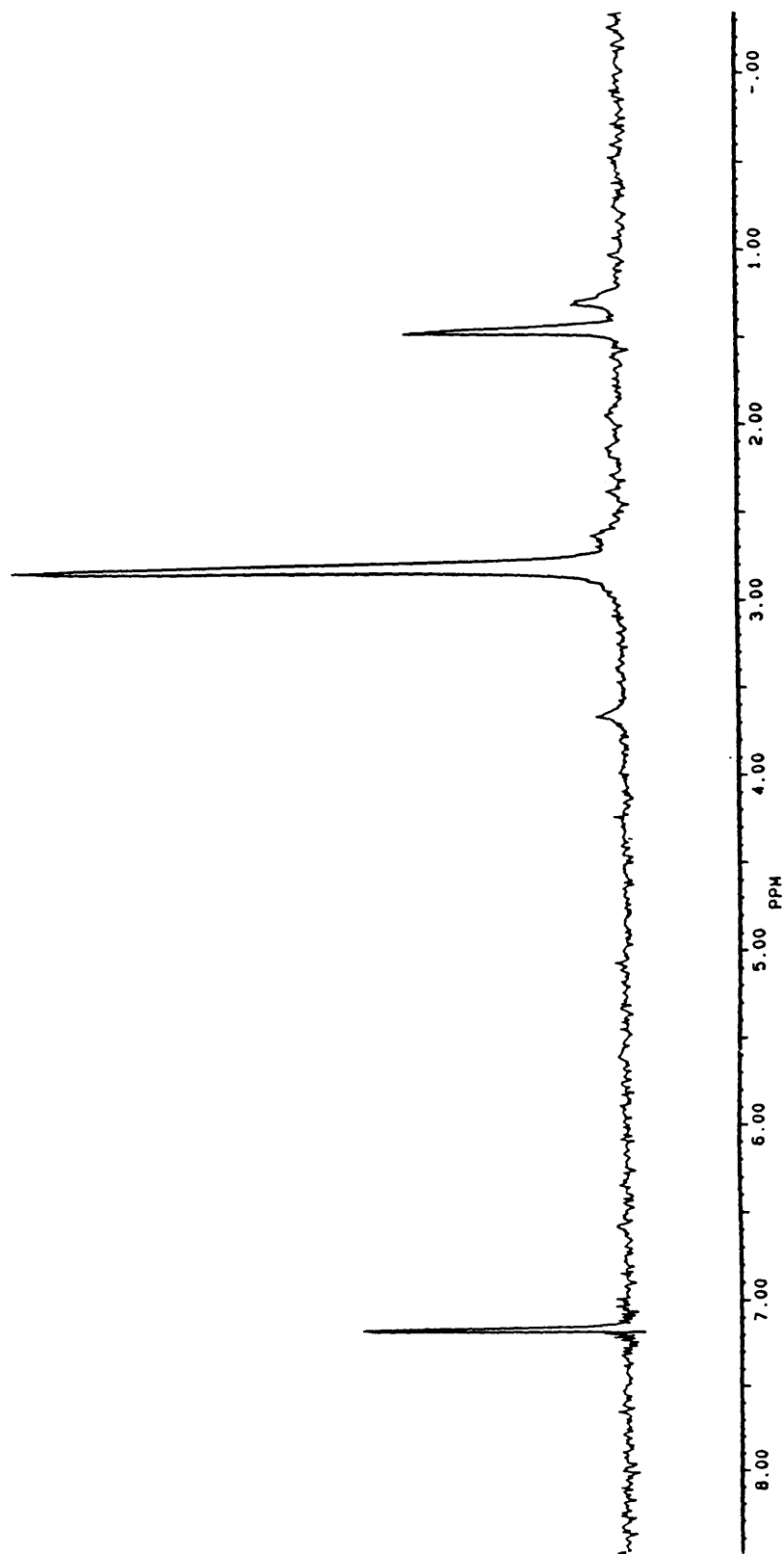
The above results suggest that two distinct exchange processes are operating: (1) a fast exchange of (only) β hydrogens between various alkyl derivatives, and (2) a much slower exchange which eventually exchanges α and β hydrogens, most likely via the reverse of Equation 7. With regard to the fast exchange process, we have made the following observations: (i) a mixture of $Cp_2(Cl)ZrCH_2CH_2C_6H_5$ ($1\text{-}d_0$) and $Cp_2(Cl)ZrCD_2CD_2C_6D_5$ ($1\text{-}d_9$) (isolated separately from $Cp_2(Cl)ZrH$ and $CH_2=CHC_6H_5$ and from $Cp_2(Cl)ZrD$ and $CD_2=CDC_6D_5$, respectively) shows complete (β) scrambling within 30 min in benzene at 25°C (These isolated samples also contained ca. 15% $2\text{-}d_0$ and $2\text{-}d_9$. Faster exchange of the β positions of $1\text{-}d_0$ and $1\text{-}d_9$ is observed, almost certainly because 2 dissolves much slower in benzene than 1. When this sample was examined 12 hr later, 2 was in solution and exchange was complete.), (ii) over the same period no deuterium incorporation into $Cp_2(Cl)ZrCH_2CH_2Ph$ is observed when it is treated with an equivalent of $CHD=CDPh$ (benzene-d_6, 25°C; ^{1}H NMR).

The fast process is remarkable, not only because it is specific for exchange between β positions, but also because it occurs rapidly after hydrozirconation is complete and without exchange with free styrene. Given these very restrictive requirements, we suggest the mechanism in the Scheme (shown for 1 only). The following points are particularly notable: (i) scrambling is catalyzed by a small amount of a zirconium(alkyl)*hydride* complex $Cp_2(H)ZrR$, produced from the Cp_2ZrH_2 present in the initial preparation of Cp_2ZrHCl[19] (Exchange between metal- and β-alkyl positions has previously been demonstrated in such a compound.[20]), (ii) the geometry of the olefin-dihydride intermediate must be that shown in the Scheme; otherwise this mechanism would interconvert 1 and 2 and thus provide facile α-exchange (Since this result apparently requires that H-D exchange is facile but olefin rotation is very slow, one might speculate that the bonding is better described as metallacyclopropane-dihydrogen than as olefin-dihydride as shown in the Scheme.[21]), (iii) chain-propagating hydride-for-chloride exchange proceeds via bridged dimers; all such $Cp_2(X)ZrH$ species are at least dimeric.
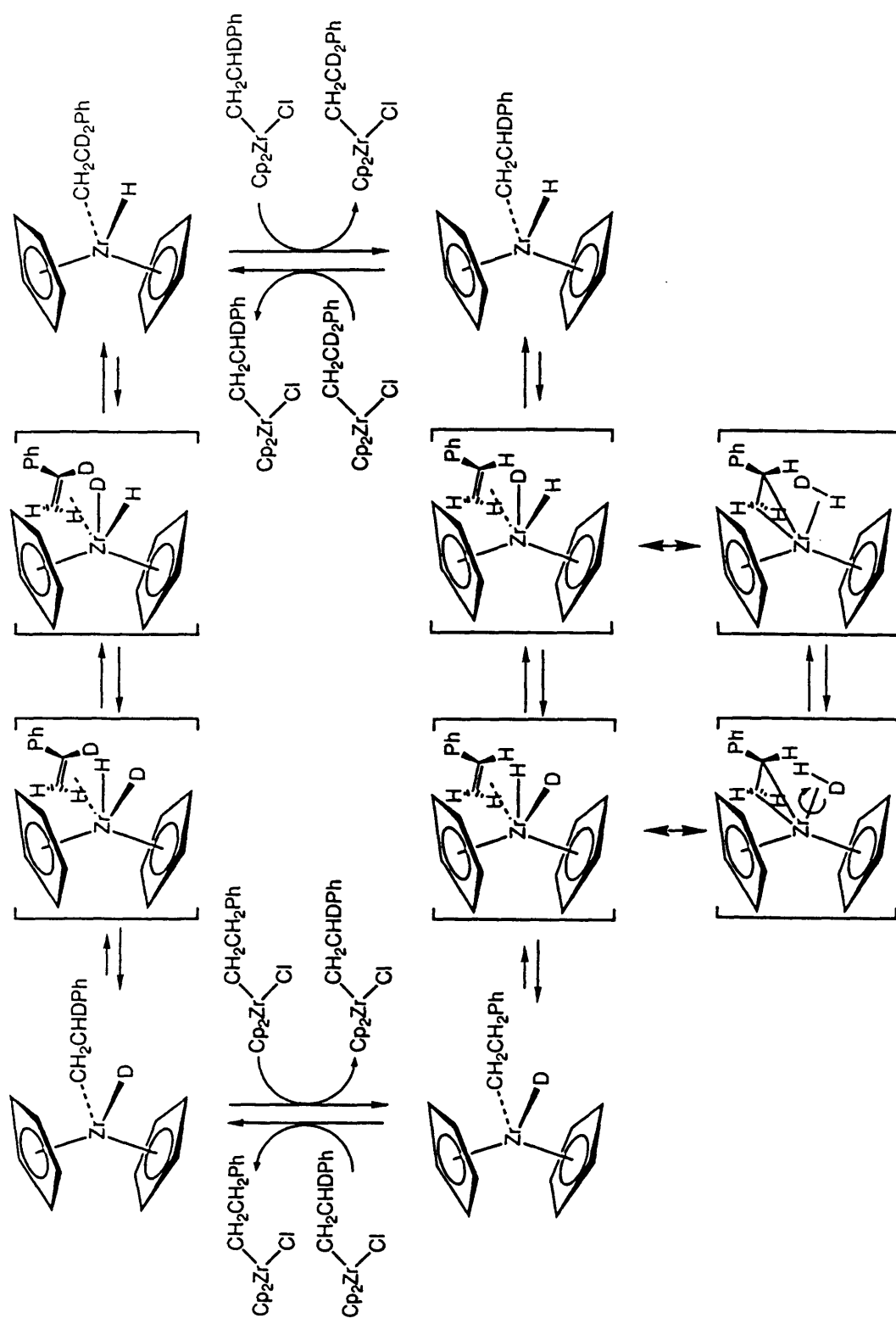
Further support that a zirconocene alkyl hydride species is important to the scrambling process (although such a species is never observed *via* ^{1}H NMR) is evidenced by reaction with acetone. In accord with the proposed mechanism, when solutions of 1-d_0 and 1-d_9 in benzene-d_6, each containing *ca.* 0.5 equivalent acetone to convert any [Zr-H] to [Zr-OCHMe$_2$], are mixed, *no H/D exchange is observed*, even after 12 hrs.

Examination For Isotopic Scrambling in Hydrozirconation of Other Olefins.

Again, the question arises: is this isotopic scrambling process unique to styrene or is it common to other aromatic olefins? Monitoring the reaction of Cp$_2$ZrDCl with allyl benzene and *trans*-α-methyl-styrene by ^{1}H NMR confirms that no unusual behavior occurs for these aromatic olefins. Apparently styrene is a special case. Reactions with *para*-substituted styrenes (CH$_2$=CHC$_6$H$_4$X, X = Me, OMe, Cl, F) show the same isotope scrambling as does styrene. Reaction with Cp*$_2$ZrHCl and *cis-d_2*-styrene has also been examined. Even though this reaction shows no other insertion products than the normal terminal one, complete scrambling in the β position also occurs for this reagent.

Conclusions

Regiospecific results of the hydrozirconation of styrene show that stable benzylic insertion product for this olefin is a special case. This perhaps is due to sterics or benzylic stabilization, but it is not clear then why other aromatic olefins do not show the same behavior.

Since stereospecific hydrozirconation *can* be effected in the neohexyl system, scrambling must not take place there; the reaction of Cp$_2$ZrDCl with CH$_2$=CHCMe$_3$ gives no detectable isotopomers other than the expected Cp$_2$(Cl)ZrCH$_2$CHDCMe$_3$. Also, *no scrambling* is found in the reactions of Cp$_2$(Cl)ZrD with CH$_2$=CHCH$_2$Ph or PhCH=CHCH$_3$. These

preliminary results suggest that styrene is the special case; perhaps the olefin complex is stabilized by conjugation relative to alkyls **1** and **2**, thus accelerating the β-elimination steps in the Scheme. Stabilization of olefin-hydride relative to inserted alkyl by phenyl has been inferred for the sterically (but *not* electronically) similar systems $Cp_2NbH(CH_2=CHR)$.[22]

It is striking that styrene is also special in that it gives significant amounts of the non-terminal hydrozirconation product. This work, however, suggests that these two manifestations of special behavior are *not* interconnected in any obvious manner.

Table 1: ^{1}H NMR Data in C_6D_6 at 25° C

Compound	Assignment	δ (ppm)	J (Hz)
$Cp_2(Cl)ZrCH_2CH_2Ph$	Cp	5.69 s	
	CH_2CH_2Ph	1.23 a	gem 14.0, 12.3
	CH_2CH_2Ph	2.78 a	vicinal 12.5, 4.4
	Ph	b	
$Cp_2(Cl)ZrCH(CH_3)Ph$	Cp	5.41 s	
	$CH(CH_3)Ph$	1.42 q	7.0
	$CH(CH_3)Ph$	2.56 d	7.0
	Ph	b	
$Cp^*_2(Cl)ZrCH_2CH_2Ph$	Cp*	1.80 s	
	CH_2CH_2Ph	0.90 a	gem 15.5, 16.9
	CH_2CH_2Ph	2.72 a	vicinal 13.5, 4.3
	Ph	7.09 t	
		7.27 t	
		7.38 d	
$Cp_2Zr(Cl)CH(Ph)CH_2CH_3$[c]	Cp	5.56 s	
		5.80 s	
	CH	2.45 dd	2.55, 11.2
	CH_2	1.94 m	
	CH_3	0.91 t	
	Ph	b	
$Cp_2(Cl)ZrCH_2CH_2CH_2Ph$[d]	Cp	5.72 s	
	$CH_2CH_2CH_2Ph$	1.08 m	
	$CH_2CH_2CH_2Ph$	1.87 m	
	$CH_2CH_2CH_2Ph$	2.57 t	
	Ph	b	

(a) AA'XX' coupling pattern was observed. (b) The phenyl region was not well enough resolved to make definite assignments. (c) Peaks are from first insertion product from Cp_2ZrHCl + trans-$CH_3CH=CHPh$. (d) NMR data from Cp_2ZrHCl + $PhCH_2CH=CH_2$ or from Cp_2ZrHCl + trans-$CH_3CH=CHPh$ after migration to terminal product (two days).

Table 2: ^{1}H NMR Data for Products of Reaction of

Cp_2ZrHCl with *para* Substituted Styrenes, $CH_2=CHC_6H_4X$

X	δ Cp (Terminal)	δ Cp (Benzylic)	Terminal:Benzylic
H	5.69	5.41	85:15
Me	5.78	5.50	88:12
OMe	5.77	5.49	89:11
Cl	5.73	5.42	81:19
F	5.74	5.44	90:10

Experimental Section

General Considerations. All air sensitive manipulations were performed by using high vacuum line or glove box techniques.[23] Argon and nitrogen gases were purified by passage over MnO on vermiculite and activated 4 Å molecular sieves. Solvents were dried over CaH_2 or Na/benzophenone and either stored under vacuum over "titanocene,"[24] sodium benzophenone ketyl, or stored under argon for Schlenk use. Benzene-d_6 was dried over 4 Å molecular sieves and stored over titanocene.

Starting Materials. Cp_2ZrCl_2 was purchased from Aldrich and used without further purification. $LiAlH_4$ and $LiAlD_4$ (Aldrich, received as a grey powder) were dissolved in ether, the solutions filtered, and the solvent removed *in vacuo* to yield a white ether soluble powder. Phenylacetylene, styrene, styrene-d_8, allylbenzene, *trans*-α-methylstyrene, and 4-methoxy-styrene, 4-methylstyrene, 4-chlorostyrene, and 4-fluorostyrene were obtained from Aldrich and used without further purification. $Cp*_2ZrHCl$ was a sample prepared by P.T. Barger according to published procedure.[25]

Cp_2ZrHCl and Cp_2ZrDCl were prepared according to Buchwald's published procedure,[9] with the following modifications: (1) $LiAlH_4$ and $LiAlD_4$ were *always* isolated from ether and redissolved before use and (2) the entire procedure was done in a glove box, thus eliminating cannula filtration and slow line filtration.

Spectra. ^{1}H NMR spectra were recorded with Varian EM-390 (90 MHz) and Bruker WM500 (500.13 MHz) spectrometers. ^{2}H NMR spectra (^{1}H decoupled) were recorded with a Bruker WM500 (76.775MHz) spectrometer.

Cp$_2$(Cl)ZrCH$_2$CH$_2$Ph (1-d_0). Cp$_2$ZrHCl (1.0 g, 3.9 mmol) was suspended in 10 mL toluene. Styrene (0.45 mL, 1.2 eq) was added *via* syringe against an Ar counterflow. The solution was stirred 3 hours until all of the Cp$_2$ZrHCl dissolved, yielding a dark red orange solution. The solution was filtered and toluene was removed *in vacuo* to yield 0.53 g (36% yield) brown powder. The product contains *ca.* 15% Cp$_2$(Cl)ZrCH(Ph)CH$_3$.

Cp$_2$(Cl)ZrCD$_2$CD$_2$C$_6$D$_5$ (1-d_9). Cp$_2$ZrDCl (1.0 g, 3.9 mmol) was suspended in 15 mL toluene. Styrene-d_8 (0.50 mL, 1.2 eq) was added *via* syringe against an Ar counterflow. The solution was stirred 5 hours until all Cp$_2$ZrHCl dissolved, yielding a dark red orange solution. The solution was filtered and toluene was removed *in vacuo* to yield 0.76 g (54% yield) dark orange sticky solid.[26] The product contains *ca.* 15% Cp$_2$(Cl)ZrCD(Ph)CD$_3$. ^{1}H NMR showed deuterium incorporation of greater than 95%.

Cis-**Styrene-d_2.** Cp$_2$ZrDCl (10.5 g, 40.5 mmol) was suspended in 50 mL toluene. Phenylacetylene (5.0 mL, 1.1 eq) was added *via* syringe against an Ar counterflow. The solution was stirred 2 hours until all of the Cp$_2$ZrDCl dissolved, yielding a dark orange solution. The toluene was removed *in vacuo* and the remaining orange goo was dissolved in 50 mL diethyl ether. The solution was cooled to 0° C, and 1.0 mL degassed D$_2$O was slowly added *via* syringe against an Ar counterflow over 30 min. The [Cp$_2$ZrO]$_x$ was filtered and the styrene was vacuum distilled to yield 5.1 mL *cis*-styrene-d_2. ^{1}H NMR showed greater than 95% deuterium incorporation.

Procedure for Hydrozirconation of Olefins. Many of the reactions reported were carried out in septum-capped NMR tubes. Approximately 15 mg of Cp$_2$ZrHCl or Cp$_2$ZrDCl was placed in an NMR tube in the glove box, approximately 0.4 mL C$_6$D$_6$ was added, and the tube was capped

with a rubber septum. Known amounts of olefin were syringed in through the septum, and the tube was shaken until all the zirconium reagent dissolved.

Procedure for acetone trapping. A small sample (*ca.* 15 mg) of $Cp_2(Cl)ZrCH_2CH_2Ph$ (1-d_0) was dissolved in 0.3 mL C_6D_6 in an NMR tube and treated with *ca.* 0.5 equivalents of acetone. A separate sample of $Cp_2(Cl)ZrCD_2CD_2C_6D_5$ (1-d_9) was prepared in a similar manner. After 30 minutes, the 1-d_0 and 1-d_9 samples were combined in the glove box, and the reaction was monitored by ^1H NMR.

References

1   The bulk of this chapter has appeared in print: Nelson, J. E.; Bercaw, J. E.; Labinger, J. A. *Organometallics* **1989**, *8*, 2484.

2   Collman, J. P.; Hegedus, L. S.; Norton, J. R.; Finke, R. G. *Principles and Applications of Organotransition Metal Chemistry* University Science Books: Mill Valley **1987**, p. 698.

3   Brown, H. C. *Hydroboration* W. A. Benjamin, Inc.: New York **1962**.

4   Wailes, P. C.; Weigold, H. *J. Organomet. Chem.* **1970**, *24*, 405.

5   (a) Wailes, P. C.; Weigold, H.; Bell, A. P.; *J. Organomet. Chem.* **1971**, *27*, 373. (b) Wailes, P. C.; Weigold, H.; Bell, A. P.; *J. Organomet. Chem.* **1972**, *43*, C32.

6   Carr, D.B.; Schwartz, J. *J. Am. Chem. Soc.* **1979**, *101*, 3521.

7   Hart, D. W.; Schwartz, J. *J. Am. Chem. Soc.* **1974**, *98*, 8115.

8   Buchwald, S. L.; LaMaire, S. J.; Nielsen, R. B.; Watson, B. T.; King, S. M. *Tetrahedron Lett.* **1987**, *28*, 3895.

9   Buchwald, S. L.; LaMaire, S. J.; *Tetrahedron Lett.* **1987**, *28*, 295.

10   Gibson, T. *Organometallics* **1987**, *6*, 918.

11   Negishi, E.; Miller, J.; Yoshida, T. *Tetrahedron Lett.* **1984**, *25*, 3407.

12   (a) Schwartz, J.; Labinger, J. A.; *Angew. Chem. Int. Ed. Engl.* **1976**, *15*, 333. (b) Labinger, J. A. In *Comprehensive Organic Synthesis*, Trost, B.M.; Fleming, I.; Eds. Pergamon Press: Oxford, in press.

13   Bock, P. L.; Boschetto, D. J.; Rasmussen, J. R.; Demers, J. P.; Whitesides, G. M. *J. Am. Chem. Soc.* **1974**, *96*, 2814.

14   Labinger, J. A.; Hart, D. W.; Seibert, W. E.; Schwartz, J. *J. Am. Chem. Soc.* **1975**, *97*, 3851.

15   See references 10, 11, and 12 as well as: Liu, Y.; Guo, Q.; Lei, X.; *Youji Huaxue* **1984**, 33 (*Chem. Abstr.* **1984**, *101*, 37 981.)

16   Erker, G.; Kropp, K.; Atwood, J. L.; Hunter, W. E. *Organometallics* **1983**, *2*, 1555.

[17] Becker, E. D. *High Resolution NMR*. Academic Press: New York. 1969, pp. 166-170.

[18] The insertion reaction of neohexene with Cp_2ZrDCl was examined to verify this. ^1H NMR shows a simple doublet and triplet as expected.

[19] Treatment of Cp_2ZrHCl with acetone to form the isopropoxide derivatives showed no detectable impurity by ^1H NMR. Thus the amount of Cp_2ZrH_2 must be less than 5%.

[20] Gell, K. I.; Schwartz, J. *J. Am. Chem. Soc.* 1978, *100*, 3246.

[21] Alternatively, the interchange of H and D in the olefin-dihydride complex might occur by the "Tarzan swing" mechanism described for $[(\eta^5-C_5Me_5)_2WH_2D]^+$: Parkin, G.; Bercaw, J. E. *Polyhedron*, 1988, *7*, 2053-2082.

[22] Burger, B. J.; Santarsiero, B. D.; Trimmer, M. S.; Bercaw, J. E. *J. Am. Chem. Soc.* 1988, *110*, 3134.

[23] Burger, B. J.; Bercaw, J. E. in "New Developments in the Synthesis, Manipulation, and Characterization of Organometallic Compounds" Wayda, A.; Darensbourg, M., eds. ACS Symposium Series, 1987, *357*, 79-98.

[24] Marvich, R. H.; Brintzinger, H. H. *J. Am. Chem. Soc.* 1971, *93*, 2046.

[25] (a) Wolczanski, P. T.; Threlkel, R. S.; Bercaw, J. E. *J. Am. Chem. Soc.* 1979, *101*, 218.

(b) Hillhouse, G.; Bercaw, J.E. unpublished results.

[26] Although powders or crystalline products were not obtained, the ^1H NMR spectrum of the product is clean.

Chapter 3

SYNTHESIS, CHARACTERIZATION, AND X-RAY STRUCTURE OF [K(THF)2]2[U(NH-2,6-i-Pr2C6H3)5] THF[1]

Abstract:

The title compound, [K(THF)2]2[U(NHAr)5]•THF (Ar = 2,6-diisopropylphenyl), is prepared by treatment of UI3(THF)4 with five equivalents of potassium 2,6-diisopropylanilide (KNHAr) in THF. Electronic absorption spectra reveal internal f-f transitions characteristic of trivalent uranium. A single crystal X-ray study reveals that the dianion is a monomer containing a trigonal bipyramidal five-coordinate uranium center. The potassium cations each interact in an η^6 and η^4 fashion with two arene rings of the arylamido ligands, and two THF molecules. Crystal data (at -70° C): Monoclinic space group $P2_1/C$, with a = 21.726(7) Å, b = 15.378(6) Å, c = 25.007(4) Å, β = 106.07(4)°, and Z = 4.

Introduction

Until recently, the lack of suitable starting materials has left the non-aqueous chemistry of trivalent uranium virtually unexplored.[2] The reported uranium trihalides are polymeric solids with poor solubilities and virtually no reactivity.[3] This is due, in part, to the fact that conventional preparative routes to uranium trihalides involve high-temperature tube-furnace techniques. $UCl_3(THF)_x$ has been prepared by the reduction of UCl_4 in THF,[4] but the composition of this material is not known and its usefulness as a precursor to trivalent uranium chemistry is limited. For example, uranium (III) reaction products are often contaminated with uranium (IV) complexes that are difficult to separate.[5]

A new solution route to a trivalent uranium halide precursor has been developed by Clark and Sattelberger.[6] The use of iodide as the halide ligand was prompted by the thermodynamic stability of uranium (IV) halides, F > Cl > Br > I.[7] In fact, uranium tetraiodide decomposes at room temperature to the triiodide.[8] A clean, reproducible, high yield synthesis of $UI_3(THF)_4$ has been developed by treating clean uranium turnings with elemental iodine as shown in Equation 1. This uranium (III) triiodide complex can be prepared on a large scale (50 g).

$$U \ + \ 1.5 \ I_2 \ \xrightarrow[\ 0°\ C\ ]{\ THF\ } \ UI_3(THF)_4 \qquad\qquad (1)$$
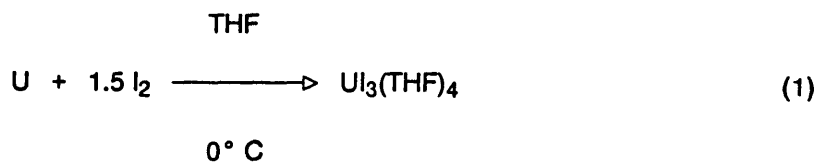
The low-temperature solution synthesis gives a monomeric, solvated product whose solubility in hydrocarbon solvents makes it a good synthetic starting material for entry into trivalent uranium chemistry. If 1,2-dimethoxyethane (dme) or pyridine (py) is used as a solvent rather than THF, $UI_3(dme)_2$ and $UI_3(py)_4$ are produced in a similar fashion, although these reactions proceed much more slowly. As well as reacting with Lewis bases, $UI_3(THF)_4$ reacts cleanly with sodium

or potassium salts, with loss of THF-insoluble NaI or KI, to give new products as shown in Scheme 1. In general, the precipitation of insoluble NaI or KI has avoided the formation of salt or "ate" complexes in the uranium (III) chemistry.
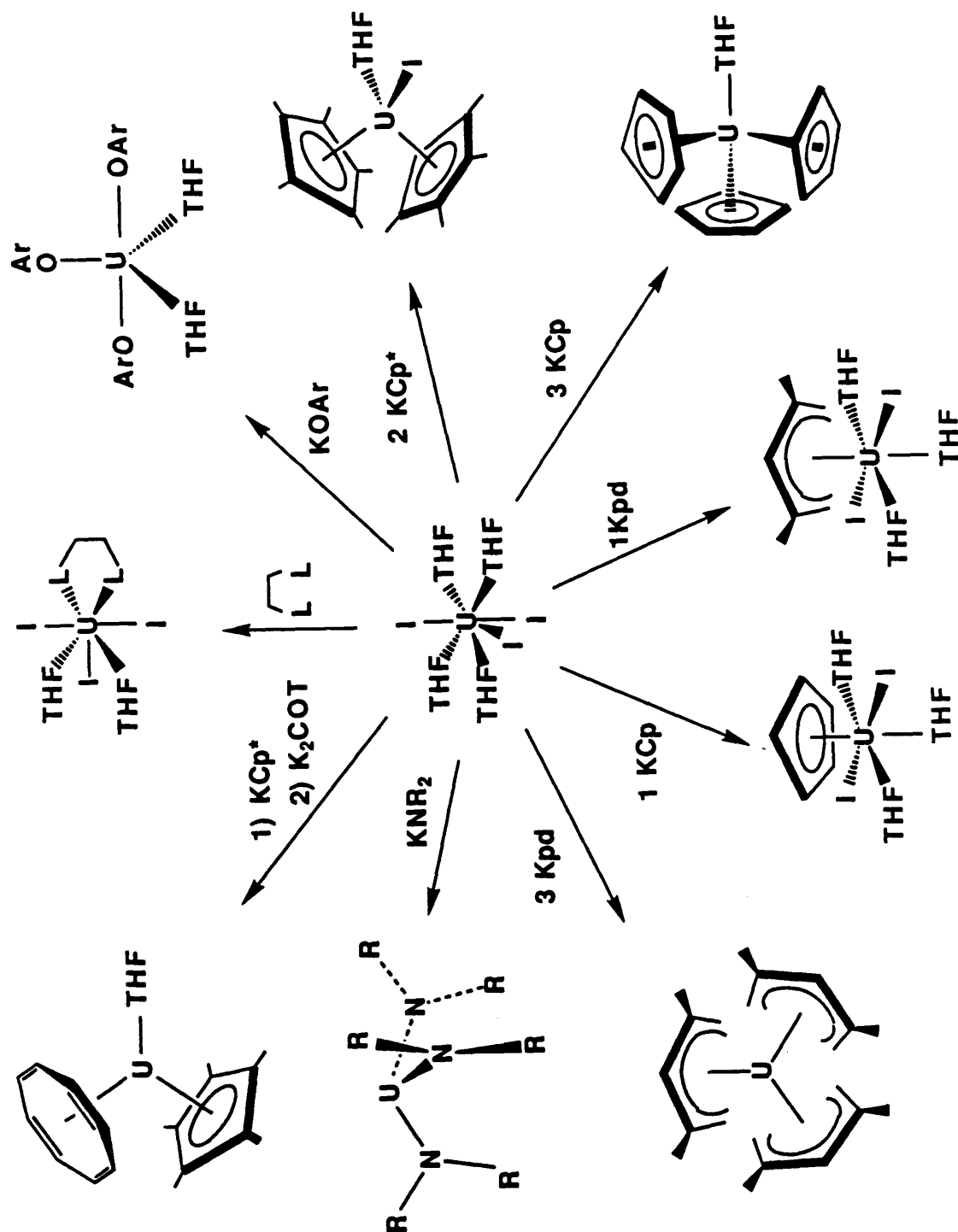
Scheme 1

Based on the successful synthesis of uranium (III) aryloxide and amide complexes noted in Scheme 1, we chose to explore the reactivity of $UI_3(THF)_4$ with potassium salts of primary amines. As well as producing new uranium amido complexes, it was hoped that primary uranium amido complexes would give new routes to uranium imido, L_nUNR, complexes through deprotonation. Currently, there is a great deal of activity in the field of metal-ligand multiple bonds, including investigations of metal organoimido complexes.[9] Thus, the synthesis of new uranium organoimido complexes is an attractive goal. Although several new uranium imido complexes have been reported,[10] no homoleptic uranium imido analog of UO_3 has been prepared to date. In fact, only recently has a neutral homoleptic transition metal imido complex, $Os(NAr)_3$ with Ar = 2,6-diisopropylphenyl, been reported.[11] Scheme 2 shows a potential route to a uranium (VI) imido complex based on the preparation of a uranium (III) amido complex followed by deprotonation and oxidation to the desired uranium (VI) imido target.

$$UI_3(THF)_4 \xrightarrow[-3\ KI]{3\ KNHAr} U(NHAr)_3 \xrightarrow[-3\ BuH]{3\ n\text{-}BuLi} Li_3[U(NAr)_3]$$

$$\downarrow Ox.$$

$$U(NAr)_3$$
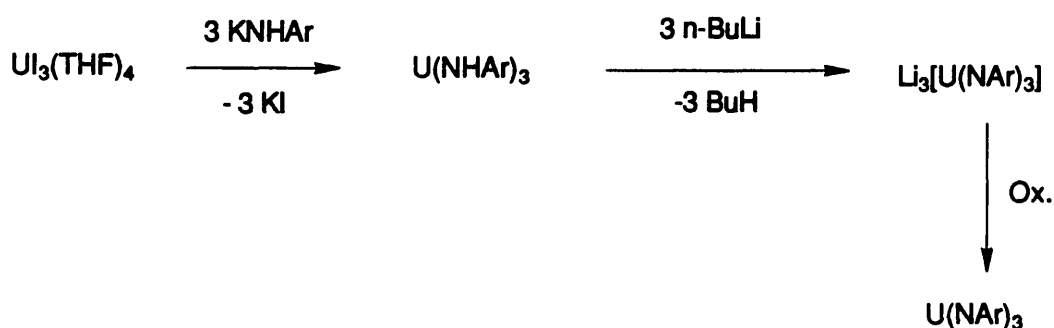
Scheme 2

New routes to uranium amido complexes from a uranium (IV) source (i.e., UCl_4) were also envisioned. Again, uranium (IV) primary amido complexes could provide precursors to imido complexes *via* similar deprotonation and oxidation steps. Scheme 3 shows a potential route into such complexes.

$$UCl_4 \xrightarrow[\text{- 3 KCl}]{\text{3 KNHAr}} U(NHAr)_3Cl \xrightarrow[\text{- LiCl}]{\text{MeLi}} U(NHAr)_3Me$$

$$\downarrow \text{-CH}_4$$

$$U(NAr)_3 \xleftarrow{\text{Ox.}} Li_2[U(NAr)_3] \xleftarrow[\text{-2 BuH}]{\text{2 n-BuLi}} U(NAr)(NHAr)_2$$
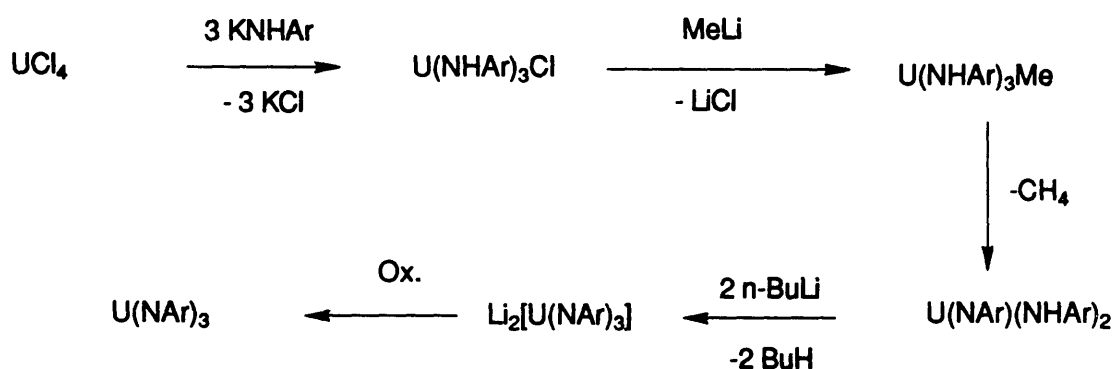
Scheme 3

This chapter discusses the reactivity of uranium (III) and (IV) halide complexes with potassium salts of primary amides.

Results and Discussion

Synthesis and Spectroscopic Characterization of New Uranium Amido Complexes.

Treatment of $UI_3(THF)_4$ with three equivalents of the potassium salt of 2,6-diisopropylaniline (NH_2Ar) yields intractable products. This is in contrast to the relatively clean products obtained by metathesis with *di*alkyl amides.[12] Interestingly, these products of the 3:1

uranium (III) reactions show ^{1}H NMR features similar to the products (also intractable) of UCl_4 with four equivalents of potassium anilide. There are ^{1}H NMR signals consistent with two sets of coordinated ligand, in roughly a 2:1 ratio.[13] Although none of these reaction products could be cleanly isolated, it is proposed that some sort of bridging complex such as (1) is formed. Since the same complex is produced whether a uranium (III) or a uranium (IV) source is used, it appears that a change in oxidation state for one of these reactions must occur. Attempts to crystallize the products using another Lewis base such as pyridine were also unsuccessful.
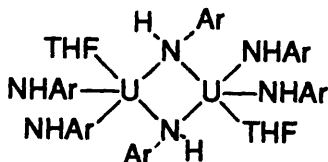
(1)

The observation of coordinated THF in the ^{1}H NMR spectra suggests that the coordination sphere of uranium (III) can accomodate more than three ligands. Therefore, the reaction of $UI_3(THF)_4$ with excess potassium anilide was examined, and found to give the brown crystalline title complex, as shown in Equation 2. Treatment of UCl_4 with excess potassium anilide (10 eq.) also gives this same complex, although not as cleanly. Although not previously seen for the $UI_3(THF)_4$ system, lithium and sodium alkali metal complex salts of the actinides are well known; their formation pervades metathesis reactions of f-element chemistry.[14]

$$UI_3(THF)_4 \ + \ \geq 5 \ KNHAR \ \longrightarrow \ [K(THF)_2]_2[U(NHAr)_5] \bullet THF \qquad (2)$$
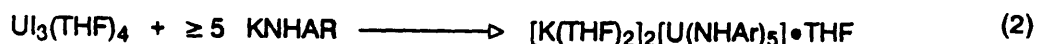
$[K(THF)_2]_2[U(NHAr)_5] \bullet THF$ is exceedingly air and moisture sensitive. It is soluble in THF and in toluene, yielding solutions which range in color from pale yellow to dark brown, depending on the concentration. The room temperature ^1H NMR spectrum in toluene-d_8 shows only broad resonances consistent with THF involved in a dynamic exchange process between free and coordinated THF. In paramagnetic trivalent uranium chemistry, coordinated THF resonances have been typically observed at high field. For example, in $U(O-2,6-Bu^t_2C_6H_3)_3(THF)$, the resonances for coordinated THF appear at δ -18.4 and δ -44.6.[15] Cooling the toluene-d_8 sample to 225 K yields an extremely complex spectrum presumably due to the low symmetry of tight ion-pairs in the hydrocarbon solvent. By contrast, the spectrum obtained in THF-d_8 displays resonances consistent with a single type of amide ligand (indicating a fluxional process equilibrates axial and equatorial positions), although peaks are broadened due to a dynamic process. Upon cooling, the anilide ligand resonances coalesce into the baseline at 180 K.

The room temperature electronic absorption spectrum of $[K(THF)_2]_2[U(NHAr)_5] \bullet THF$

recorded in THF solution from 1600 - 200 nm is shown in Figure 1. The absorption spectrum

shows a manifold of weak (ϵ = 30-80 $M^{-1}cm^{-1}$) absorption bands in the near-IR region and three

intense (ϵ = 11,000-47,000 $M^{-1}cm^{-1}$) absorption bands in the ultraviolet region. The band

positions and weak intensity of the absorption features between 1600 - 600 nm are consistent

with Laporte-forbidden internal f-f transitions of the uranium(III) center. These band maxima

show a striking similarity to other U(III) inorganic[16] $[UI_3(THF)_4]$ and organometallic[17]

$[Cp_3UOEt_2]$ complexes, and even the U(III) aquo ion stabilized in perchloric acid.[18] Thus the f-f

bands in the spectrum for $[K(THF)_2]_2[U(NHAr)_5] \bullet THF$ serve as an electronic "fingerprint" for

trivalent uranium, in support of the structural assignment of a U(III) amido complex anion. The

shoulder at 320 nm (ϵ = 11,230 $M^{-1}cm^{-1}$) is difficult to see in Figure 1, but becomes obvious

upon spectrum expansion. The band is tentatively assigned to an internal f-d transition. The

intensity of the band maxima at 290 nm (ϵ = 29,700 $M^{-1}cm^{-1}$) and 239 nm (ϵ = 46,700 $M^{-1}cm^{-1}$)

are indicative of fully-allowed charge transfer excitations. With five arene chromophores in the

complex, the 239 nm absorption feature is tentatively assigned to the arene π - π^* (benzenoid

B-band) transition in the anilide ligand. The 290 nm band is tentatively assigned to a nitrogen-

to-uranium ligand-to-metal charge transfer (LMCT) excitation.

Figure 1: UV-VIS Spectrum of [K(THF)$_2$]$_2$[U(NHAr)$_5$]•THF
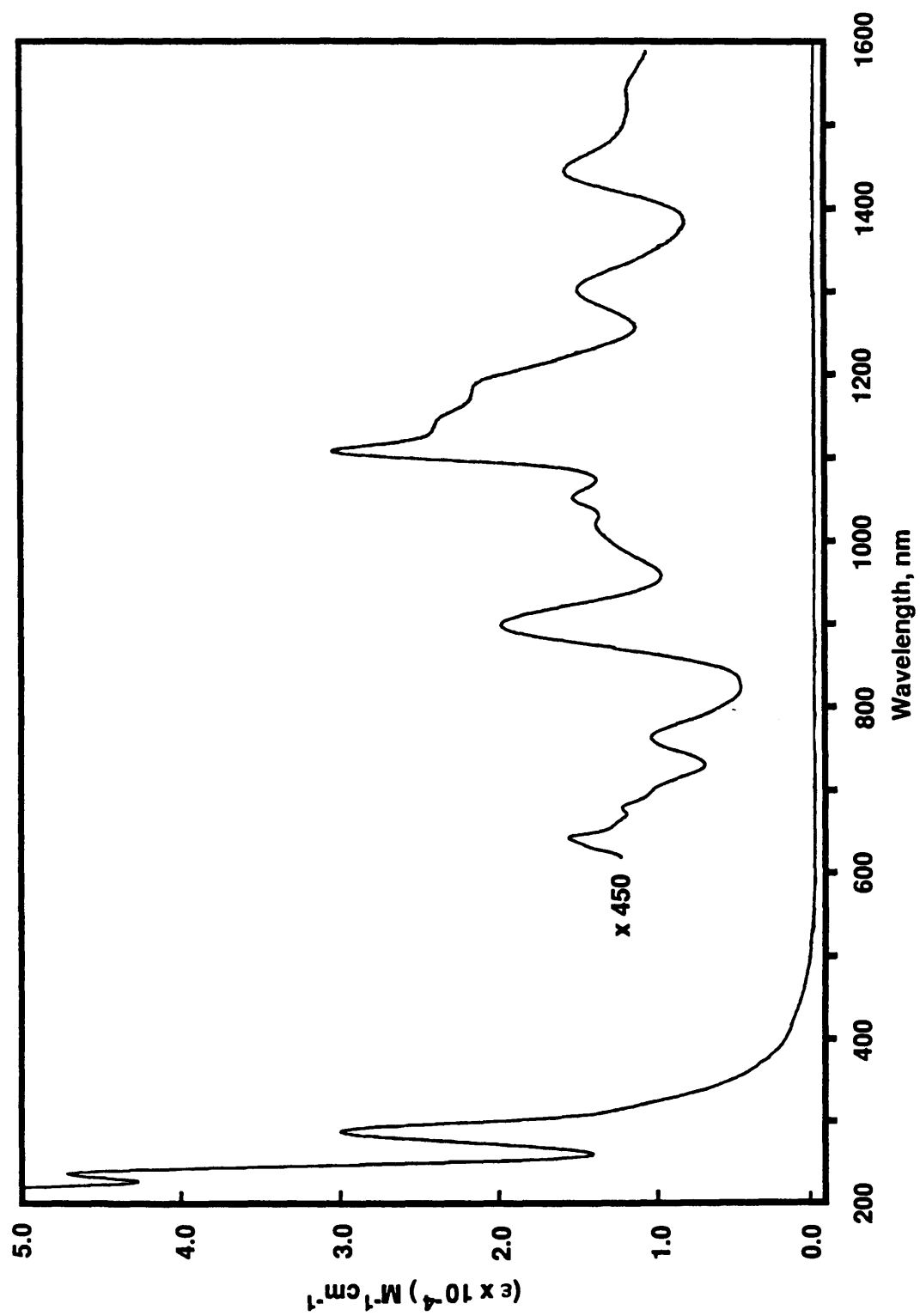
The infrared spectrum (4000-450 cm^{-1}) shows a weak, broad feature at 3300 cm^{-1}, indicative of a secondary N-H stretch. The strong band at 1583 cm^{-1} is assigned to the C=C aromatic stretch, and the vibrations at 774 cm^{-1} and 707 cm^{-1} are consistent with C-H out-of-plane bending modes expected for a 1,2,3-trisubstituted arene ring. In addition, infrared absorption bands indicative of both coordinated (1041, 884, 838 cm^{-1}) and nonligated (1054, 906 cm^{-1}) THF are observed.[19]

Structure and Bonding of [K(THF)$_2$]$_2$[U(NHAr)$_5$]•THF.

In the solid state, [K(THF)$_2$]$_2$[U(NHAr)$_5$]•THF is a monomeric complex, displaying a five coordinate uranium center in approximately trigonal-bipyramidal coordination geometry. An ORTEP drawing of the anion portion of the complex emphasizing the coordination is shown in Figure 2. The uranium atom lies within the plane formed by the equatorial amide nitrogen atoms to within 0.006(1) Å. Each potassium cation interacts with one equatorial and one axial amide ligand, increasing the angle subtended by these ligands (N(2)-U-N(5) = 95.9(9)°, N(3)-U-N(4) = 92.9(7)°), as well as decreasing the angle formed by the axial ligands (N(2)-U-N(4) = 166.0(7)°. In addition, each potassium atom is also ligated by two tetrahydrofuran molecules.

The U-N bond distances (Table 3) vary from 2.26(3) Å to 2.38(2) Å, with an average value of 2.34 Å. The trigonal bipyramidal coordination geometry about the uranium center is similar to that found in the U(IV) alkoxide complex [Li(THF)$_4$][U(O-2,6-iPr$_2$-C$_6$H$_3$)$_5$],[20] which possesses an average U-O bond distance of 2.17(2) Å. These uranium-ligand bond lengths are comparable when corrected for the 0.13-0.15 Å increase of ionic radius in U(III) with respect to U(IV).[21] The average U-N bond length is also similar to that determined for the amido complexes U(NPh$_2$)$_4$ (2.27(2) Å)[22] and U[N(SiMe$_3$)$_3$] (2.320(4) Å).[23] The U-N-C angles range from 141(2)° to 156(2)°, with an average value of 149(2)°. Although the protons on the primary amido ligands were not located in the final difference Fourier map, the values of these angles preclude

Figure 2: Ball-and-Stick View of the [U(NHAr)₅]²⁻ Anion
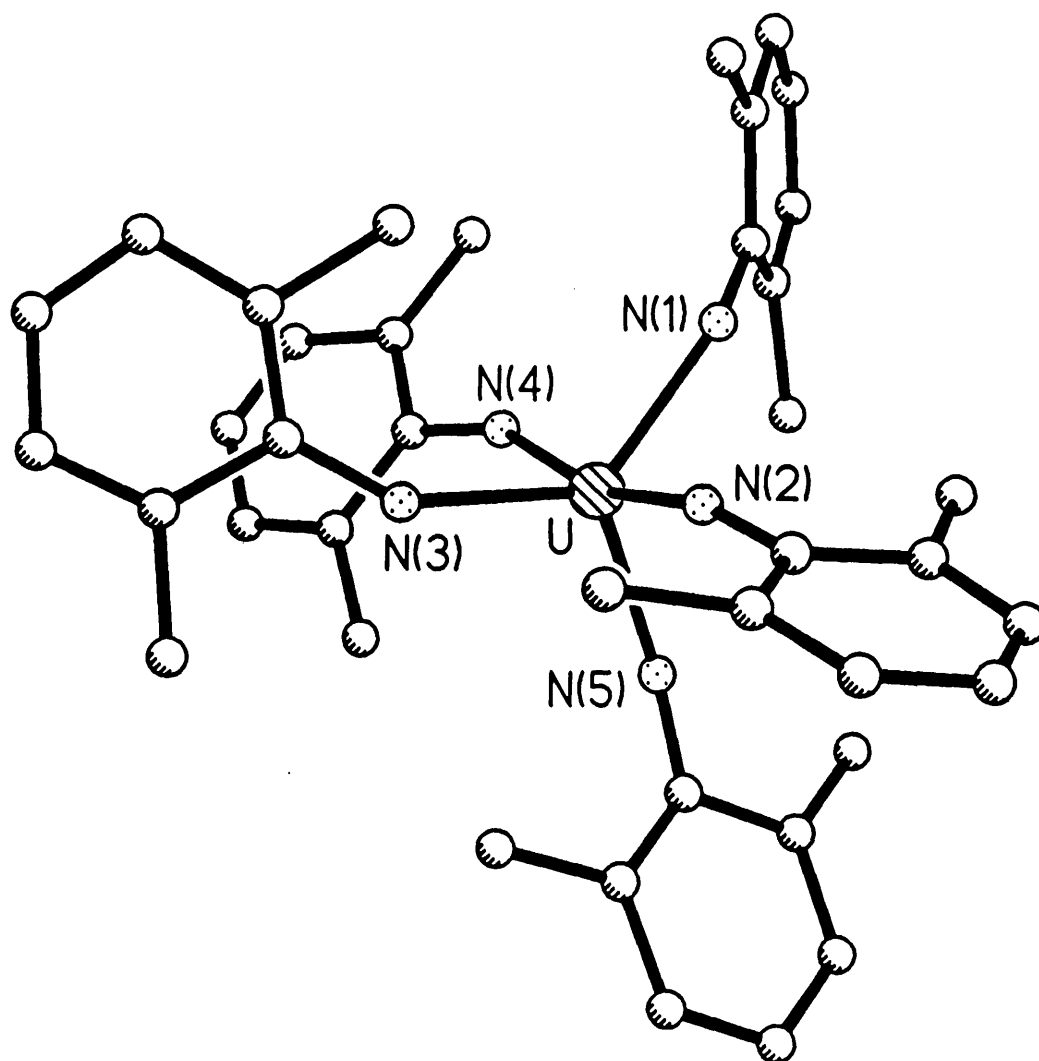
Table 1: Selected Bond Distances (Å) and Angles (°) for [K(THF)$_2$]$_2$[U(NHAr)$_5$]•THF

U-N(1)	2.35(1)		U-N(2)	2.32(2)
U-N(3)	2.38(2)		U-N(4)	2.37(2)
U-N(5)	2.26(3)			
K(1)-O(1)	2.72(2)		K(1)-O(3)	2.72(2)
K(2)-O(2)	2.62(2)		K(2)-O(4)	2.78(3)
K(1)-C(31)	3.38(3)		K(1)-C(32)	3.15(3)
K(1)-C(33)	3.06(3)		K(1)-C(34)	3.24(3)
K(1)-C(41)	3.14(3)		K(1)-C(42)	3.06(3)
K(1)-C(43)	3.11(3)		K(1)-C(44)	3.24(3)
K(1)-C(45)	3.30(3)		K(1)-C(46)	3.34(3)
K(2)-C(21)	3.29(3)		K(2)-C(24)	3.30(3)
K(2)-C(25)	3.09(3)		K(2)-C(26)	3.11(3)
K(2)-C(51)	3.26(3)		K(2)-C(52)	3.38(3)
K(2)-C(53)	3.34(3)		K(2)-C(54)	3.21(3)
K(2)-C(55)	3.15(2)		K(2)-C(56)	3.22(3)
N(1)-U-N(2)	88.1(6)		N(1)-U-N(3)	129.4(9)
N(1)-U-N(4)	80.9(6)		N(1)-U-N(5)	118.3(9)
N(2)-U-N(3)	87.2(8)		N(2)-U-N(4)	166.0(7)
N(2)-U-N(5)	95.9(9)		N(3)-U-N(4)	92.9(7)
N(3)-U-N(5)	112.3(8)		N(4)-U-N(5)	97.1(9)
U-N(1)-C(11)	148(1)		U-N(2)-C(21)	156(2)
U-N(3)-C(31)	141(2)		U-N(4)-C(41)	152(2)
U-N(5)-C(51)	149(2)			

the identification of these ligands as imido groups, which typically display near linear U-N-C angles.

In many structurally characterized "ate" complexes, the alkali metal cation does not interact with the anion, but is complexed by neutral oxygen or nitrogen donor atom ligands. In other members of this class, the alkali metal cation coordinates to a halide ligand, or to the heteroatom of the amide or alkoxide functional group. A striking feature of the solid state structure of $[K(THF)_2]_2[U(NHAr)_5] \bullet THF$ is that the potassium counterions interact with the arene rings of the aryl amido ligands, rather than the nitrogen atoms. Each potassium cation displays close contacts with all six carbons of one aryl ring to give η^6-coordination, and four carbons of a second ring to give η^4-coordination as shown in Figure 3. The potassium-carbon distances range from 3.06(3) Å to 3.38(3) Å, with an average value of 3.22(3) Å. All other potassium-carbon contact distances are longer than 3.5 Å. (The mean distance of the potassium ions from the arene planes is 2.915(7) Å.) These η^6-π interactions are exceedingly rare in alkali metal arene complexes.[24] There is precedent for alkali metal cation interactions with unsaturated organic ligands bound to d-transition metal anions;[25] the complex $K[Co(C_2H_4)(PMe_3)_3]_2$ displays $\eta2$-coordination of the ethylene to the potassium ion, with a mean K-C distance of 3.12 Å.[10a] The average K-C distance for $[K(THF)_2]_2[U(NHAr)_5] \bullet THF$ of 3.22 Å perhaps can be better compared to the average η^6 K-C distances found in $K[Al_7O_6Me_{16}] \bullet C_6H_6$ (3.33 Å),[26] $K[AlMe_3NO_3] \bullet C_6H_6$ (3.38 Å),[27] and $[K(db-18-c-6)][Al_2Me_6Cl] \bullet 2C_6H_6$ (3.39 Å).[28]

Figure 3: A View of the Coordination of the Potassium Cation

Emphasizing the η^4 and η^6 π-Interactions
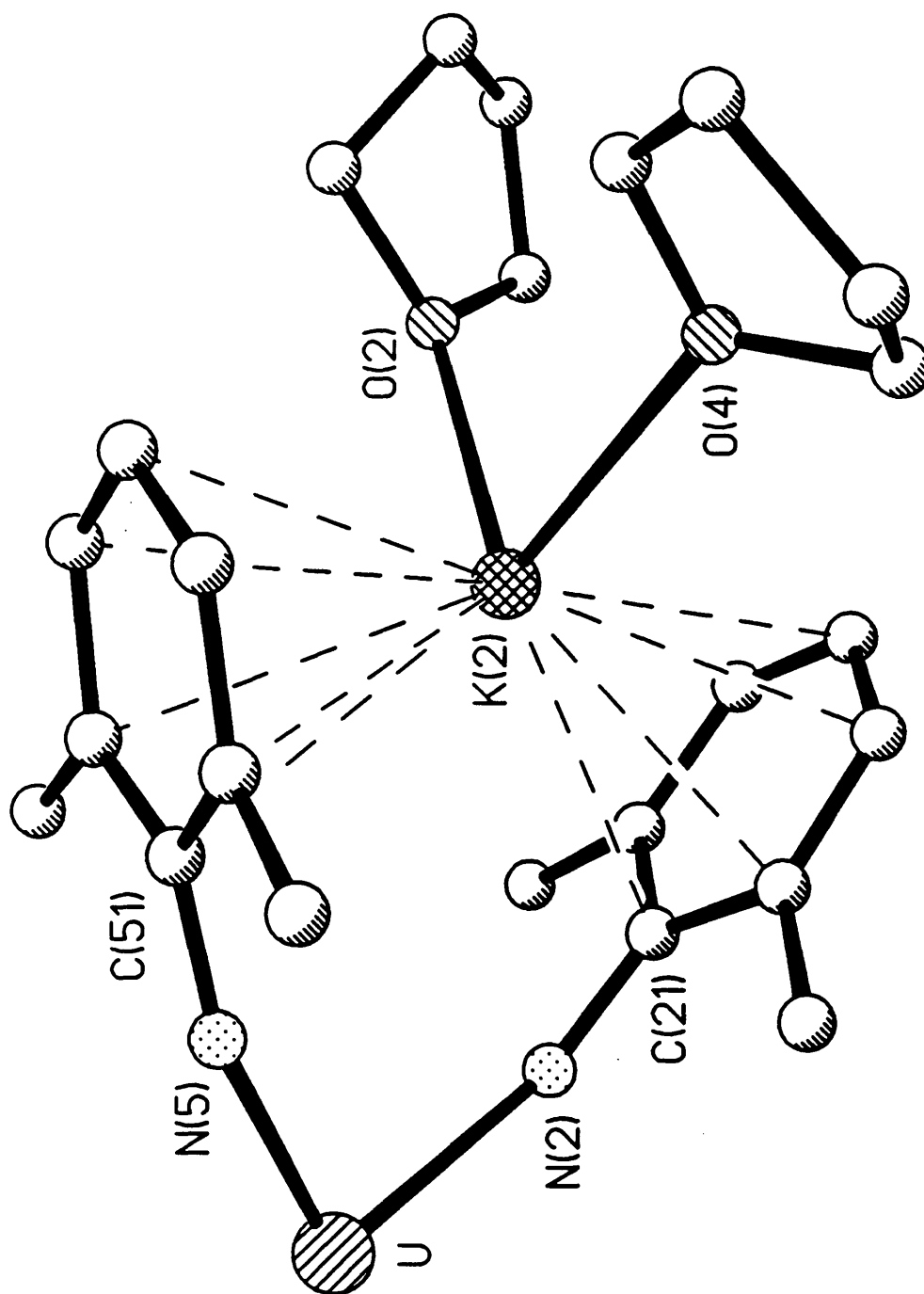
Conclusions

$[K(THF)_2]_2[U(NHAr)_5] \cdot THF$ is the first example where metathesis of $UI_3(THF)_4$ with potassium salts produced an alkali metal salt complex. It is interesting to note that the reaction of three equivalents of KNHAr with $UI_3(THF)_4$ does not proceed in a manner analogous to the reactions with secondary amides. Although reaction of the uranium starting material does appear to produce an amido complex, addition of excess potassium anilide is necessary to yield a monomeric product. This is perhaps due to an apparent lack of steric bulk in the 2,6-diisopropyl ligand. Use of a different solvent or addition of another Lewis base may help in the isolation of a $U(NHAr)_3$ complex.

The electronic spectrum (characteristic f-f bands) and the x-ray data (non-linear U-N-R bonds) seem conclusive evidence that $[K(THF)_2]_2[U(NHAr)_5] \cdot THF$ has been correctly assigned as a uranium (III) complex, even though the nitrogen protons were not located. Since the ^1H NMR spectra for the reactions of UCl_4 with KNHAr were nearly identical to the spectra for the $UI_3(THF)_4$ reactions, it appears the uranium (IV) complexes undergo a reduction to yield the uranium (III) species. Since these reactions were not extremely clean, the chemistry was not examined in detail.

Although the initial goal of producing a $U(NHAr)_3$ complex was not directly achieved, the $[K(THF)_2]_2[U(NHAr)_5] \cdot THF$ complex has shown interesting features. This complex could perhaps be envisioned as $[U(NHAr)_3][KNHAr(THF)_2]_2 \cdot THF$, and may display similar reactivity to a $U(NHAr)_3$ complex. $[K(THF)_2]_2[U(NHAr)_5] \cdot THF$ may well indeed prove a convenient precursor toward high valent uranium imido complexes.

Experimental Section

General Considerations. All air sensitive manipulations were performed in a helium-filled glovebox or by using Schlenk techniques. Hexane, THF, and toluene were dried over sodium-potassium alloy and distilled under nitrogen. Solvents were tested with sodium benzophenone ketyl prior to use and discarded if a purple color was not maintained. Deuterated solvents were degassed, dried, and stored over sodium amalgam.

Starting Materials. KH (Aldrich) was purchased as a 60% dispersion in mineral oil, washed with three aliquots of hexane, filtered and pumped to dryness to yield a white powder. 2,6-Diisopropylaniline (NH₂Ar) was obtained from Aldrich (90%) and distilled and stored under N_2 prior to use. Potassium 2,6-diisopropylanilide (KNHAr) was prepared by slow addition of a slight excess of NH₂Ar to a toluene suspension of KH and allowed to stir for 12 hr. The gelatinous product was collected by vacuum filtration on a medium porosity frit, washed with hexane until the washings were colorless, and dried *in vacuo* to give a white powder. $UI_3(THF)_4$[6] was prepared as previously reported.

Precautions for Handling Radioactive Materials. Depleted uranium (^{238}U) is a weak α emitter (4.196 MeV, half life 4.468×10^9 years); therefore all manipulations were carried out in a radiation laboratory with a monitored fume hood. Personnel wore lab coats and surgical gloves at all times. Radioactive wastes, both solid and liquid, were disposed of in approved receptacles.

Spectra. ^1H NMR spectra were recorded with an IBM Instruments Corp. AF-250 and on Bruker WM-300 instruments. Chemical shifts are reported in ppm (δ) relative to the residual solvent proton impurity set at δ 2.09 for toluene-d_8 and δ 1.73 for THF-d_8. Infrared spectra were recorded as Nujol mulls between KBr salt plates under an N_2 purge using a Bio-Rad Digilab FTS-40 spectrometer. Elemental analyses were performed using a Perkin-Elmer 2400 CHN Elemental Analyzer and standard air sensitive techniques. Electronic absorption spectra were

obtained with a Perkin-Elmer Lambda 9 UV/VIS/NIR Spectrophotometer using matched 1.0-cm or 1.0-mm quartz cells equipped with Sol-Seal joints. Extinction coefficients were measured from the baseline. The true extinction coefficients of bands that appear as shoulders are probably significantly smaller.

[K(THF)$_2$]$_2$[U(NHAr)$_5$] THF. In the glove box, UI$_3$(THF)$_4$ (5.05 g, 5.56 mmol) was dissolved in 50 mL THF in a 125 mL Erlenmeyer flask equipped with a magnetic stir bar to give a royal blue solution. While stirring, KNHAr (7.30 g, 33.8 mmol) was added as a solid over a period of 10 min. The reaction proceeds smoothly with the immediate formation of a dark brown solution along with the precipitation of white and grey solids. After stirring 24 hours at room temperature in the glovebox, the solution was vacuum filtered through a Celite pad and washed with THF until the filtrate was colorless. The THF was removed *in vacuo* to provide a brown product. The solid residue was extracted into 100 mL toluene, allowed to stir several hours, filtered through a Celite pad, and washed with toluene until the filtrate was colorless. The toluene was removed *in vacuo* to afford 5.04 g (3.23 mmol, 58% yield) of brown microcrystalline solid. The brown product may be recrystallized from THF/hexane to give 69% recrystallized yield.

Anal. Calcd. for UK$_2$N$_5$O$_5$C$_{80}$H$_{130}$: C, 61.67; H, 8.41; N, 4.49. Found: C, 62.45; H, 8.54; N, 4.56.

^{1}H NMR data (THF-d$_8$, 22°C): δ 5.61 (s, C*H*Me$_2$), δ 4.78 (s, meta), δ 1.12 (s, para), δ -5.49 (s, CH*Me$_2$*).

IR data (cm^{-1}): 3272 (vw); 1400 (s); 1379 (s); 1357 (m); 1328 (s); 1253 (s, br); 1215 (m); 1169 (w); 1150 (m); 1138 (m); 1111 (m); 1054 (s); 1041 (m); 906 (s); 884 (s); 838 (s); 744 (s); 624 (w); 538 (m).

UV-VIS-NIR absorption spectrum in THF solution: λ_{max}, nm (ϵ, M^{-1}cm^{-1}): 239 (46,680); 290 (29,720); 320s (11,230); 623 (44); 661 (36); 750 (31); 888 (55); 1015 (40); 1047 (44); 1107 (81); 1145 (65); 1190 (59); 1307 (43); 1456 (45); 1557 (35).

Structural Determination. Crystallographic data are summarized in Table 2. Single crystals of $[K(THF)_2]_2[U(NHAr)_5] \bullet THF$ were grown by layering a saturated THF solution with hexane and slowly cooling to -40 °C. Most crystals mounted for inspection fractured easily, and the compound appeared to lose solvent from the lattice at room temperature and in the X-ray beam, necessitating low temperature data collection. This resulted in some broadening of the Bragg reflections, however, limiting the quality of the data acquired. A single crystal measuring 0.12 x 0.31 x 0.45 mm was mounted on a glass fiber and transferred directly to the cold stream of an Enraf-Nonius CAD4 Automated Diffractometer operating at -70 °C. Cell constants and the orientation matrix were determined from the setting angles of 25 reflections with $12° < 2\theta < 30°$. Data was collected utilizing MoKα radiation. Examination of the systematic absences uniquely identified the space group as $P2_1/c$. A semi-empirical absorption correction was applied to the data based on the average relative intensity curve of azimuthal scans. The structure was solved by a combination of Patterson and difference Fourier methods. The uranium and potassium positions were refined anisotropically; all other atoms were refined with isotropic thermal parameters. The difference Fourier map revealed a THF of solvation present in the lattice. The positional and thermal parameters of this molecule were refined, but tended to oscillate, leading to relatively large shifts in the final least-squares cycle. The Δ/σ values for all other atoms were less than 0.1 in the final refinement. Positional and equivalent thermal parameters are given in Table 3.

Table 2: Crystal and Intensity Collection Data for [K(THF)$_2$]$_2$[U(NHAr)$_5$]•THF

Temperature	-70°C
Space Group	P2$_1$/c
a (Å)	21.726(7)
b (Å)	15.378(6)
c (Å)	25.007(8)
β (°)	106.07(4)
V (Å^3)	8028(10)
Z	4
fw	1558.19
d (calcd, g/cm^3)	1.289
μ (cm^{-1})	20.68
crystal size (mm)	0.21x 0.31 x 0.45
radiation	MoKα (λ = 0.70926Å)
scan type, range	θ -2θ, 2<2θ<45°
scan speed (deg/min)	1.12-8.24, variable
scan width (deg)	1.30 + 0.35 tanθ
reflections collected	11294; +h, +k, ±l
unique reflections	10475
reflections F$_o^2$ > 2.5σF$_o^2$	4035
min/max transmission	0.86
variables	388
R	0.083
R$_w$	0.092
GOF	1.781
p	0.04
max Δ/σ in final cycle	1.51
Maximum peak in final difference Fourier (e/Å^3)	1.51

Figure 4: Labeling Scheme for [K(THF)₂]₂[U(NHAr)₅]•THF
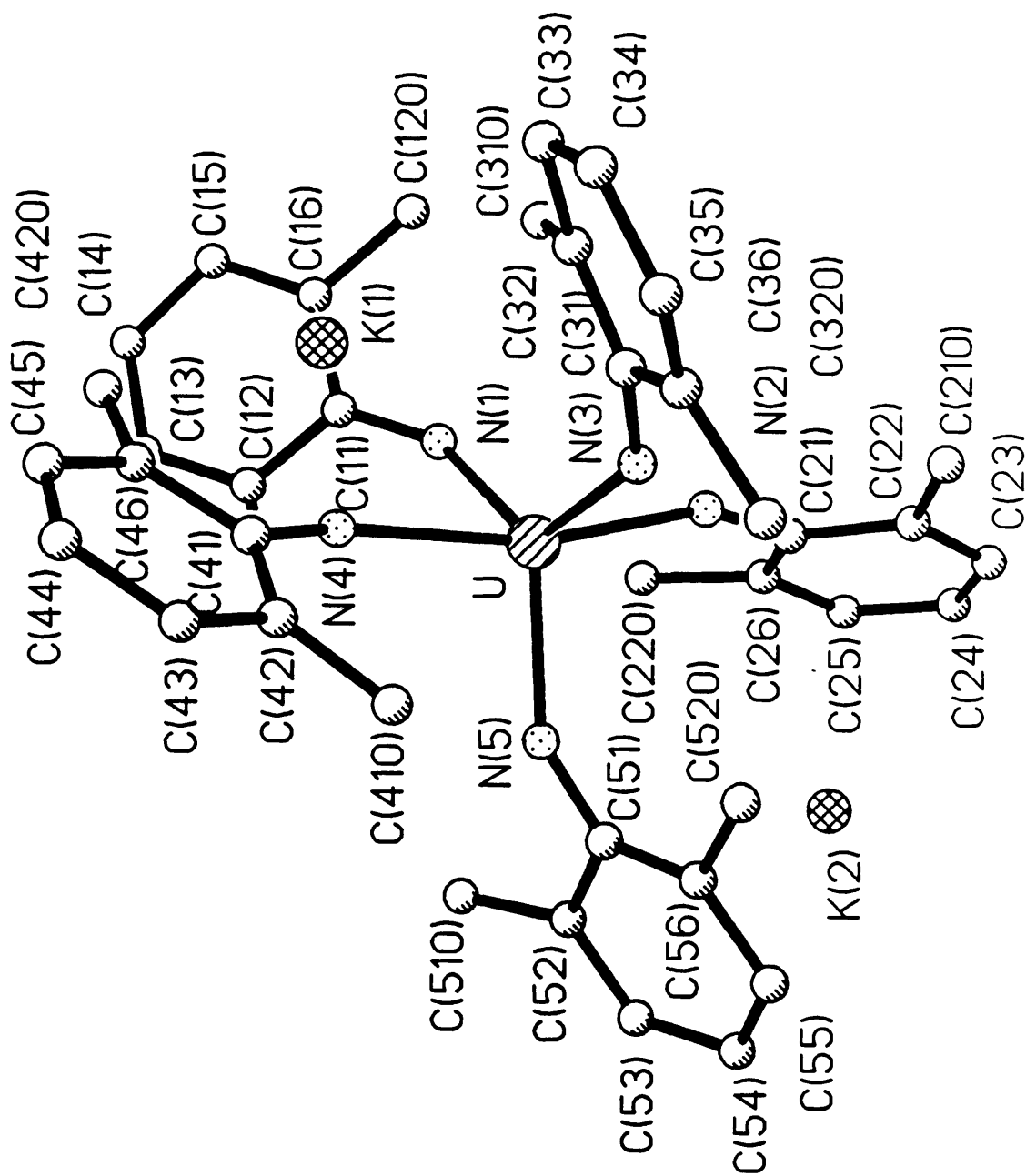
Table 3: Final Atomic Coordinates and Parameters for [K(THF)₂]₂[U(NHAr)₅]•THF

Atom	x	y	z	B
U	0.25044(5)	-0.0034(1)	0.20019(4)	2.40(2) †
K1	0.0893(3)	-0.2674(5)	0.1616(3)	4.3(2) †
K2	0.3572(3)	0.2328(5)	0.1134(3)	4.0(2) †
N1	0.2900(8)	-0.002(2)	0.2975(6)	2.7(4)
N2	0.3548(9)	0.014(2)	0.1957(8)	4.2(5)
N3	0.242(1)	-0.121(1)	0.1370(8)	2.7(5)
N4	0.156(1)	-0.044(1)	0.2233(8)	3.0(5)
N5	0.213(1)	0.122(2)	0.156(1)	5.0(7)
C11	0.277(1)	-0.000(3)	0.3480(9)	3.3(5)
C12	0.229(1)	0.054(2)	0.358(1)	2.6(6)
C13	0.211(1)	0.052(2)	0.408(1)	2.8(6)
C14	0.238(1)	-0.009(2)	0.4479(9)	3.7(6)
C15	0.288(1)	-0.067(2)	0.4438(9)	2.3(6)
C16	0.304(1)	-0.063(2)	0.3927(9)	2.3(6)
C21	0.405(1)	0.057(2)	0.188(1)	4.7(8)
C22	0.436(1)	0.029(2)	0.1463(9)	2.9(7)
C23	0.485(1)	0.083(2)	0.139(1)	3.6(7)
C24	0.503(1)	0.157(2)	0.169(1)	4.4(8)
C25	0.475(1)	0.182(2)	0.210(1)	4.0(7)
C26	0.428(1)	0.133(2)	0.221(1)	3.6(7)
C31	0.226(1)	-0.210(2)	0.131(1)	3.0(6)
C32	0.237(1)	-0.274(2)	0.173(1)	2.8(6)
C33	0.215(1)	-0.363(2)	0.170(1)	4.3(8)
C34	0.186(1)	-0.389(2)	0.115(1)	2.8(6)
C35	0.172(1)	-0.332(2)	0.068(1)	4.0(7)
C36	0.195(1)	-0.247(2)	0.075(1)	4.5(8)
C41	0.095(1)	-0.077(2)	0.210(1)	2.7(6)
C42	0.055(1)	-0.073(2)	0.1524(9)	2.3(6)
C43	-0.006(1)	-0.112(2)	0.140(1)	3.7(7)
C44	-0.029(1)	-0.154(2)	0.182(1)	3.4(7)
C45	0.008(1)	-0.159(2)	0.234(1)	2.8(6)
C46	0.071(1)	-0.117(2)	0.253(1)	4.7(8)
C51	0.213(1)	0.181(2)	0.118(1)	3.5(7)
C52	0.214(1)	0.275(2)	0.137(1)	3.0(6)
C53	0.220(1)	0.341(2)	0.099(1)	2.9(6)
C54	0.225(1)	0.322(2)	0.044(1)	3.6(7)
C55	0.221(1)	0.235(2)	0.027(1)	3.2(6)
C56	0.212(1)	0.167(2)	0.063(1)	3.1(6)
C110	0.202(1)	0.130(2)	0.315(1)	3.6(7)
C111	0.228(1)	0.218(2)	0.341(1)	2.9(6)
C112	0.128(1)	0.133(2)	0.304(1)	4.0(7)
C120	0.357(1)	-0.124(2)	0.383(1)	4.1(7)
C121	0.365(1)	-0.211(2)	0.421(1)	3.5(7)
C122	0.421(2)	-0.078(2)	0.397(1)	6.1(9)

Atom	x	y	z	B
C210	0.416(1)	-0.055(2)	0.117(1)	5.1(8)
C211	0.458(1)	-0.128(2)	0.150(1)	5.1(8)
C212	0.428(2)	-0.053(2)	0.055(1)	6.3(9)
C220	0.396(1)	0.154(2)	0.267(1)	4.7(8)
C221	0.448(2)	0.146(3)	0.325(1)	8(1)
C222	0.367(2)	0.240(3)	0.259(2)	9(1)
C310	0.281(1)	-0.240(2)	0.2316(9)	2.0(6)
C311	0.351(1)	-0.226(2)	0.226(1)	4.6(8)
C312	0.282(1)	-0.308(2)	0.279(1)	4.5(8)
C320	0.189(1)	-0.188(2)	0.024(1)	3.8(7)
C321	0.253(2)	-0.194(2)	0.011(1)	7(1)
C322	0.133(2)	-0.220(2)	-0.027(1)	7(1)
C410	0.077(1)	0.024(2)	0.110(1)	4.4(8)
C411	0.058(1)	-0.070(2)	0.053(1)	4.6(8)
C412	0.051(2)	0.069(2)	0.104(1)	7(1)
C420	0.107(1)	-0.118(2)	0.313(1)	3.0(6)
C421	0.069(1)	-0.127(2)	0.354(1)	4.9(8)
C422	0.160(1)	-0.189(2)	0.323(1)	4.2(8)
C510	0.203(1)	0.297(2)	0.1922(9)	2.3(6)
C511	0.132(1)	0.298(2)	0.189(1)	4.8(8)
C512	0.237(1)	0.384(2)	0.215(1)	3.9(7)
C520	0.208(1)	0.074(2)	0.041(1)	4.3(8)
C521	0.168(1)	0.063(2)	-0.022(1)	5.2(8)
C522	0.278(1)	0.045(2)	0.041(1)	4.6(8)
O1	-0.006(1)	-0.331(2)	0.0751(9)	6.9(6)
O2	0.388(1)	0.245(2)	0.0195(9)	6.9(6)
O3	0.062(1)	-0.394(2)	0.2292(8)	6.5(6)
O4	0.402(1)	0.401(2)	0.1385(9)	7.6(7)
O5	0.297(2)	0.528(3)	0.397(1)	17(1)
C1*	-0.039(2)	-0.286(3)	0.022(2)	10(1)
C2*	-0.048(2)	-0.364(2)	-0.019(1)	5.9(9)
C3*	-0.069(2)	-0.431(2)	0.013(1)	7(1)
C4*	-0.023(2)	-0.423(3)	0.078(1)	8(1)
C5*	0.448(2)	0.217(3)	0.008(1)	9(1)
C6*	0.458(2)	0.276(3)	-0.033(2)	12(2)
C7*	0.417(2)	0.346(3)	-0.031(2)	9(1)
C8*	0.360(2)	0.311(3)	-0.022(2)	9(1)
C9*	0.043(1)	-0.400(2)	0.285(1)	4.9(8)
C10*	0.104(1)	-0.437(2)	0.324(1)	5.0(8)
C11*	0.134(2)	-0.477(2)	0.285(1)	7(1)
C12*	0.100(2)	-0.467(3)	0.230(1)	8(1)
C13*	0.436(2)	0.435(3)	0.192(1)	7(1)
C14*	0.399(2)	0.513(3)	0.198(1)	10(1)
C15*	0.372(2)	0.554(3)	0.135(1)	8(1)
C16*	0.377(2)	0.470(3)	0.101(2)	12(2)
C17*	0.298(2)	0.421(4)	0.377(2)	13(2)

Atom	x	y	z	B
C18*	0.352(3)	0.443(4)	0.346(2)	6(2)
C19*	0.372(4)	0.421(6)	0.400(3)	28(4)
C20*	0.377(2)	0.537(3)	0.402(2)	12(2)

----

† Refined anisotropically.
Anisotropically refined atoms are given in the form of the
isotropic equivalent displacement parameter defined as:

$(4/3) * [a^{2*}B(1,1) + b^{2*}B(2,2) + c^{2*}B(3,3) + ab(\cos \gamma)^*B(1,2)$

$+ ac(\cos \beta)^*B(1,3) + bc(\cos \alpha)^*B(2,3)]$

Table 4: Anisotropic Displacement Parameters for [K(THF)$_2$]$_2$[U(NHAr)$_5$]•THF

Name	B(1,1)	B(2,2)	B(3,3)	B(1,2)	B(1,3)	B(2,3)	Beqv
U	2.60(3)	1.44(4)	2.88(3)	0.1(1)	0.32(3)	0.0(1)	2.40(2)
K1	4.2(4)	2.4(4)	4.9(3)	1.0(3)	-0.9(3)	-0.1(3)	4.3(2)
K2	3.9(3)	3.5(4)	4.2(3)	0.8(3)	0.4(3)	-0.6(3)	4.0(2)

The form of the anisotropic displacement parameter is:
exp[-0.25(h2a2B(1,1) + k2b2B(2,2) + l2c2B(3,3) + 2hkabB(1,2) + 2hlacB(1,3) + 2klbcB(2,3))] where a,b, and c are reciprocal lattice constants.

Table 5: Complete Bond Distances (Å) for [K(THF)₂]₂[U(NHAr)₅]•THF

Atom 1	Atom 2	Distance	Atom 1	Atom 2	Distance	Atom 1	Atom 2	Distance
U	N1	2.35(1)	K2	C53	3.34(3)			
U	N2	2.32(2)	K2	C54	3.21(3)	C23	C24	1.36(4)
U	N3	2.38(2)	K2	C55	3.15(2)	C24	C25	1.38(4)
U	N4	2.37(2)	K2	C56	3.22(3)	C25	C26	1.37(4)
U	N5	2.26(3)	K2	O2	2.62(2)	C26	C220	1.53(4)
K1	C31	3.38(3)	K2	O4	2.78(3)	C31	C32	1.41(4)
K1	C32	3.15(3)	N1	C11	1.37(3)	C31	C36	1.49(4)
K1	C33	3.06(3)	N2	C21	1.33(4)	C32	C33	1.45(4)
K1	C34	3.24(3)	N3	C31	1.41(4)	C32	C310	1.59(3)
K1	C41	3.14(3)	N4	C41	1.38(3)	C33	C34	1.41(3)
K1	C42	3.06(3)	N5	C51	1.33(4)	C34	C35	1.44(4)
K1	C43	3.11(3)	C11	C12	1.41(4)	C35	C36	1.39(4)
K1	C44	3.24(3)	C11	C16	1.47(4)	C36	C320	1.55(4)
K1	C45	3.30(3)	C12	C13	1.41(4)	C41	C42	1.45(3)
K1	C46	3.34(3)	C12	C110	1.58(4)	C41	C46	1.44(4)
K1	O1	2.72(2)	C13	C14	1.38(4)	C42	C43	1.42(4)
K1	O3	2.75(2)	C14	C15	1.42(4)	C42	C410	1.48(4)
K2	C21	3.29(3)	C15	C16	1.42(4)	C43	C44	1.43(4)
K2	C24	3.30(3)	C16	C120	1.54(4)	C44	C45	1.32(3)
K2	C25	3.09(3)	C21	C22	1.47(4)	C45	C46	1.48(4)
K2	C26	3.11(3)	C21	C26	1.43(4)	C46	C420	1.49(3)
K2	C51	3.26(3)	C22	C23	1.40(4)	C51	C52	1.52(4)
K2	C52	3.38(3)	C22	C210	1.49(4)	C51	C56	1.37(4)

Atom 1	Atom 2	Distance	Atom 1	Atom 2	Distance	Atom 1	Atom 2	Distance
C52	C53	1.42(4)	C410	C411	1.55(4)	C1*	C2*	1.55(5)
C52	C510	1.51(4)	C410	C412	1.54(5)	C2*	C3*	1.46(5)
C53	C54	1.43(4)	C420	C421	1.49(5)	C3*	C4*	1.65(4)
C54	C55	1.39(4)	C420	C422	1.55(4)	C5*	C6*	1.45(6)
C55	C56	1.44(4)	C510	C511	1.52(4)	C6*	C7*	1.41(7)
C56	C520	1.53(4)	C510	C512	1.55(4)	C7*	C8*	1.44(6)
C110	C111	1.53(4)	C520	C521	1.58(4)	C9*	C10*	1.53(4)
C110	C112	1.56(4)	C520	C522	1.56(4)	C10*	C11*	1.45(5)
C120	C121	1.63(4)	O1	C1*	1.49(4)	C11*	C12*	1.39(4)
C120	C122	1.53(5)	O1	C4*	1.48(5)	C13*	C14*	1.48(6)
C210	C211	1.54(4)	O2	C5*	1.46(5)	C14*	C15*	1.64(5)
C210	C212	1.62(5)	O2	C8*	1.47(4)	C15*	C16*	1.57(6)
C220	C221	1.59(4)	O3	C9*	1.56(4)	C17*	C18*	1.61(8)
C220	C222	1.45(5)	O3	C12*	1.39(5)	C17*	C19*	1.6(1)
C310	C311	1.58(4)	O4	C13*	1.43(4)	C18*	C19*	1.34(9)
C310	C312	1.57(4)	O4	C16*	1.42(5)	C19*	C20*	1.8(1)
C320	C321	1.52(5)	O5	C17*	1.72(7)			
C320	C322	1.57(4)	O5	C20*	1.71(6)			

Numbers in parentheses are estimated standard deviations in the least significant digits.

Table 6: Complete Bond Angles (°) for [K(THF)₂]₂[U(NHAr)₅]•THF

Atom 1	Atom 2	Atom 3	Angle	Atom 1	Atom 2	Atom 3	Angle	Atom 1	Atom 2	Atom 3	Angle
N1	U	N2	88.1(6)	C33	K1	C42	131.4(8)	C42	K1	C43	26.6(7)
N1	U	N3	129.4(9)	C33	K1	C43	157.0(9)	C42	K1	C44	46.3(7)
N1	U	N4	80.9(6)	C33	K1	C44	166.9(7)	C42	K1	C45	52.9(7)
N1	U	N5	118.3(9)	C33	K1	C45	143.8(7)	C42	K1	C46	46.2(7)
N2	U	N3	87.2(8)	C33	K1	C46	123.6(7)	C42	K1	O1	100.1(7)
N2	U	N4	166.0(7)	C33	K1	O1	110.6(8)	C42	K1	O3	130.2(8)
N2	U	N5	95.9(9)	C33	K1	O3	87.9(8)	C43	K1	C44	25.9(8)
N3	U	N4	92.9(7)	C34	K1	C41	135.1(7)	C43	K1	C45	43.6(7)
N3	U	N5	112.3(8)	C34	K1	C42	134.0(8)	C43	K1	C46	52.4(7)
N4	U	N5	97.1(9)	C34	K1	C43	147.4(7)	C43	K1	O1	79.3(7)
C32	K1	C33	27.0(8)	C34	K1	C44	167.5(6)	C43	K1	O3	113.6(8)
C32	K1	C34	43.4(7)	C34	K1	C45	168.5(6)	C44	K1	C45	23.3(6)
C32	K1	C41	93.5(7)	C34	K1	C46	148.0(7)	C44	K1	C46	44.0(7)
C32	K1	C42	104.6(7)	C34	K1	O1	86.1(7)	C44	K1	O1	81.8(7)
C32	K1	C43	130.7(8)	C34	K1	O3	95.1(7)	C44	K1	O3	88.0(8)
C32	K1	C44	146.2(7)	C41	K1	C42	27.0(6)	C45	K1	C46	25.7(7)
C32	K1	C45	130.6(7)	C41	K1	C43	46.2(6)	C45	K1	O1	102.2(7)
C32	K1	C46	105.4(7)	C41	K1	C44	52.7(7)	C45	K1	O3	77.3(7)
C32	K1	O1	126.3(8)	C41	K1	C45	45.0(7)	C46	K1	O1	125.7(8)
C32	K1	O3	108.4(7)	C41	K1	C46	25.5(8)	C46	K1	O3	89.1(8)
C33	K1	C34	25.5(6)	C41	K1	O1	125.2(7)	O1	K1	O3	89.3(7)
C33	K1	C41	118.6(8)	C41	K1	O3	114.4(7)	C21	K2	C24	50.1(8)

Atom 1	Atom 2	Atom 3	Angle	Atom 1	Atom 2	Atom 3	Angle	Atom 1	Atom 2	Atom 3	Angle
C21	K2	C25	44.5(8)	C25	K2	C55	163.2(8)	C54	K2	C55	25.3(7)
C21	K2	C26	25.6(7)	C25	K2	C56	137.2(8)	C54	K2	C56	45.0(7)
C21	K2	C51	86.0(8)	C25	K2	O2	110.8(8)	C54	K2	O2	84.3(7)
C21	K2	C53	126.7(8)	C25	K2	O4	84.0(7)	C54	K2	O4	86.1(7)
C21	K2	C54	138.3(8)	C26	K2	C51	95.6(7)	C55	K2	C56	26.2(7)
C21	K2	C55	119.2(8)	C26	K2	C53	123.4(8)	C55	K2	O2	78.9(7)
C21	K2	C56	94.5(7)	C26	K2	C54	145.8(8)	C55	K2	O4	110.5(7)
C21	K2	O2	116.9(8)	C26	K2	C55	138.2(8)	C56	K2	O2	98.0(7)
C21	K2	O4	127.1(7)	C26	K2	C56	112.0(8)	C56	K2	O4	129.0(7)
C24	K2	C25	24.6(8)	C26	K2	O2	128.5(8)	O2	K2	O4	88.5(8)
C24	K2	C26	43.6(8)	C26	K2	O4	102.1(7)	U	N1	C11	148.(1)
C24	K2	C51	135.9(7)	C51	K2	C53	44.8(7)	U	N2	C21	156.(2)
C24	K2	C53	160.7(7)	C51	K2	C54	53.1(7)	U	N3	C31	141.(2)
C24	K2	C54	170.5(8)	C51	K2	C55	45.3(7)	U	N4	C41	152.(2)
C24	K2	C55	154.8(8)	C51	K2	C56	24.4(7)	U	N5	C51	149.(2)
C24	K2	C56	140.9(8)	C51	K2	O2	122.1(7)	N1	C11	C12	122.(2)
C24	K2	O2	87.1(7)	C51	K2	O4	120.3(8)	N1	C11	C16	123.(3)
C24	K2	O4	89.7(8)	C53	K2	C54	25.1(7)	C12	C11	C16	115.(2)
C25	K2	C26	25.5(8)	C53	K2	C55	43.9(7)	C11	C12	C13	123.(2)
C25	K2	C51	120.5(7)	C53	K2	C56	50.7(7)	C11	C12	C110	118.(2)
C25	K2	C53	136.9(8)	C53	K2	O2	108.0(7)	C13	C12	C110	119.(2)
C25	K2	C54	161.6(9)	C53	K2	O4	79.0(7)	C12	C13	C14	119.(3)

Atom 1	Atom 2	Atom 3	Angle	Atom 1	Atom 2	Atom 3	Angle	Atom 1	Atom 2	Atom 3	Angle
C13	C14	C15	124.(2)	K2	C26	C25	76.(2)	C31	C36	C320	118.(3)
C14	C15	C16	115.(2)	K2	C26	C220	109.(2)	C35	C36	C320	120.(2)
C11	C16	C15	125.(2)	C21	C26	C25	120.(3)	K1	C41	N4	112.(2)
C11	C16	C120	116.(2)	C21	C26	C220	116.(3)	K1	C41	C42	73.(1)
C15	C16	C120	119.(2)	C25	C26	C220	124.(3)	K1	C41	C46	85.(2)
K2	C21	N2	110.(2)	N3	C31	C32	127.(2)	N4	C41	C42	119.(2)
K2	C21	C22	88.(2)	N3	C31	C36	120.(2)	N4	C41	C46	119.(2)
K2	C21	C26	70.(2)	C32	C31	C36	112.(2)	C42	C41	C46	122.(2)
N2	C21	C22	121.(3)	K1	C32	C31	87.(2)	K1	C42	C41	80.(2)
N2	C21	C26	120.(3)	K1	C32	C33	73.(2)	K1	C42	C43	79.(2)
C22	C21	C26	119.(3)	K1	C32	C310	114.(2)	K1	C42	C410	116.(2)
C21	C22	C23	116.(2)	C31	C32	C33	129.(2)	C41	C42	C43	117.(2)
C21	C22	C210	118.(3)	C31	C32	C310	114.(2)	C41	C42	C410	121.(2)
C23	C22	C210	126.(3)	C33	C32	C310	117.(2)	C43	C42	C410	122.(2)
C22	C23	C24	123.(3)	K1	C33	C32	80.(2)	K1	C43	C42	75.(2)
K2	C24	C23	88.(2)	K1	C33	C34	85.(2)	K1	C43	C44	82.(2)
K2	C24	C25	69.(2)	C32	C33	C34	112.(2)	C42	C43	C44	122.(2)
C23	C24	C25	121.(3)	K1	C34	C33	70.(2)	K1	C44	C43	72.(2)
K2	C25	C24	86.(2)	K1	C34	C35	86.(2)	K1	C44	C45	81.(2)
K2	C25	C26	78.(1)	C33	C34	C35	125.(3)	C43	C44	C45	120.(3)
C24	C25	C26	121.(3)	C34	C35	C36	118.(2)	K1	C45	C44	76.(2)
K2	C26	C21	84.(2)	C31	C36	C35	122.(3)	K1	C45	C46	79.(2)

Atom 1	Atom 2	Atom 3	Angle	Atom 1	Atom 2	Atom 3	Angle	Atom 1	Atom 2	Atom 3	Angle
C44	C45	C46	123.(3)	K2	C55	C54	80.(1)	C32	C310	C312	111.(2)
K1	C46	C41	70.(2)	K2	C55	C56	79.(1)	C311	C310	C312	110.(2)
K1	C46	C45	76.(2)	C54	C55	C56	120.(2)	C36	C320	C321	105.(2)
K1	C46	C420	123.(2)	K2	C56	C51	80.(2)	C36	C320	C322	111.(2)
C41	C46	C45	115.(2)	K2	C56	C55	75.(1)	C321	C320	C322	110.(3)
C41	C46	C420	124.(3)	K2	C56	C520	113.(2)	C42	C410	C411	112.(2)
C''	C46	C420	120.(3)	C51	C56	C55	123.(3)	C42	C410	C412	112.(3)
K?	C'1	N5	113.(2)	C51	C56	C520	120.(3)	C411	C410	C412	110.(2)
K2	C51	C52	81.(2)	C55	C56	C520	117.(2)	C46	C420	C421	117.(2)
K2	C51	C56	76.(2)	C12	C110	C111	110.(2)	C46	C420	C422	109.(2)
N5	C51	C52	115.(2)	C12	C110	C112	108.(2)	C421	C420	C422	110.(2)
N5	C51	C56	128.(3)	C111	C110	C112	107.(2)	C52	C510	C511	111.(2)
C'2	C'1	C56	117.(3)	C16	C120	C121	112.(2)	C52	C510	C512	111.(2)
C'1	C'2	C53	118.(2)	C16	C120	C122	111.(3)	C511	C510	C512	113.(2)
C'1	C'2	C510	121.(2)	C121	C120	C122	108.(2)	C56	C520	C521	115.(2)
C'3	C'2	C510	121.(2)	C22	C210	C211	108.(2)	C56	C520	C522	108.(2)
K?	C'3	C52	80.(2)	C22	C210	C212	110.(3)	C521	C520	C522	104.(2)
K?	C'3	C54	73.(2)	C211	C210	C212	108.(3)	K1	O1	C1*	128.(2)
C'?	C'3	C54	122.(3)	C26	C220	C221	108.(3)	K1	O1	C4*	117.(2)
K?	C'4	C53	82.(1)	C26	C220	C222	111.(3)	C1*	O1	C4*	114.(2)
K?	C'4	C55	75.(1)	C221	C220	C222	112.(3)	K2	O2	C5*	128.(2)
C'3	C54	C55	119.(3)	C32	C310	C311	108.(2)	K2	O2	C8*	122.(2)

Atom 1	Atom 2	Atom 3	Angle		Atom 1	Atom 2	Atom 3	Angle		Atom 1	Atom 2	Atom 3	Angle
C5*	O2	C8*	106.(3)		O1	C4*	C3*	97.(3)		C14*	C15*	C16*	98.(3)
K1	O3	C9*	139.(2)		O2	C5*	C6*	107.(3)		O4	C16*	C15*	109.(3)
K1	O3	C12*	110.(2)		C5*	C6*	C7*	103.(4)		O5	C17*	C18*	91.(4)
C9*	O3	C12*	104.(2)		C6*	C7*	C8*	108.(4)		O5	C17*	C19*	89.(4)
K2	O4	C13*	127.(2)		O2	C8*	C7*	100.(3)		C18*	C17*	C19*	50.(4)
K2	O4	C16*	120.(2)		O3	C9*	C10*	102.(2)		C17*	C18*	C19*	63.(5)
C13*	O4	C16*	111.(3)		C9*	C10*	C11*	101.(2)		C17*	C19*	C18*	67.(4)
C17*	O5	C20*	91.(3)		C10*	C11*	C12*	114.(3)		C17*	C19*	C20*	93.(5)
O1	C1*	C2*	100.(3)		O3	C12*	C11*	105.(3)		C18*	C19*	C20*	77.(5)
C1*	C2*	C3*	101.(3)		O4	C13*	C14*	103.(3)		O5	C20*	C19*	82.(4)
C2*	C3*	C4*	107.(3)		C13*	C14*	C15*	106.(3)					

Numbers in parentheses are estimated standard deviations in the least significant digits.

References

1   The bulk of this chapter has been submitted for publication: Nelson, J.E.; Clark, D.L.;

        Burns, C.J.; Sattelberger, A.P. *Inorg. Chem.* **1991.**

2   Katz, J.J.; Morss, G.T.; Seaborg, G.T. *The Chemistry of the Actinide Elements;* Chapman

        and Hall: New York, **1966,** Vol. 1 and 2, and references therein.

3   (a) Taylor, J.C.; Wilson, P.W. *Acta. Cryst.* **1974,** *B30,* 2803. (b) Levy, J.H.; Taylor, J.C.;

        Wilson, P.W. *Acta. Cryst.* **1975,** *B31,* 880.

4   Moody, D.C.; Odom, J.D. *J. Inorg. Nucl. Chem.* **1979,** *41,* 533.

5   See, for example: (a) Moody, D.C.; Zozulin, A.J.; Salazar, K.V. *Inorg. Chem.* **1982,** *21,*

        3856. (b) Moody, D.C.; Penneman, R.A.; Salazar, K.V. *Inorg. Chem.* **1979,** *18,* 208. (c)

        Sanots, I.; Marques, N.; De Matos, A.P. *Inorg. Chim. Acta* **1985,** *110,* 149. (d) Cymbaluk,

        T.H.; Liu, J.-Z.; Ernst, R.D. *J. Organomet. Chem.* **1983,** *255,* 311. (e) Zozulin, A.J.;

        Moody, D.C.; Ryan, R.R. *Inorg. Chem.* **1982,** *21,* 3083. (f) Andersen, R.A. *Inorg. Chem.*

        1979, *18,* 1507.

6   Clark, D.L.; Sattelberger, A.P.; Bott, S.G.; Vrtis, R.N. *Inorg. Chem.* **1989,** *28,* 1771.

7   (a) Cotton, F.A.; Wilkinson, G. *Advanced Inorganic Chemistry;* Wiley: New York, 1988;

        Chapter 21. (b) Brown, D. *Halides of the Lanthanides and Actinides;* Wiley-Interscience:

        New York, 1968, Chapter 5.

8   (a) Bagnall, K.W.; Brown, D.; Jones, P.J.; du Preez, J.G.H. *J. Chem Soc.* **1965,** 350. (b)

        du Preez, J.G.H.; Zeelie, B.; *Inorg. Chim. Acta* **1986,** *118,* L25. (c) du Preez, J.G.H.;

        Zeelie, B. *J. Chem. Soc., Chem. Commun.* **1986,** 743.

9   Nugent, W.A.; Mayer, J.M. *Metal-Ligand Multiple Bonds;* John Wiley and Sons: New

        York, 1988.

10   (a) Burns, C.J.; Smith, W.H.; Huffman, J.C.; Sattelberger, A.P. *J. Am. Chem. Soc.* **1990,**

        112, 3237. (b) Zalkin, A.; Brennan, J.G.; Andersen, R.A. *Acta. Cryst.* **1988,** *C44,* 1553. (c)

Brennen, J.G.; Andersen, R.A. *J. Am. Chem. Soc.* **1985**, *107*, 514. (d) Cramer, R.E.; Panchanatheswaren, K.; Gilje, J.W. *J. Am. Chem. Soc.* **1984**, *106*, 1853. (e) Cramer, R.E.; Edelmann, F.; Mori, A.L.; Roth, S.; Gilje, J.W.; Tatsumi, K.; Nakamura, A. *Organometallics* **1988**, *7*, 841.

[11]   Anhous, J.T.; Kee, T.P.; Schofield, M.H.; Schrock, R.R. *J. Am. Chem. Soc.* **1990**, *112*, 1642.

[12]   Although both sodium and potassium salts seem to work for these metathesis reactions, the reactions appear cleaner when the potassium reagents are used. D.L. Clark, personal communication.

[13] ^{1}H NMR data (benzene-d_6, 22° C): δ 13.2 (t, 4 H, meta), δ 9.9 (d, 2 H, para), δ 2.8 (s, 24 H, CH*Me$_2$*); δ 3.5 (t, 2 H, meta), δ 2.5 (d, 1 H, para), δ -14.2 (s, 12 H, CH*Me$_2$*). Resonances at δ -40 and δ -60 are tentatively assigned as coordinated THF.

[14]   (a) Cotton, F.A.; Marler, D.O.; Schwotzer, W. *Inorg. Chem.* **1984**, *23*, 4211. (b) Lauke, H.; Swepson, P.J.; Marks, T.J. *J. Am. Chem. Soc.* **1984**, *62*, 6841. (c) Secaur, C.A.; Day, V.W.; Ernst, R.D.; Kennelly, W.J.; Marks, T.J. *J. Am. Chem. Soc.* **1976**, *98*, 3713. (d) Cotton, S. A.; Hart, F.A.; Hursthouse, M.B.; Welch, J.A. *J. Chem. Soc., Chem. Commun.* **1972**, 1225. (e) Atwood, J.L.; Hunter, W.E.; Rogers, R.D.; Holten, J.; McMeeking, J.; Pearce, R.; Lappert, M.F. *J. Chem. Soc., Chem. Commun.* **1978**, 140. (f) Schumann H.; Muller, J.; Brunks, N.; Lauke, H.; Pickardt, J.; Schwartz, H.; Eckart, K. *Organometallics* **1984**, *3*, 69. (g) Tilley, T.D.; Andersen, R.A. *Inorg. Chem.* **1981**, *20*, 3267. (h) Watson, P.L.; Whitney, J.F.; Harlow, R.L. *Inorg. Chem.* **1981**, *20*, 3271.

[15]   Van Der Sluys, W.G.; Burns, C.J.; Huffman, J.C.; Sattelberger, A.P. *J. Am. Chem. Soc.* **1988**, *110*, 5924.

[16]   Clark, D.L.; Sattelberger, A.P., manuscript in preparation.

[17]   Zanella, P.; Rossetto, G.; DePaoli, G.; Traverso, O. *Inorg. Chim. Acta.* **1988**, *110*, 5924.

[18]   Cohen, D.; Carnall, W.T. *J. Phys. Chem.* **1960**, *44*, L155.

[19]   Lewis, J.; Miller, J.R.; Richards, R.L.; Thompson, A. *J. Chem. Soc.* **1965**, 5850.

20   Blake, P.C.; Lappert, M.F.; Taylor, R.G.; Atwood, J.L.; Zhang, H. *Inorg. Chim. Acta,* **1987,** *139,* 13.

21   Shannon, R.D. *Acta. Cryst.* **1976,** *a32,* 751.

22   Reynolds, J.G.; Zalkin, A.; Templeton, D.H.; Edelstein, N.M. *Inorg. Chem.* **1977,** *16,* 1090.

23   Stewart, J.L. Ph.D. Thesis, University of California, Berkely, **1981.**

24   Bock, H.; Ruppert, K.; Havlas, Z.; Fenske, D. *Angew. Chem. Int. Ed. Engl.* **1990,** *29,* 1042.

25   (a) Klein, J.F.; Gross, J.; Bassett, J.M.; Schubert, U. *Z. Naturforsch, Teil B.* **1980,** *35,* 614. (b) Klein, J.F.; Witty, H.; Schubert, U. *J. Chem. Soc., Chem. Commun.* **1983,** 231. (c) Jonas, K.; Kruger, F. *Angew. Chem. Int. Ed. Engl.* **1980,** *19,* 520.

26   Atwood, J.L.; Hrncir, D.C.; Priester, R.D.; Rogers, R.D. *Organometallics* **1983,** *2,* 985.

27   Atwood, J.L.; Crissinger, K.D.; Rogers, R.D. *J. Organomet. Chem.* **1978,** *115,* 1.

28   Atwood, J.L.; Hrncir, D.C.; Rogers, R.D. *J. Inclusion Phen.* **1983,** *1,* 199.